Arctic Report Card 2022
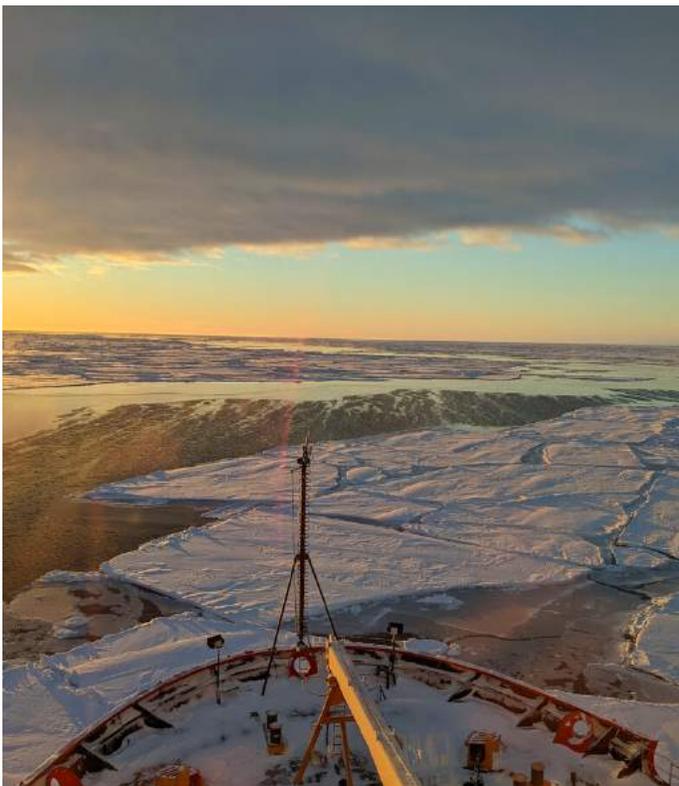
The warming Arctic reveals shifting seasons, widespread disturbances, and the value of diverse observations

M.L. Druckenmiller, R.L. Thoman, and T.A. Moon; Eds.

December 2022

Matthew L. Druckenmiller, Richard L. Thoman, Twila A. Moon; Editors
Kelley A. Uhlig; NOAA Coordinating Editor

www.arctic.noaa.gov/Report-Card

How to Cite Arctic Report Card 2022

Citing the complete report or Executive Summary:

Druckenmiller, M. L., R. L. Thoman, and T. A. Moon, Eds., 2022: *Arctic Report Card 2022*, https://doi.org/10.25923/yjx6-r184.

Citing an essay (example):

Mudryk, L., A. Elias Chereque, C. Derksen, K. Luojus, and B. Decharme, 2022: Terrestrial Snow Cover. *Arctic Report Card 2022*, M. L. Druckenmiller, R. L. Thoman, and T. A. Moon, Eds., https://doi.org/10.25923/yxs5-6c72.

(Note: Each essay has a unique DOI assigned)

Front cover photo credits

Center: Coastal thaw along Qikiqtaruk, Yukon, 2016 – Jeff T. Kerby, USA

Bottom Right: Ex-Tropical Typhoon Merbok approaches Alaska's coastline on September 16, 2022 – NOAA NESDIS/STAR GOES-West, Silver Spring, MD, USA & NWS Alaska Region, Anchorage, AK, USA.

Bottom Left: US Coast Guard Cutter Healy (WAGB-20) breaks ice near 81°N, 179°W during the 2022 US Synoptic Arctic Survey* on October 10, 2022 – Sarah Kaye, US Coast Guard, USA & National Science Foundation, Alexandria, VA, USA.
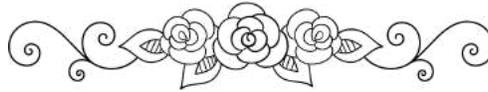*The US Synoptic Arctic Survey is an NSF-funded expedition (NSF/OPP-2053098, 2052626, 2051642, 2052101, 2053003, 2052513, 2053110, 2053084, 2210615, among others) with technical support provided through the Ship-based Science Technical Support in the Arctic (STARC) Program (NSF/OPP-2222245, 2037251).*

In Memoriam

Dr. Kevin R. Wood

1962 – 2022

NOAA's Arctic Report Card production team would like to honor the extensive contributions of Kevin R. Wood over the last 10 years. Kevin contributed scientifically to several essays and led the development of the Arctic Report Card video and script. His passion for scientific communication and storytelling shone through in these efforts and helped make the Arctic Report Card the authoritative and accessible publication that it is.

Fair winds and following seas…

Table of Contents

2022 Headlines

The warming Arctic reveals shifting seasons, widespread disturbances, and the value of diverse observations

Shifting seasons and climate-driven disturbances, such as wildfires, extreme weather, and unusual wildlife mortality events, are becoming increasingly difficult to assess within the context of what has been previously considered normal.

Headlines

- The average **surface air temperature** over the Arctic for this past year (October 2021-September 2022) was the 6th warmest since 1900. The last seven years are collectively the warmest seven years on record.
- Low pressure across the Alaska Arctic and northern Canada sustained warm summer temperatures over the Beaufort Sea and Canadian Archipelago.
- The Arctic continues to warm **more than twice as fast** as the rest of the globe, with even greater warming in some locations and times of year.

In the oceans

- 2022 Arctic **sea ice** extent was similar to 2021 and well below the long-term average.
- August 2022 mean **sea surface temperatures** continued to show warming trends for 1982-2022 in most ice-free regions of the Arctic Ocean. SSTs in the Chukchi Sea were anomalously cool in August 2022.
- Most regions of the Arctic continued to show increased ocean plankton blooms, or **ocean primary productivity**, over the 2003-22 period, with the greatest increases in the Eurasian Arctic and Barents Sea.
- Satellite records from 2009 to 2018 show **increasing maritime ship traffic in the Arcti**c as sea ice declines. The most significant increases in maritime traffic are occurring from the Pacific Ocean through the Bering Strait and Beaufort Sea.
- **NASA's Oceans Melting Greenland mission** used cutting-edge technology to demonstrate that rising ocean temperatures along Greenland's continental shelf are contributing to ice loss through melting glaciers at the ice sheet's margins.

On the land

- June 2022 **terrestrial snow cover** was unusually low over both the North American (2nd lowest in the 56-year record) and Eurasian Arctic (3rd lowest in the record). Winter accumulation was above average, but early snow melt in a warming Arctic contributed to the overall low snow cover.
- A significant increase in **Arctic precipitation** since the 1950s is now detectable across all seasons. Wetter-than-normal conditions were observed from October 2021 through September 2022, in what was the 3rd wettest year of the past 72 years.

- The **Greenland Ice Shee**t experienced its 25th consecutive year of ice loss. In September 2022, unprecedented late-season warming created surface melt conditions over 36% of the ice sheet, including at the 10,500 ft ice sheet summit.
- **Tundra greenin**g declined from the record high values of the previous two years, with high productivity in most of the North American Arctic, but unusually low productivity in northeastern Siberia. Wildfires, extreme weather events, and other disturbances have become more frequent, influencing the variability of tundra greenness.
- Striking differences were observed between **lake ice** durations in Eurasia and North America, with substantially longer than average ice durations in Eurasia and predominantly shorter in North America. Freeze-up of Arctic lakes is occurring later in most of North America, especially in Canada.
- The distribution, conservation status, and ecology of most **Arctic pollinators** are poorly known though these insects are critically important to Arctic ecosystems and the food systems of Arctic Indigenous Peoples and Arctic residents. Coordinated long-term monitoring, increased funding, and emerging technologies can improve our understanding of Arctic pollinator habitats and status, and inform effective conservation strategies.

Arctic birds

- In 2022, despite an outbreak of highly pathogenic avian influenza affecting birds throughout North America and variable spring weather conditions, the population sizes of most **Arctic geese** remained high with increasing or stable trends. Multiple geese species provide food and cultural significance for many peoples.
- In contrast, communities in the northern Bering and southern Chukchi Sea region reported higher-than-expected **seabird die-offs** for the sixth consecutive year. Tracking the duration, geographic extent, and magnitude of seabird bird die-offs across Alaska's expansive and remote coastline is only possible through well-coordinated communication and a dedicated network of Tribal, State, and Federal partners.

Consequences of rapid Arctic environmental change for people

- People experience the **consequences of a rapidly changing Arctic** as the combined effects of physical conditions, responses of biological resources, impacts on infrastructure, decisions influencing adaptive capacities, and environmental and international influences on economics and well-being.
- Living and innovating in Arctic environments over millennia, Indigenous Peoples have evolved **holistic knowledge providing resilience and sustainability**. Indigenous expertise is augmented by scientific abilities to reconstruct past environments and to model and predict future changes. Decision makers (from communities to governments) have the skills necessary to apply this experience and knowledge to help mitigate and adapt to a rapidly changing Arctic.
- **Addressing unprecedented Arctic environmental changes** requires listening to one another, aligning values, and collaborating across knowledge systems, disciplines, and sectors of society.

Executive Summary

M. L. Druckenmiller[1,2], R. L. Thoman[3,4], and T. A. Moon[1,2]

[1]National Snow and Ice Data Center, University of Colorado Boulder, Boulder, CO, USA
[2]Cooperative Institute for Research in Environmental Sciences, University of Colorado Boulder, Boulder, CO, USA
[3]Alaska Center for Climate Assessment and Policy, University of Alaska Fairbanks, Fairbanks, AK, USA
[4]International Arctic Research Center, University of Alaska Fairbanks, Fairbanks, AK, USA

Few parts of the world demonstrate such extreme seasonal shifts in temperature, land and ocean cover, ecological processes, and wildlife movement and behavior as the Arctic. These extreme shifts across the annual cycle are a source of the Arctic region's heightened sensitivity to climate changes and climate-related disturbances. The Arctic is also a region of sparse in-situ observations, especially relative to its importance in understanding the Earth's changing climate and associated societal consequences.

The 2022 Arctic Report Card (ARC2022) provides an updated annual view into the state of the Arctic by checking in on key *vital signs*—eight defining elements of the Arctic's climate and environmental system. This report also samples critical and emerging topics across the Arctic, bringing into focus diverse collections of observations that help to assess the overall trajectory of Arctic change.

ARC2022 reveals an Arctic experiencing widespread shifts in seasonal climate. Many observations throughout the Report Card are organized within periods of the year defined by predictable climatological or ecological conditions (e.g., the "snow season" or the "breeding season" for a particular animal species). These periods are shifting, and in turn, altering ecological and landscape processes, and increasingly misaligning with human expectations and decision-making. For example, June snow cover extent in the Arctic is rapidly declining at a rate of -18.9 ± 6.6% per decade, marking a dramatic shift in how the snow season is defined and experienced across the North. In early September 2022, the Greenland Ice Sheet experienced an unprecedented late-season surface melt event across 36% of the ice sheet surface. This was followed by a small but again unprecedented late September melt event caused by the remnants of Hurricane Fiona, challenging how researchers define the Greenland summer melt season.

As seasons shift, climate-driven disturbances, such as wildfires, extreme weather, and unusual wildlife mortality events, become increasingly difficult to assess within the context of what has been previously considered normal. To better track changing climate and remain well positioned to assess accelerating change and disturbances, ARC2022 has implemented a new climate baseline period across its *vital sign* essays. The Report Card now uses 1991-2020 as the new 30-year baseline, updated from the previous 1981-2010 baseline. This shift also aligns our reporting with other leading climate science organizations that monitor climate trends on Arctic to global scales, such as the World Meteorological Organization.

Arctic annual surface air temperatures during October 2021-September 2022 were the sixth warmest dating back to 1900, continuing a decades-long trend in which Arctic air temperatures have warmed faster than the global average. Strongly driven by this warming, Arctic sea ice continues to decline in thickness and extent. Increasingly, the Arctic provides powerful glimpses into what ice loss may mean

for the future of communities and ecosystems, as well as shipping and marine access in the far north. In summer 2022, both the Northern Sea Route and Northwest Passage were open while unusually low ice concentrations and areas of open water were observed near the North Pole.

What does this mean for the future of Arctic shipping? The emergence and availability of satellite-based ship data since 2009 are helping to address this important question. As of 2022, satellite-based records reveal increasing maritime ship traffic within all Arctic high seas and national exclusive economic zones, aligning with the "ship-ice hypothesis," which posits that Arctic shipping will increase as sea ice diminishes. This raises important questions on topics ranging from the future of Arctic trade routes to the introduction of enhanced anthropogenic stresses on Arctic Peoples and ecosystems. The Arctic Ocean and peripheral seas are remote, ecologically sensitive, and environmentally variable waters where socio-economic and geopolitical realities cannot be ignored.

Sea ice loss is also intricately connected to other key Arctic marine *vital signs*. Arctic sea surface temperature (SST) is a valuable indicator of the role of the ice-albedo feedback cycle. As sea ice melts due to warming, much more incoming solar heat is absorbed by the exposed darker ocean surface and, in turn, the warmer ocean melts more sea ice, or impedes ice thickening throughout fall and winter. August average SSTs show warming trends since records began in 1982 for most regions of the Arctic Ocean that are ice-free, with the northern Barents Sea as a notable exception due in part to a period of warm SSTs during the 1980s and '90s. In 2022, SSTs showed unusually cool August SSTs in the Chukchi Sea, coincident with late-summer sea ice in the region that was kept in place by persistent north winds.

Ocean temperatures are not only rising at the surface, but also at depth, further influencing Arctic environments, such as the Greenland Ice Sheet. Findings from the NASA *Oceans Melting Greenland* mission confirmed the important role that warming ocean temperatures play in influencing ice loss through glacier melt at the ice sheet margins. These types of observations give us new insights into the processes affecting a melting Greenland. With melt occurring at the ocean boundaries and across the ice sheet surface, the Greenland Ice Sheet again lost ice in 2022, the 25th consecutive year of ice loss.

ARC2022 includes the inaugural *vital sign* essay on Arctic precipitation. Using reanalysis data products, which allow scientists to overcome the challenges of sparse gauge measurements in the Arctic, this new essay assesses variations and the emergence of trends in Arctic precipitation. Significant increases in Arctic precipitation across all seasons since the mid-1900s are detected, consistent with observed increases in global total atmospheric moisture. However, regional variations exist across the Arctic, with some regions experiencing notable seasonal decreases in precipitation (e.g., the Bering Sea during spring and summer).

Summer storms played a substantial role in shaping 2022 Arctic events. For example, storms in the Bering Sea may have been responsible for the satellite-observed higher-than-average primary productivity (i.e., the transformation of dissolved inorganic carbon into organic material) in the region due to enhanced vertical mixing of nutrients. These same storms in the Pacific Arctic also disrupted ship-based measurements of nutrients and primary productivity during summer 2022 that are critical for complementing satellite observations. Five of the nine monitored Arctic regions showed high productivity in 2022, with the Arctic overall in line with the long-term positive trend over the satellite record (2003-22).

Typhoon Merbok—fueled by unusually warm water in the North Pacific—was another storm that dramatically shaped 2022 in the Bering Sea region. In mid-September, hurricane-force winds, 50-foot

waves, and far-reaching storm surge impacted coastal and river communities along over 1,000 miles of coastline. Homes, roads, and infrastructure were damaged, and the storm severely disrupted the communities' fall hunting and harvesting in preparation for the oncoming winter.

Long-term precipitation records also suggest important connections to other ongoing changes in the Arctic. For example, an increase in prolonged wet periods (measured as consecutive wet days) across a large area spanning from Svalbard eastward through the Siberian seas to the Chukchi Sea generally coincides with reduced sea ice coverage during the warm season of the year when moisture is readily transferred from the ocean to atmosphere. The new precipitation essay also provides an annual and seasonal overview of Arctic precipitation anomalies in the context of long-term changes. For this past year (October 2021-September 2022), wetter-than-normal conditions predominated over much of the Arctic. Summer 2022 was an exception, with generally dry conditions across the North. In Alaska, these dry conditions fed severe wildfires in early summer.

The Arctic's intensifying hydrologic cycle and warming air temperatures are key drivers of many changes across the Arctic terrestrial environment—from snow cover to lake ice break-up to tundra vegetation productivity. During the 2021-22 season, despite an above-average accumulation of snow, the Arctic overall experienced an early and rapid snow melt, consistent with the expected changes to snow cover in a warmer Arctic. For example, the spring snow-free period across much of Eurasia was 30-50% longer than normal. North America and Eurasia experienced the second and third lowest June snow extents, respectively, in the 56-year record. However, for Arctic lakes in 2022, striking differences were observed between lake ice durations in North America and Eurasia, with predominantly shorter ice durations in North America and substantially longer durations in Eurasia. On the tundra, vegetation productivity (greening) in 2022 declined from the record-high values of the previous two years, but still represented the fourth highest value since observations began in 2000.
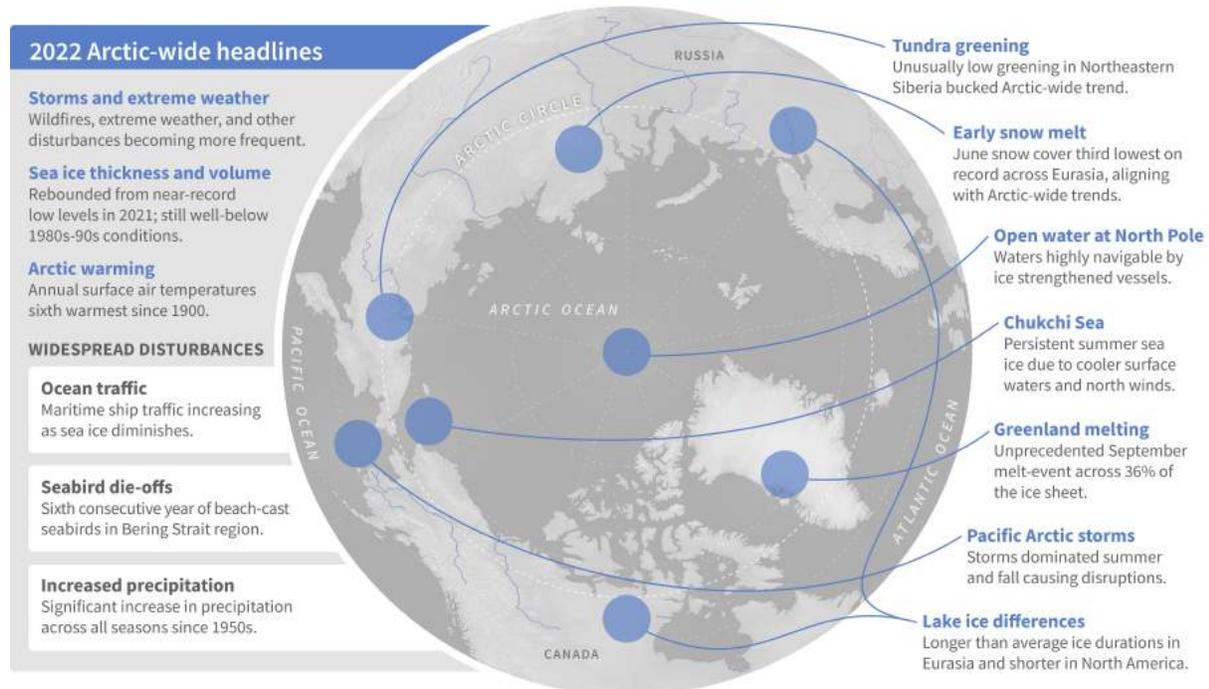
A sample of notable events and widespread disturbances from across the Arctic. Image by Climate.gov.

ARC2022 includes a discussion on climate consequences felt by Arctic Peoples. This essay from the Study of Environmental Arctic Change (SEARCH) illuminates how people experience change as the combined effects of altered physical conditions, infrastructure vulnerability, access to resources, and local to global economic drivers. This lesson is not only true of human well-being; environments, animals, and the Arctic system itself are experiencing multiple stressors, and it is the combined, cumulative effect that sustained Arctic observing aims to understand.

Northern migratory animals in particular are unique as they experience environmental, climatic, and anthropogenic stresses accumulated across many different regions, often well beyond the Arctic. Drawing on observations from a network of Tribal, State, and Federal partners in Alaska, seabird die-offs across the northern Bering Sea and southern Chukchi Sea were reported for the sixth straight year in 2022, maintaining concerns that massive ecological shifts in a warming and less ice-covered ocean are stressing these top predators in the food chain.

Arctic Geese, like seabirds, serve as important indicators of environmental changes and disturbances, including the spread of disease. In 2022, despite an outbreak of highly pathogenic avian influenza in North America and variable spring weather conditions, Arctic geese have remained high and stable in population. Given the scale and pace of change across the Arctic, however, there is a need for monitoring across a broad range of climate-sensitive indicator species, not just top predators. For example, this year's report showcases the critical function that pollinating insects play in Arctic ecosystems and the status of inventorying their populations internationally.

Overall, ARC2022 provides 15 essays highlighting an Arctic in transition. Long-term trends are reinforced by another year of observations, while regional differences across the Arctic are increasingly apparent. The Arctic remains a varied and expansive region to monitor. To understand its transition, local to international partnerships, especially with Arctic Peoples and Indigenous communities, are vital to the use of diverse observations and knowledge, as well as to identifying solutions to long-term climate impacts and abrupt disturbances.

ARC2022 explores observations from geographic regions and locations across the Arctic. The ARC2022 map provides a reference for notable locations mentioned in this year's report. Please also visit About Arctic Report Card 2022 for more information about the report.

January 13, 2023

Surface Air Temperature

T. J. Ballinger[1], J. E. Overland[2], M. Wang[2,3], J. E. Walsh[1], B. Brettschneider[4], R. L. Thoman[1,5], U. S. Bhatt[6], E. Hanna[7], I. Hanssen-Bauer[8], and S. -J. Kim[9]

[1]International Arctic Research Center, University of Alaska Fairbanks, Fairbanks, AK, USA
[2]Pacific Marine Environmental Laboratory, NOAA, Seattle, WA, USA
[3]Cooperative Institute for Climate, Ocean, and Ecosystem Studies, University of Washington, Seattle, WA, USA
[4]National Weather Service Alaska Region, NOAA, Anchorage, AK, USA
[5]Alaska Center for Climate Assessment and Policy, University of Alaska Fairbanks, Fairbanks, AK, USA
[6]Geophysical Institute, University of Alaska Fairbanks, Fairbanks, AK, USA
[7]Department of Geography and Lincoln Climate Research Group, Lincoln, UK
[8]Norwegian Meteorological Institute, Oslo, Norway
[9]Korea Polar Research Institute, Incheon, Republic of Korea

Highlights

- Annual water year (October 2021-September 2022) surface air temperatures (north of 60° N) were the sixth warmest dating back to 1900.
- Winter (January-March) 2022 was characterized by above-normal (≥3°C) air temperature anomalies in the Eurasian Arctic and Arctic Ocean contrasted by below-normal (≤-2°C) air temperature anomalies over most of the North American high latitudes.
- An extensive region of low pressure in the eastern Arctic supported warm Eurasian and Arctic Ocean winter temperatures, while low pressure across the Alaska Arctic and northern Canada sustained warm summer temperatures over the Beaufort Sea and Canadian Archipelago.

Over recent decades, Arctic air temperatures have warmed at a greater rate relative to global means. This amplified regional warming, known as Arctic Amplification (AA), is associated with various localized land-ocean-sea ice interactions and large-scale atmospheric and oceanic energy transports (Previdi et al. 2021). AA is a well-established phenomenon that is connected to changes in Arctic weather and climate extremes that impact the region's climate system (Walsh et al. 2020). Recent research has emphasized that the magnitude of AA is sensitive to multiple constraints, including how the southern limit of the Arctic region is defined, which datasets (i.e., observational versus modeled) are analyzed, and what time periods are considered (England et al. 2021; Chylek et al. 2022; Rantanen et al. 2022). As examples, Chylek et al. (2022) and Rantanen et al. (2022) showed that land and ocean areas poleward of 60° N have warmed ~2-3 faster than the global mean during the last three decades.

As a long-standing practice in the Arctic Report Card, this year's Surface Air Temperature essay examines Arctic annual temperatures for northern lands (60-90° N), and includes ocean and total area (land and ocean) temperature estimates across this domain. A summary of seasonal air temperature anomalies is also discussed with an emphasis on patterns observed during the past year.

Arctic annual land and ocean temperatures

This past water year (October 2021-September 2022) marked the sixth warmest for Arctic Ocean and land areas north of 60° N since 1900 (Fig. 1a). Surface air temperatures were 0.73°C warmer than the 1991-2020 mean, continuing the common, recent pattern where annual temperatures have both exceeded the 30-year Arctic mean and been warmer than the global mean. Including the past year, the ten warmest years observed in the Arctic have all occurred since 2011 (Fig. 1a).
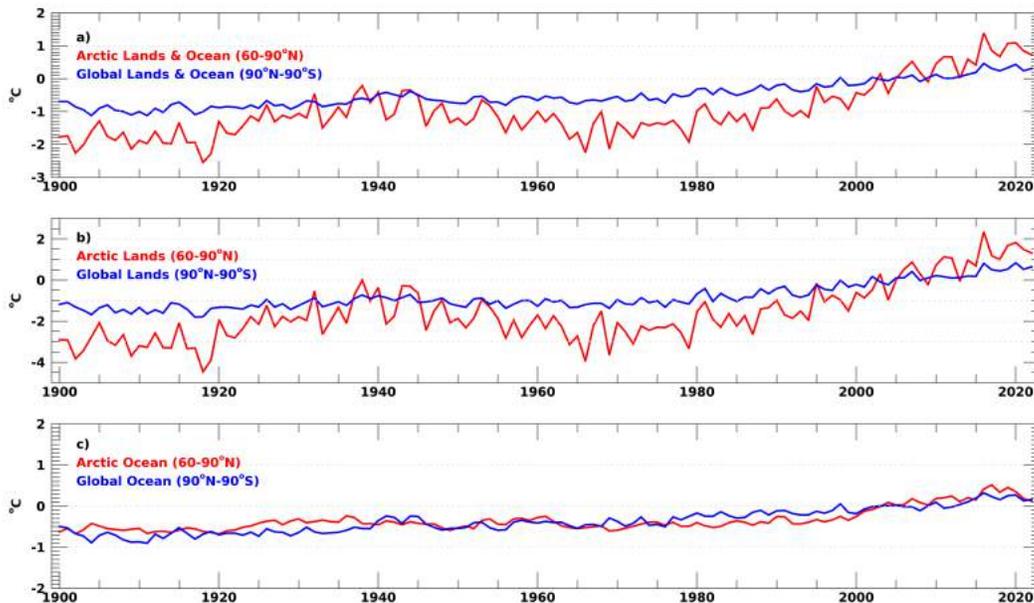

Fig. 1. Water year (October through September) Arctic and global-average surface air temperature anomalies (°C) for (a) land and ocean areas, (b) land-only, and (c) ocean-only for 1900-2022. Anomalies are presented with respect to the 1991-2020 baseline. Source: SAT data are from NASA GISTEMP (see Methods and data section for details).

Considered independently, Arctic lands (Fig. 1b) and the Arctic Ocean (Fig. 1c) also experienced notable annual warm anomalies during 2022. Land temperatures were 1.31°C above the 1991-2020 mean, ranking fifth warmest, while this past year's Arctic Ocean mean temperature anomaly (0.13°C) was the thirteenth warmest, both since 1900. Over the last half century, increased temperatures are apparent in both environments with greater year-to-year variability observed over land compared to the ocean due to thermal inertia and heat capacity differences between these environments.

Seasonal Arctic air temperatures in 2022

Arctic air temperature anomalies, compared to the 1991-2020 mean, are presented for seasons spanning the water year (October-September) defined as follows: autumn 2021 (October-December [OND]), winter (January-March [JFM]), spring (April-June [AMJ]) and summer (July-September [JAS]) 2022 (Fig. 2). These seasonal definitions also follow important annual cycles discussed in this year's Arctic Report Card, including the Greenland Ice Sheet's period of peak ablation during summer and the spring onset of snow and sea ice melt on the Arctic Ocean.
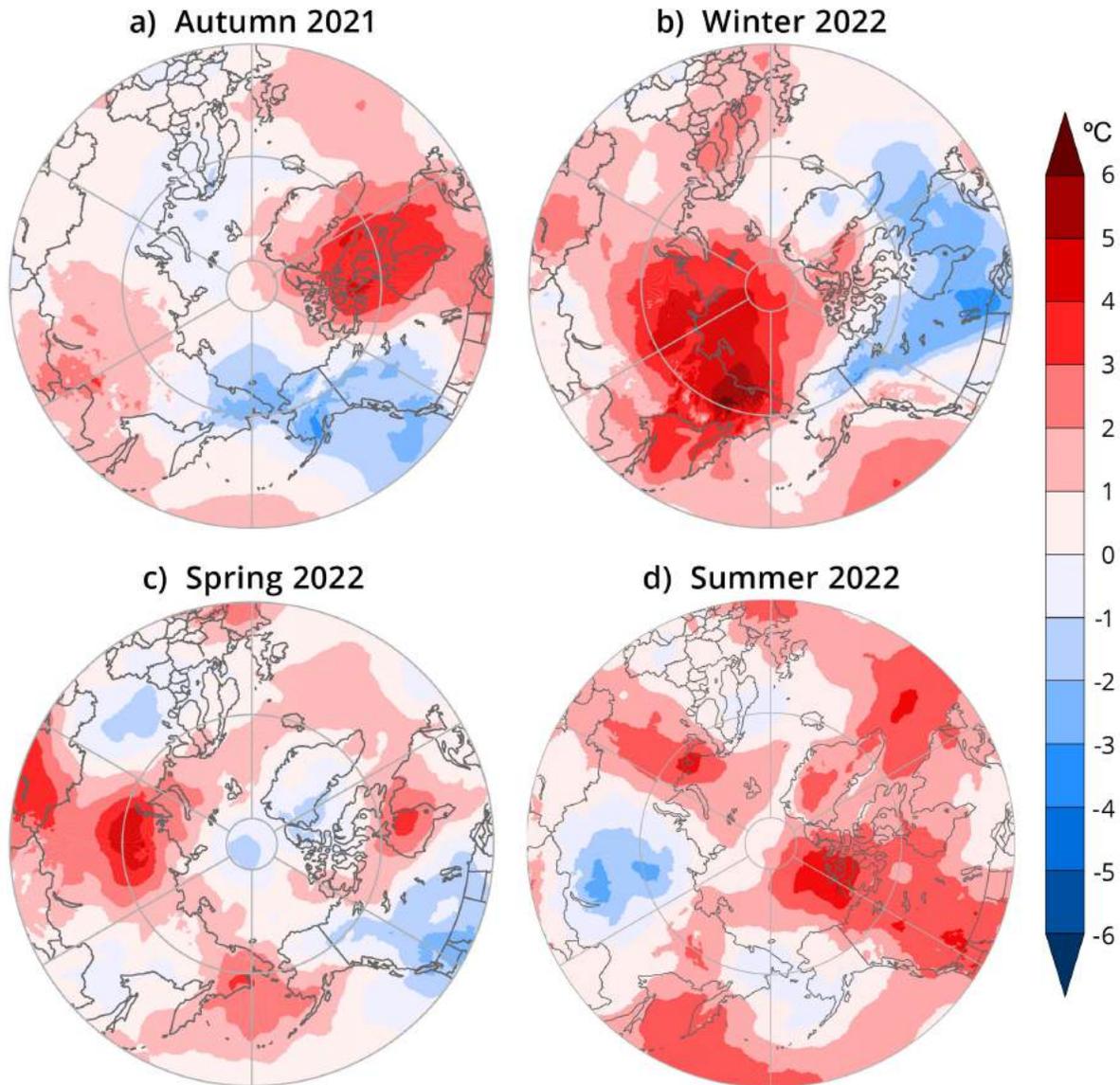
Fig. 2. Near-surface (925 hPa) seasonal air temperature anomalies (in °C) for (a) autumn 2021, (b) winter 2022, (c) spring 2022, and (d) summer 2022. Temperature anomalies are shown relative to their 1991-2020 means. Source: ERA5 reanalysis air temperature data are obtained from the Copernicus Climate Change Service (see Methods and data section for details).

Autumn 2021. Warm air temperature anomalies of at least 1°C above the 1991-2020 mean spread over most of Arctic Canada, Greenland, and central Siberia (Fig. 2a). Broad warm anomalies of 3°C were found over Hudson Bay and the Canadian Archipelago to the north extending eastward over Baffin Bay and the northern Labrador Sea. These anomalies were supported by two sea-level pressure anomaly patterns. One of these patterns showed higher-than-normal pressure over the central Arctic and Greenland—with unusually strong Greenland Blocking in October—while the second pattern was characterized by below-normal pressure over the Beaufort Sea and Canadian Archipelago. These two patterns worked in tandem to transport warm, southerly air across this area and sustained above-normal air temperatures (Fig. 3a). In stark contrast to autumn 2020 (see Ballinger et al. 2021), the Arctic Ocean experienced near-normal autumn temperatures.
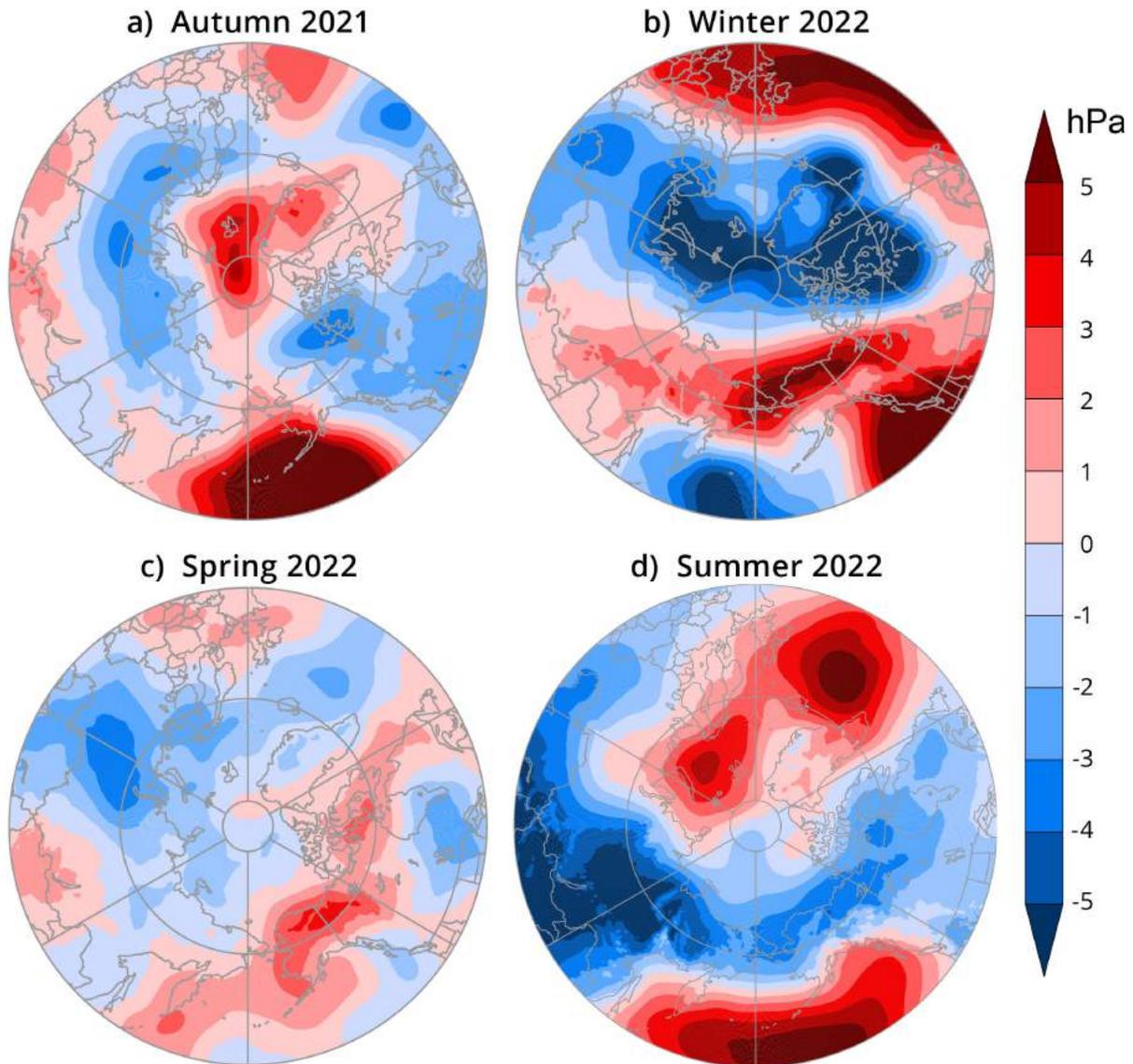
Fig. 3. Seasonal sea-level pressure (SLP) anomalies (in hPa) for (a) autumn 2021, (b) winter 2022, (c) spring 2022, and (d) summer 2022. SLP anomalies are shown relative to their 1991-2020 means. Source: ERA5 reanalysis SLP data are obtained from the Copernicus Climate Change Service (see Methods and data section for details).

Cold anomalies stretched from Chukotka eastward across northwestern North America (Fig. 2a). Areas within the Chukchi Sea and northern Bering Sea and adjacent North Slope and southcentral Alaska saw the coldest seasonal temperature patterns (≤-2°C) in the Arctic. Colder-than-normal autumn air temperatures were associated with the development of relatively thicker sea ice compared to previous years (see essay *Sea Ice*). Record and near-record cold events were noted in western Alaska in November, including the lowest November mean temperature in the past 75 years at both King Salmon and Cold Bay, Alaska (NOAA NWS 2022). This stretch of cold temperatures was a result of northerly winds aided by the aforementioned negative pressure anomaly over the Beaufort Sea and Canadian Archipelago in tandem with a large high-pressure anomaly (≥5 hPa) in the North Pacific (Fig. 3a).

Winter 2022. A distinct, contrasting Eurasian-North American temperature dipole was present during winter of 2022 (Fig. 2b). This was characterized by above-normal air temperatures in the Eurasian Arctic and cold departures over the North American high latitudes, as a result of positive Arctic Oscillation/North Atlantic Oscillation conditions prevailing during much of this season. A large region of ≥3°C warm anomalies was concentrated on the central Arctic extending south to western Siberia and stretching across the continent. The above-average temperatures were associated with 4-5 hPa lower-than-normal surface pressure over the Barents and Kara Seas that facilitated warm airflow over land and ocean areas to the east (Fig. 3b) and coincided with positive precipitation anomalies over Norway (see essay *Precipitation*).

Contrasting winter cold temperature anomalies (≤-2°C) were noted over northern North America, extending from northeastern Alaska southeastward over Hudson Bay and Labrador Sea to the east (Fig. 2b). Colder-than-normal air temperatures over these areas were supported by low pressure north of Hudson Bay (≤-5 hPa) and a broad region of high pressure upstream extending eastward from central Siberia to western North America (Fig. 3b).

Spring 2022. Arctic Ocean air temperatures hovered around average, with relatively small air temperature anomalies over Arctic lands during spring of 2022 (Fig. 2c). This was typified by warm anomalies (≥1°C) in central and eastern Siberia and atop Hudson Bay. A small area of maximum Arctic air temperature anomalies (4-5°C) was found just west of the Ural Mountains associated with low pressure anomalies (≤-2 hPa) that transported warm air into the area (Fig. 3c). Record warm June-averaged air temperatures were found over Svalbard (5-6°C; Mamen et al. 2022). Similar to autumn of 2021, near-normal air temperatures were found over the Arctic Ocean. Negative temperature anomalies (≤-1°C) were dispersed over northwestern North America, northwestern Greenland and adjacent Ellesmere Island, and westernmost Eurasia.

Summer 2022. Summer air temperatures were described by multiple, regional warm anomalies (≥1°C), including over westernmost Eurasia, easternmost Eurasia, and the Beaufort Sea and Canadian Archipelago (Fig. 2d). Low pressure anomalies, suggestive of frequent storms, across Arctic Alaska and northern Canada supported the warm air temperatures in the latter areas. Similar to preceding autumn and spring temperature patterns, the central Arctic Ocean air temperatures remained near to slightly above-normal with some warm anomalies extending from coastal areas into the marginal seas. Cold anomalies were observed in central Eurasia and were associated with low pressure anomalies to the east that caused cold, northerly winds (Fig 3d).

Methods and data

The NASA Goddard Institute for Space Studies (GISS) surface temperature analysis version 4 (GISTEMP v4) is used to describe Arctic and global air temperatures since 1900 (Fig. 1). GISTEMP4 air temperatures over global lands are obtained from the NOAA Global Historical Climatology Network version 4 (GHCN v4) and global ocean surface temperatures originate from the NOAA Extended Reconstructed Sea Surface Temperature version 5 (ERSST v5) dataset. The process of merging these products to create the GISTEMP product is described in Hansen et al. (2010) and Lenssen et al. (2019). Past ARC SAT essays have used different versions of the CRUTEM product (e.g., Osborn et al. 2021). We elect to use GISTEMP this year as it has been shown to exhibit similar variability and trends as CRUTEM and analogous products that resolve multidecadal Arctic and global air temperatures (Rantanen et al. 2022), but has more thorough spatial coverage.

Seasonal air temperature and surface pressure plots are created from ERA5 reanalysis (Hersbach et al. 2020). Two-meter air temperatures in ERA5 exhibit a warm bias over the Arctic Ocean (Yu et al. 2021). Therefore, we elect to show 925 hPa level air temperatures (Fig. 2), which are constrained by aerial (e.g., radiosonde and aircraft) and satellite observations. We note that initial analyses found 925 hPa Arctic air temperatures from ERA5 to be consistent with other reanalyses in terms of their temporal variability and spatial patterns (not shown). All values and fields are presented as anomalies with respect to the 1991-2020 mean.

References

Ballinger, T. J., and Coauthors, 2021: Surface air temperature. *Arctic Report Card 2021*, T. A. Moon, M. L. Druckenmiller, and R. L. Thoman, Eds., https://doi.org/10.25923/53xd-9k68.

Chylek, P., C. Folland, J. D. Klett, M. Wang, N. Hengartner, G. Lesins, and M. K. Dubey, 2022: Annual mean Arctic amplification 1970-2020: Observed and simulated by CMIP6 climate models. *Geophys. Res. Lett.*, **49**, e2022GL099371, https://doi.org/10.1029/2022GL099371.

England, M. R., I. Eisenman, N. J. Lutsko, and T. J. W. Wagner, 2021: The recent emergence of Arctic amplification. *Geophys. Res. Lett.*, **48**, e2021GL094086, https://doi.org/10.1029/2021GL094086.

Hersbach, H., and Coauthors, 2020: The ERA5 global reanalysis. *Q. J. Roy. Meteor. Soc.*, **146**, 1999-2049, https://doi.org/10.1002/qj.3803.

Hansen, J., R. Ruedy, M. Sato, and K. Lo, 2010: Global surface temperature change. *Rev. Geophys.*, **48**, RG4004, https://doi.org/10.1029/2010RG000345.

Lenssen, N., G. Schmidt, J. Hansen, M. Menne, A. Persin, R. Ruedy, and D. Zyss, 2019: Improvements in the GISTEMP uncertainty model. *J. Geophys. Res.-Atmos.*, **124**, 6307-6326, https://doi.org/10.1029/2018JD029522.

Mamen, J., H. T. T. Tajet, and K. Tunheim, 2022: Klimatologisk månedsoversikt, June 2022, MET info no. 6/2022 (In Norwegian), ISSN 1894-759X.

NOAA National Weather Service (NWS), 2022: NOWData - NOAA Online Weather Data [Cold Bay Area & King Salmon Area], accessed 12 September 2022, https://www.weather.gov/wrh/Climate?wfo=afg.

Osborn, T. J., P. D. Jones, D. H. Lister, C. P. Morice, I. R. Simpson, J. P. Winn, E. Hogan, and I. C. Harris, 2021: Land surface air temperature variations across the globe updated to 2019: the CRUTEM5 dataset. *J. Geophys. Res.-Atmos.*, **126**, e2019JD032352, https://doi.org/10.1029/2019JD032352.

Previdi, M., K. L. Smith, and L. M. Polvani, 2021: Arctic amplification of climate change: a review of underlying mechanisms. *Environ. Res. Lett.*, **16**, 093003, https://doi.org/10.1088/1748-9326/ac1c29.

Rantanen, M., A. Y. Karpechko, A. Lipponen, K. Nordling, O. Hyvärinen, K. Ruosteenoja, T. Vihma, and A. Laaksonen, 2022: The Arctic has warmed nearly four times faster than the globe since 1979. *Commun. Earth Env.*, **3**, 168, https://doi.org/10.1038/s43247-022-00498-3.

Walsh, J. E., T. J. Ballinger, E. S. Euskirchen, E. Hanna, J. Mård, J. E. Overland, H. Tangen, and T. Vihma, 2020: Extreme weather and climate events in northern areas: A review. *Earth-Sci. Rev.*, **209**, 103324, https://doi.org/10.1016/j.earscirev.2020.103324.

Yu, Y., W. Xiao, Z. Zhang, X. Cheng, F. Hui, and J. Zhao, 2021: Evaluation of 2-m air temperature and surface temperature from ERA5 and ERA-I using buoy observations in the arctic during 2010-2020. *Remote Sens.*, **13**, 2813, https://doi.org/10.3390/rs13142813.

November 14, 2022

Terrestrial Snow Cover

L. Mudryk[1], A. Elias Chereque[2], C. Derksen[1], K. Luojus[3], and B. Decharme[4]

[1]Climate Research Division, Environment and Climate Change Canada, Toronto, ON, Canada
[2]Department of Physics, University of Toronto, Toronto, ON, Canada
[3]Arctic Research Centre, Finnish Meteorological Institute, Helsinki, Finland
[4]Centre National de Recherches Météorologiques, Météo-France, Toulouse, France

Highlights

- June Arctic snow cover extent (SCE) anomalies were strongly negative over both North America (2nd lowest in the 56-year record) and Eurasia (3rd lowest in the record).
- The 2021/22 Arctic snow season saw a combination of above-average snow accumulation but early snow melt consistent with the expected changes to snow cover in a warmer Arctic.

Introduction

Many components of the Arctic land surface are directly influenced by snow cover from fall through spring, including the surface energy budget, ground thermal regime, permafrost, and terrestrial and freshwater ecosystems (Brown et al. 2017; Meredith et al. 2019). Even following the snow cover season, the influence of spring snow melt timing persists through impacts on river discharge timing and magnitude, surface water, soil moisture, vegetation phenology, and fire risk (Meredith et al. 2019).

Multiple datasets derived from satellite observations and snowpack models driven by atmospheric reanalyses are used to assess Arctic seasonal snow cover. Collectively, this approach provides a reliable picture of Arctic snow cover variability over the last five decades. We characterize snow conditions across the Arctic land surface using three quantities: how much total land area is covered by snow (snow cover extent - SCE), how long throughout the year snow covers the land surface (snow cover duration - SCD), and how much water is stored in solid form by the snowpack (snow water equivalent - SWE; the product of snow depth and density). We examine each of these quantities in turn for the Arctic snow season spanning fall 2021 through spring 2022.

Snow cover extent and duration

SCE anomalies (relative to the 1991-2020 climatology) in spring 2022 are shown separately for the North American and Eurasian terrestrial sectors of the Arctic in Fig. 1. May anomalies were near the average of the last 30 years in the North American sector (ranked 29th lowest in the 56-year record available since 1967) but below average over the Eurasian sector (ranked 9th lowest). Rapid snow loss in June resulted in very low SCE across both sectors (2nd and 3rd lowest, respectively).
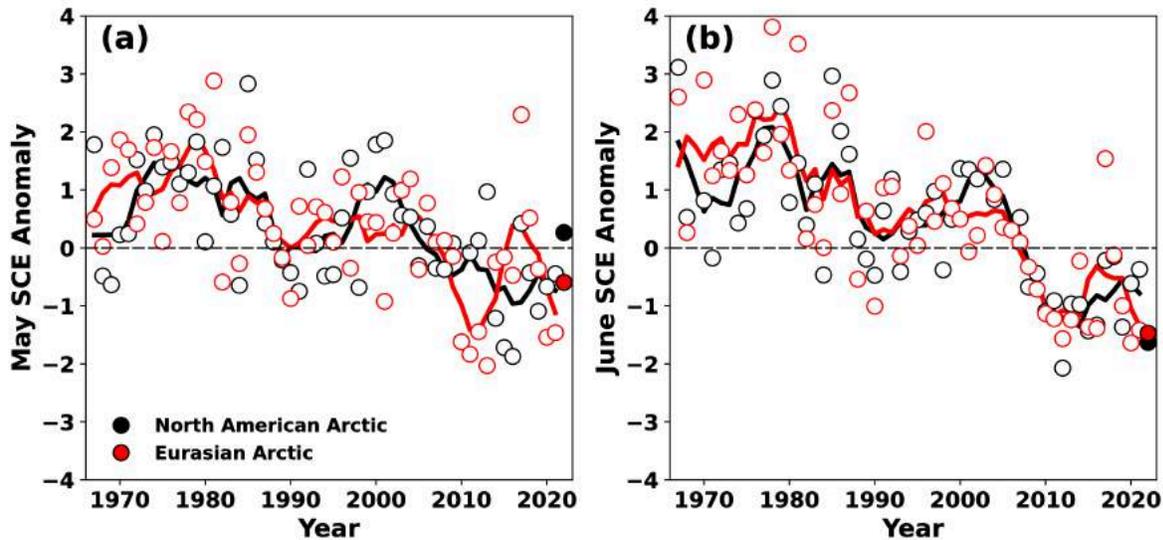
Fig. 1. Standardized monthly snow cover extent anomalies relative to the 1991-2020 climatology for Arctic land areas (>60° N) for (a) May, and (b) June, from 1967 to 2022. Solid black and red lines depict 5-year running means for North America and Eurasia, respectively. Filled circles are used to highlight 2022 anomalies. Source: NOAA snow chart Climate Data Record (CDR).

Snow cover duration (SCD) anomalies (relative to a 1998-1999 to 2017-2018 climatology) across the Arctic region for the 2021/22 snow season are shown in Fig. 2 for both snow onset and snow melt periods of the year (see Methods and data). Onset anomalies indicate snow cover during autumn 2021 began earlier than normal over Alaska, Eastern Siberia, and Scandinavia and began later than normal over central Arctic Canada and parts of central Siberia, a pattern consistent with autumn temperature anomalies (see essay *Surface Air Temperature*) and above-normal precipitation over Alaska and Scandinavia (see essay *Precipitation*). Melt anomalies during spring 2022 show anomalously low SCD (indicating early melt) across much of the Arctic with three strong maximums: east of the Ural Mountains, across eastern Siberia, and over the Canadian Arctic Archipelago consistent with spring and summer 2022 temperature anomalies (see essay *Surface Air Temperature*). Similar to spring 2021, the duration of the spring 2022 snow-free period across broad expanses of Eurasia was 30-50% longer than normal.
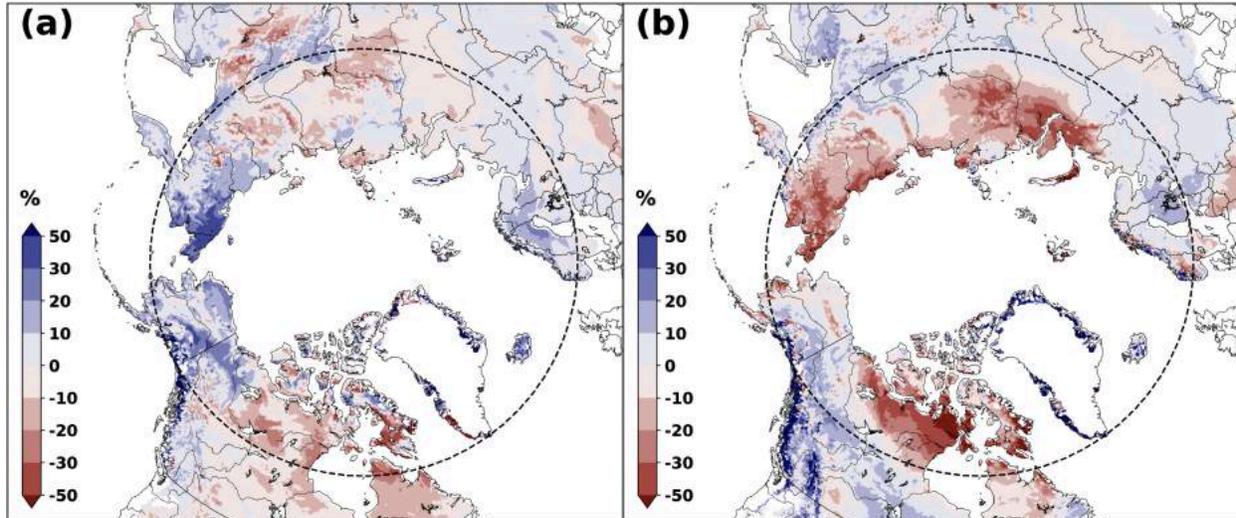
Fig. 2. Snow cover duration anomalies (% difference relative to average number of snow-free days) for the 2021/22 snow year: (a) snow onset (Aug-Jan); and (b) snow melt (Feb-Jul). Red (blue) indicates increased (decreased) snow-free days compared to the 1998/99 through 2017/18 mean. The dashed circle marks the latitude 60° N; land north of this defines Arctic land areas considered in this study. Source: NOAA IMS data record.

Snow mass and snow water equivalent

For Arctic regions as a whole, snow mass tends to peak annually during April, when snowfall has accumulated since the preceding autumn but before increasing temperatures during May and June lead to snow melt. Snow mass anomalies for April 2021 (Fig. 3; calculated by aggregating SWE across the Arctic land surface to measure the total mass of water stored by snow across the region) indicate snow accumulation was moderately above the 1991-2020 average across both the Eurasian and North American Arctic. Figure 4 shows the unaggregated SWE field to illustrate how this accumulation varied regionally from just before peak (March) through to the end of the melt period (June). Before May, both continents had mixed distributions of SWE: the northern regions of Arctic Eurasia had lower SWE than normal with higher than normal SWE located further south; in North America, the central Canadian Arctic and northern Alaska had lower than normal SWE while higher than normal accumulations were present south of the Brooks Range and across the Yukon Territory. Melt during May caused widespread reductions in SWE across the Eurasian Arctic and further reduced the snowpack where it was already lower than average in the North American Arctic, consistent with the pattern of SCD anomalies shown in Fig. 2. Similar to the previous year, the 2021/22 Arctic snow season saw a combination of increased snow accumulation (expressed as higher than average April snow mass in Fig. 3) but early snow melt (expressed by shorter than average snow melt periods in Fig. 2b) consistent with the expected changes to Arctic snow cover in a warmer Arctic (Meredith et al. 2019).
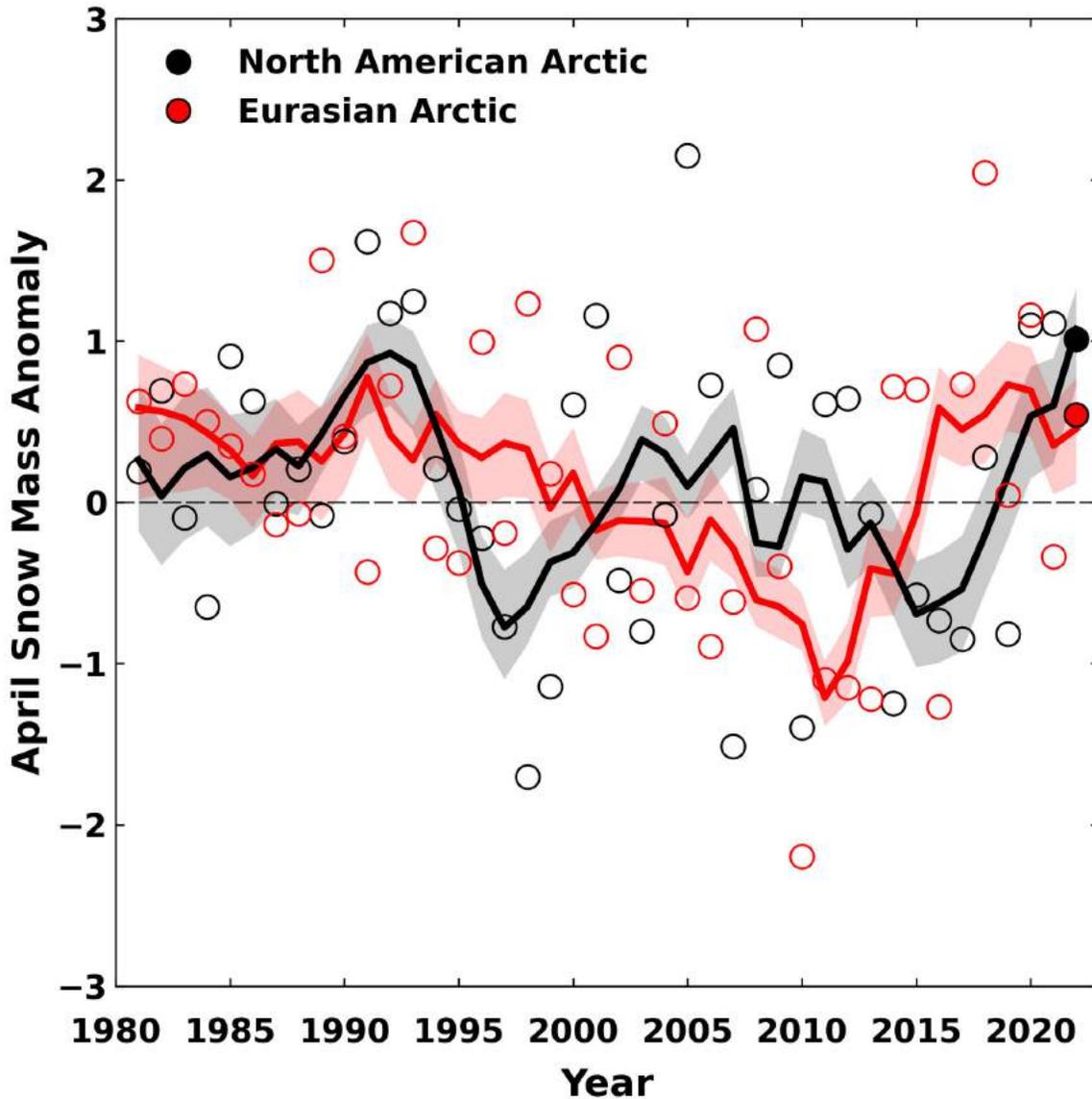
Fig. 3. Standardized April snow mass anomalies for Arctic land areas across the North American (black) and Eurasian (red) sectors. Anomalies (relative to the 1991-2020 average) represent the ensemble mean from a suite of four independent snow analyses (see Methods and data). Filled circles are used to highlight 2022 anomalies. Solid black and red lines depict 5-yr running means; shading depicts the spread among the running means of individual datasets. Source: snow analyses as described in Methods and data.
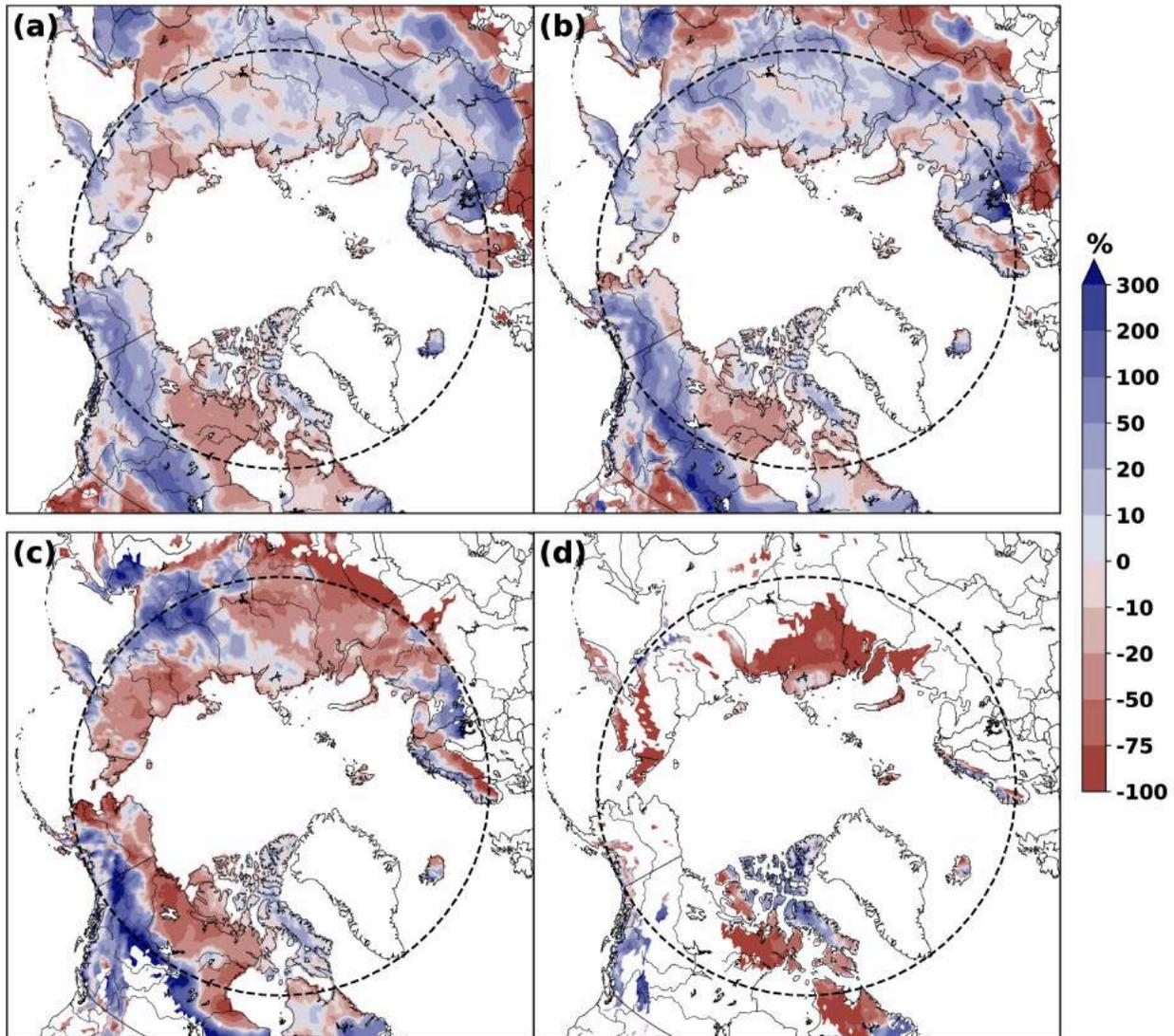
Fig. 4. Snow water equivalent (SWE) anomalies (% difference from the 1991-2020 average) in 2022 for (a) March, (b) April, (c) May, and (d) June. Anomalies represent the ensemble mean from a suite of four independent snow analyses (see Methods and data). The dashed circle marks the latitude 60° N.

Summary and long-term trends

In summary, snow accumulation during the 2021/22 winter was moderately above average across the Arctic. Despite that, spring snow extent was below normal, consistent with the last 15 years. Since 2008, North American June SCE has been below the long-term average every year, while Eurasian June SCE has been below the long-term average for all but 1 year. Long-term trends for total Arctic SCE, derived from the data presented in Fig. 1, are negative: -3.8 ±1.9% per decade, and -18.9 ± 6.6% per decade for May and June, respectively (1981-2022 trends relative to a baseline of 1991-2020). These trends are more strongly negative compared to a range of other sources, as discussed in Mudryk et al. (2017, 2020). The April trend in Arctic snow mass over the 1981-2022 period is more moderate, reflecting large interannual variability. Calculated from the data presented in Fig. 3, the snow mass trend is -1.4 ± 1.9% per decade.

Methods and data

Snow cover extent (SCE) anomalies are derived from the NOAA snow chart climate data record, which extends from 1967 to present (Estilow et al. 2015; Robinson et al. 2012). Monthly anomalies of total areal snow cover over land for a given Arctic sector (North America or Eurasia, > 60° N) are computed and standardized relative to the 1991-2020 period (each observation differenced from the mean and divided by the standard deviation and thus unitless).

Snow cover duration (SCD) fields are derived from the NOAA daily Interactive Multisensor Snow and Ice Mapping System (IMS) snow cover product (U.S. National Ice Center 2008). The IMS snow cover product is used for this analysis since the NOAA snow chart climate data record has spurious trends during autumn (Brown and Derksen 2013; Mudryk et al. 2017) that could alter SCD fields during the onset period. Anomalies in the total number of days with snow cover were computed separately for each half of the snow season: August 2021 to January 2022, referred to as "onset period," and February 2022 to July 2022, referred to as "melt period." IMS availability starts in 1998, so a 1999-2018 climatological period is used (including information from Aug-Dec 1998 for snow onset). Anomalies for each season are presented as percent differences from the climatological number of snow-free days. In the Arctic, this varies from approximately three months near 60° N, to approximately two months at 70° N, and decreases to less than a month over the Canadian Arctic Archipelago. Because the Arctic is generally always snow covered between November and April, Arctic region snow onset anomalies are indicative of conditions during September and October, while Arctic region snow melt anomalies are indicative of conditions during May and June.

Four snow water equivalent (SWE) analyses were used to generate multi-dataset SWE fields from March-June for the 1981-2022 period: (1) the European Space Agency Snow CCI SWE version 2 product derived through a combination of satellite passive microwave brightness temperatures and climate station snow depth observations (Luojus et al. 2022); (2) the Modern-Era Retrospective Analysis for Research and Applications version 2 (MERRA-2, GMAO 2015; Gelaro et al. 2017) daily SWE fields; (3) SWE output from the ERA5-Land analysis (Muñoz Sabater 2019); and (4) the physical snowpack model Crocus (Brun et al. 2013) driven by ERA5 meteorological forcing. Availability of climate station snow data limits the accuracy of the Snow CCI SWE product during May and June, hence we only use it during March and April. An approach using gridded products is required because in situ observations alone are too sparse to be representative of hemispheric snow conditions, especially in the Arctic where stations are particularly sparse. We consider multiple datasets because averaging multiple SWE products has been shown to be more accurate than individual datasets when validated with in situ observations (Mortimer et al. 2020). The ensemble-mean SWE field is used to calculate monthly SWE anomalies relative to the 1991-2020 period, which are presented as percent differences. For April, the SWE fields for each product are also aggregated across Arctic land regions (> 60° N) for both North American and Eurasian sectors to produce multiple estimates of April snow mass. These monthly snow mass values are used to calculate standardized anomalies relative to the 1991-2020 period for each data product. The standardized anomalies are then averaged to produce an ensemble-mean time series.

Acknowledgments

2020. Neither the European Commission nor ECMWF is responsible for any use that may be made of the Copernicus information or data it contains.

References

Brown, R. D., and C. Derksen, 2013: Is Eurasian October snow cover extent increasing? *Environ. Res. Lett.*, **8**, 024006, https://doi.org/10.1088/1748-9326/8/2/024006.

Brown, R., and Coauthors, 2017: Arctic terrestrial snow cover. In: Snow, Water, Ice and Permafrost in the Arctic (SWIPA) 2017. pp. 25-64. Arctic Monitoring and Assessment Programme (AMAP), Oslo, Norway.

Brun, E., V. Vionnet, A. Boone, B. Decharme, Y. Peings, R. Valette, F. Karbou, and S. Morin, 2013: Simulation of Northern Eurasian local snow depth, mass, and density using a detailed snowpack model and meteorological reanalyses. *J. Hydrometeor.*, **14**, 203-219, https://doi.org/10.1175/JHM-D-12-012.1.

Estilow, T. W., A. H. Young, and D. A. Robinson, 2015: A long-term Northern Hemisphere snow cover extent data record for climate studies and monitoring. *Earth Syst. Sci. Data*, **7**, 137-142, https://doi.org/10.5194/essd-7-137-2015.

Gelaro, R., and Coauthors, 2017: The Modern-era retrospective analysis for research and applications, Version 2 (MERRA-2). *J. Climate*, **30**, 5419-5454, https://doi.org/10.1175/JCLI-D-16-0758.1.

GMAO (Global Modeling and Assimilation Office), 2015: MERRA-2tavg1_2d_lnd_Nx:2d, 1-Hourly, Time-Averaged, Single-Level, Assimilation, Land Surface Diagnostics V5.12.4, Goddard Earth Sciences Data and Information Services Center (GESDISC), accessed: 16 August 2022, https://doi.org/10.5067/RKPHT8KC1Y1T.

Luojus, K., and Coauthors, 2022: ESA Snow Climate Change Initiative (Snow_cci): Snow Water Equivalent (SWE) level 3C daily global climate research data package (CRDP) (1979 - 2020), version 2.0. NERC EDS Centre for Environmental Data Analysis, accessed: 16 August 2022, https://doi.org/10.5285/4647cc9ad3c044439d6c643208d3c494.

Meredith, M., and Coauthors, 2019: Polar Regions. IPCC Special Report on the Ocean and Cryosphere in a Changing Climate, H. -O. Pörtner, and co-editors, in press, https://www.ipcc.ch/srocc/.

Mortimer, C., L. Mudryk, C. Derksen, K. Luojus, R. Brown, R. Kelly, and M. Tedesco, 2020: Evaluation of long-term Northern Hemisphere snow water equivalent products. *Cryosphere*, **14**, 1579-1594, https://doi.org/10.5194/tc-14-1579-2020.

Mudryk, L. R., P. J. Kushner, C. Derksen, and C. Thackeray, 2017: Snow cover response to temperature in observational and climate model ensembles. *Geophys. Res. Lett.*, **44**, 919-926, https://doi.org/10.1002/2016GL071789.

Mudryk, L., M. Santolaria-Otín, G. Krinner, M. Ménégoz, C. Derksen, C. Brutel-Vuilmet, M. Brady, and R. Essery, 2020: Historical Northern Hemisphere snow cover trends and projected changes in the CMIP6 multi-model ensemble. *Cryosphere*, **14**, 2495-2514, https://doi.org/10.5194/tc-14-2495-2020.

Muñoz Sabater, J., 2019: ERA5-Land hourly data from 1950 to present. Copernicus Climate Change Service (C3S) Climate Data Store (CDS), accessed 8 September 2022, https://doi.org/10.24381/cds.e2161bac.

Robinson, D. A., T. W. Estilow, and NOAA CDR Program, 2012: NOAA Climate Data Record (CDR) of Northern Hemisphere (NH) Snow Cover Extent (SCE), Version 1 [r01]. NOAA National Centers for Environmental Information, accessed: 16 August 2022, https://doi.org/10.7289/V5N014G9.

U.S. National Ice Center, 2008: IMS Daily Northern Hemisphere Snow and Ice Analysis at 1 km, 4 km, and 24 km Resolutions, Version 1. Boulder, Colorado USA. NSIDC: National Snow and Ice Data Center, accessed: 22 Aug 2022, https://doi.org/10.7265/N52R3PMC.

November 10, 2022

Precipitation

J. E. Walsh[1], S. Bigalke[2], S. A. McAfee[3], R. Lader[1], M. C. Serreze[4], and T. J. Ballinger[1]

[1]International Arctic Research Center, University of Alaska Fairbanks, Fairbanks, AK, USA
[2]Plants, Soils and Climate Department, Utah State University, Logan, UT, USA
[3]Department of Geography, University of Nevada Reno, Reno, NV, USA
[4]National Snow and Ice Data Center, University of Colorado Boulder, Boulder, CO, USA

Highlights

- Wetter-than-normal conditions predominated over much of the Arctic during the October 2021 through September 2022 water year, which was the 3rd wettest of the past 72 years.
- A significant increase in Arctic precipitation since the mid-20th century is now detectable across seasons and datasets.
- Significant increases in heavy precipitation events are detectable in the North Atlantic subarctic, while much of the central Arctic shows increases in consecutive wet days and decreases in consecutive dry days.

Introduction

Globally, precipitation over land has likely increased since 1950, consistent with increases in total atmospheric moisture (IPCC 2021). Climate models project an increase in Arctic precipitation, a transition from snowfall- to rainfall-dominated climates, and a higher frequency of heavy precipitation events (e.g., Sillmann et al. 2013; Kusunoki et al. 2015; McCrystall et al. 2021). However, previous assessments of precipitation and precipitation extremes across the Arctic over the period of observations have not shown coherent trends (Walsh et al. 2020). Results depend on the time period, the region examined, and the data sources (in situ gauge records, satellite retrievals, output from atmospheric reanalysis).

Gauge measurements of precipitation are especially problematic in the Arctic, where challenges include the sparse gauge network itself, which is unable to provide representative measurements in many northern regions. Moreover, precipitation gauges are known to suffer from undercatch of snow in cold, windy conditions (Ye et al. 2021). For this reason, gridded reanalysis products are increasingly used to assess variations and the expected emergence of trends in Arctic precipitation. For example, Yu and Zhong (2021) and White et al. (2021) used the ERA-Interim and ERA5 reanalyses, respectively, to show that trends of Arctic precipitation vary regionally and seasonally over the past few decades. In this essay, we use the more recent and more highly regarded ERA5 reanalysis to provide an annual and seasonal overview of the 2021/22 water year (October 2021-September 2022) Arctic precipitation anomalies and place these anomalies into a context of recent and ongoing changes.

2021/22 water year precipitation at a glance

The Arctic experienced notable precipitation anomalies in the 2021/22 water year. The outstanding features were (1) a predominance of positive seasonal departures from the climatological means and (2) shorter-duration heavy precipitation that broke existing records at various locations within the Arctic. Overall, the pan-Arctic (north of 60° N) precipitation for the 2021-22 water year in the ERA5 reanalysis was the 3rd highest since 1950, trailing only the 2019/20 and 2017/18 water years. The Arctic autumn, winter, and summer all ranked among the 10 wettest of their corresponding seasons in the post-1950 period.

Figure 1 shows the ERA5-derived seasonal departures from the 1991-2020 means. For the October-December (OND) period, large positive departures are apparent in the Bering Sea extending into Interior Alaska and also along the western coast of Norway. Weaker positive departures are the rule over much of northern Russia and northeastern Canada. The Alaska anomalies are consistent with an anomalous ridge of high pressure south of the Aleutian Islands, with a corresponding eastward flux of moisture across the Bering Sea into Alaska (see essay *Surface Air Temperature*, Fig. 3a). The positive departures over northern Asia were associated with below normal pressures over the region and may have been augmented by enhanced moisture availability during the increasingly long open water seasons in the seas north of Eurasia. Among notable heavy events, Bergen, Norway broke its October precipitation record and new records for December precipitation were set at Fairbanks in Interior Alaska and at Nome on the western Alaska coast. Fairbanks also experienced a high-impact freezing rain event with more than 3 cm of total precipitation (rain plus melted snow) on 26 December, nearly twice the monthly average.
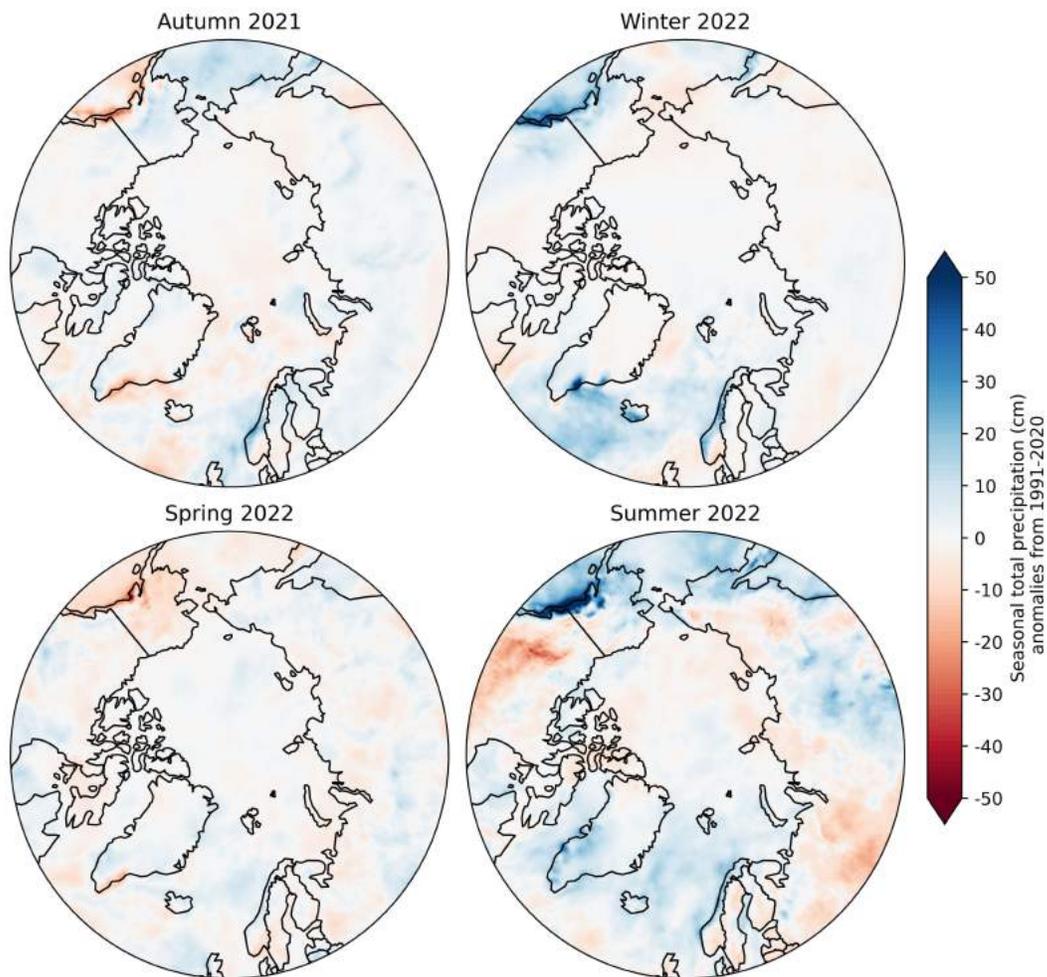
Fig. 1. Seasonal departures of precipitation from the 1991-2020 climatological means for autumn 2021 (OND, upper left), winter 2022 (JFM, upper right), spring 2022 (AMJ, lower left), and summer 2022 (JAS, lower right). Blue shades denote above-normal precipitation, red shades denote below-normal precipitation. Data source: ERA5 reanalysis.

The primary features of the January-March (JFM) pattern are broad areas of positive precipitation departures from normal in the North Atlantic subarctic, the Gulf of Alaska, and the southeastern Alaska panhandle. The positive departures over Alaska link to anomalously high pressure over western Canada and low pressure anomalies farther offshore (see essay *Surface Air Temperature*, Fig. 3b). The positive precipitation departures extending from Greenland to Norway were attributable to winter storm events. Seasonally-averaged sea level pressures were more than 5 hPa below average from northeastern Canada to northern Europe, indicative of an active cyclone pattern in the Atlantic sector of the Arctic. A late-January storm set 32 records for heavy precipitation in Norway and contributed to the positive seasonal departures there in the winter panel of Fig. 1. The autumn and winter precipitation anomalies point to the importance of large-scale circulation in controlling the regional distribution of Arctic precipitation.

Spring is normally dry in the Arctic, and the April-June (AMJ) period of 2022 was characterized by generally small departures from the relatively low seasonal means (Fig. 1). Correspondingly, the atmospheric circulation anomalies were relatively weak (see essay *Surface Air Temperature*, Fig. 3c). For the 60-90° N region as a whole, AMJ precipitation was very close to the 1951-2022 median. A notable feature of Fig. 1's spring panel is the broad area of negative (dry) departures extending across the North American subarctic from northeastern Canada to Alaska. Positive sea level pressure anomalies coincided with this broad band of dry conditions (see essay *Surface Air Temperature*, Fig. 3c). The dry conditions are especially apparent in central and southern Alaska, where all three months (April-June) had well below-normal precipitation. Drought conditions developed during May over southwestern Alaska and northern Cook Inlet. Moderate drought conditions expanded into much of Interior Alaska in June, setting the stage for severe wildfires in the early summer season.

Finally, the summer (JAS) was characterized by contrasting extremes (Fig. 1), with wet conditions predominating. Overall, the Arctic's summer was the 3rd wettest of the past 72 years. Southeastern and southern Alaska were exceptionally wet with some locations recording their wettest JAS period on record. Western Alaska experienced heavy rain and coastal flooding from ex-typhoon Merbok in late September. New monthly records for July rainfall were set at various locations in northern Norway, including Holt, Harstad, Grunnfarnes, and Skibotn. However, very dry conditions prevailed over parts of northern Canada and northeastern Europe, contributing to low water levels in rivers of eastern Europe.

Historical variations and trends

Figure 2 compares time series of seasonal precipitation from ERA5 and the station-based dataset of the Global Precipitation Climatology Center (GPCC) during 1950-2021. While there is considerable interannual variability, these variations are generally consistent across the two datasets. Both show increases of about 10% in the yearly total precipitation. Increases in both time series are smallest in the summer and most pronounced for winter. In all cases, the trends are statistically significant at the 0.01 level. The consistency of the trends across seasons and datasets argues that precipitation over the Arctic as a whole is increasing, as expected from climate model simulations. For the more recent period 1979-2021, when ERA5's assimilation of satellite data increased, the trends in ERA5 (and also GPCC) precipitation are even larger and statistically significant for the full water year and for all seasons except AMJ. The AMJ trends for 1979-2021 are weaker than for 1950-2021 and insignificant in both datasets.
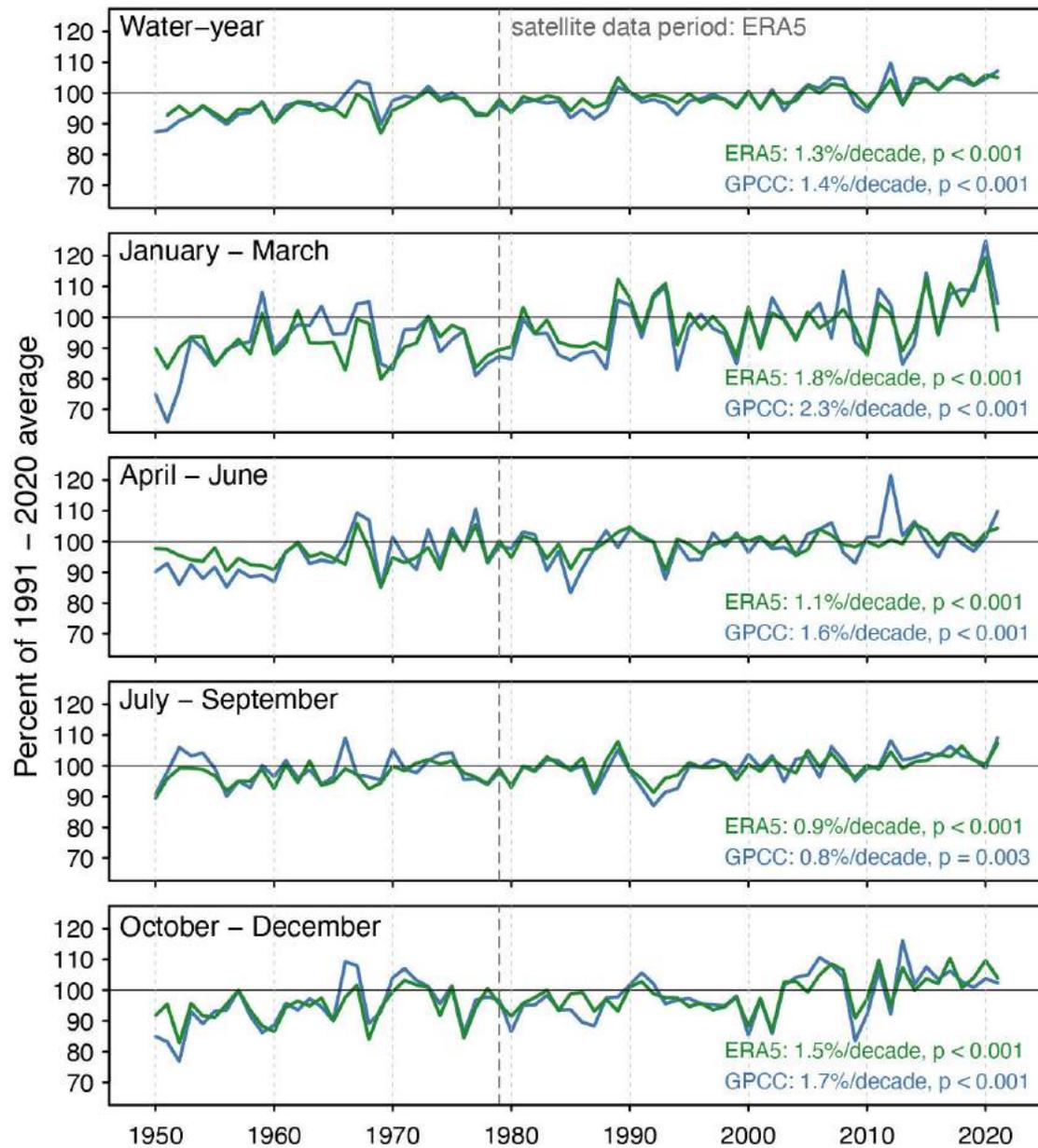
Fig. 2. Time series of Arctic (60-90° N) precipitation for the water-years ending in 1951 through 2021 and for each 3-month season, expressed as a percentage of the 1991-2020 average. Results are from ERA5 (green lines) and GPCC 1.0° data (blue lines). GPCC values are for land only; ERA5 values are for land + ocean. Seasonal time series are for JFM, AMJ, JAS, and OND in 2nd through 5th panels. Linear slopes and significance levels are shown in lower right of each panel.

The spatial patterns of linear trends based on ERA5 are presented in Fig. 3. While there are scattered areas of decrease (brown shading) in every season, areas of increase (green shading) predominate. Consistent with the area-averaged trends in Fig. 2, nearly all areas of statistically significant change are increases. Increased precipitation is especially pronounced in the Bering Sea and southern Alaska during autumn, the subpolar North Atlantic during winter, and southeastern Alaska during winter and summer. The southwestern coast of Norway is dominated by increases in all seasons. A notable area of decrease is the Bering Sea during spring and summer.
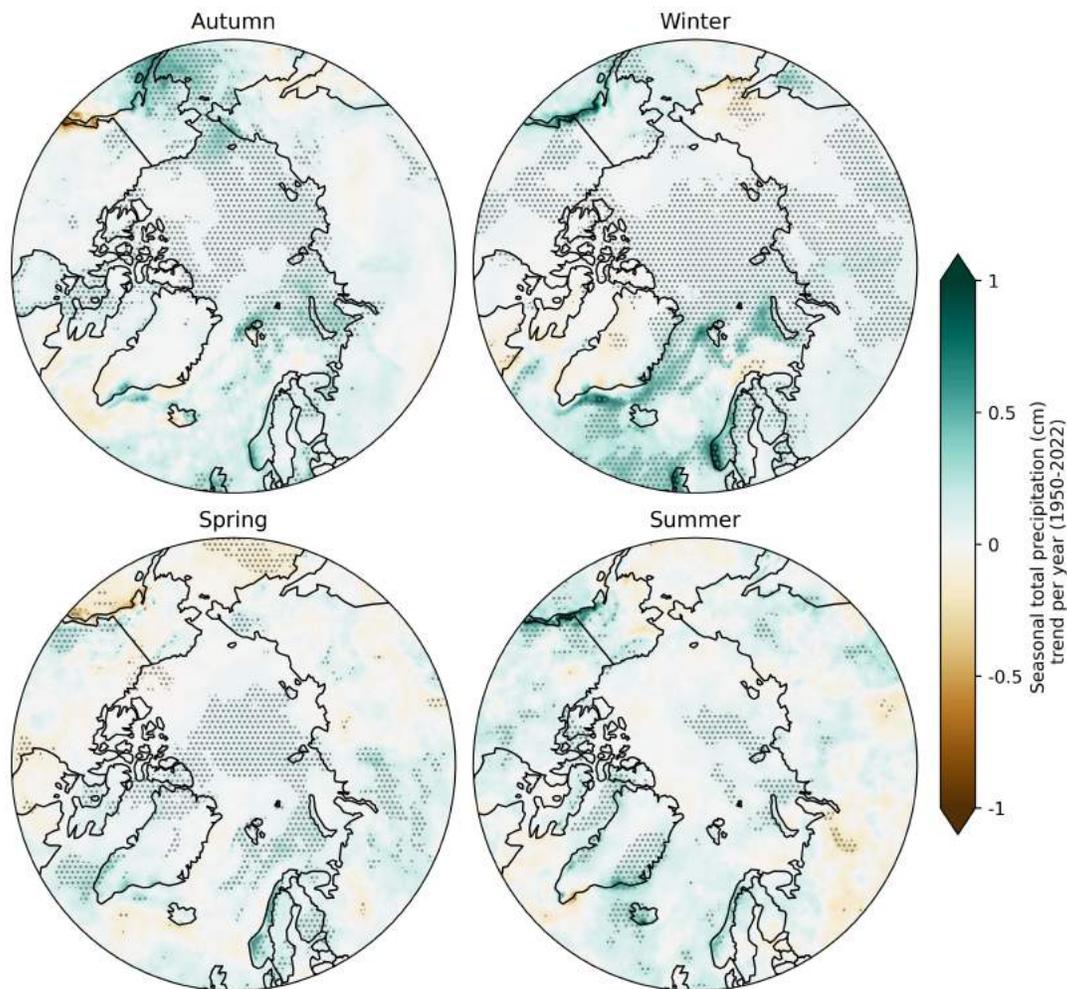
Fig. 3. Seasonal precipitation trends (cm/year) derived from ERA5 reanalysis. Seasons are referenced to the start of the water year: Oct-Dec (upper left), Jan-Mar (upper right), Apr-Jun (lower left), Jul-Sep (lower right). Green shades denote increases and brown shades denote decreases. Stippling denotes trends significant at the 0.05 level.

Indicators of precipitation extremes

Heavy precipitation events based on ERA5, as captured by the yearly maximum 1-day (R×1) and 5-day precipitation (R×5), show no coherent trends over most of the Arctic, although large and significant increases are apparent over eastern Greenland, Svalbard, and northern Norway (Fig. 4). These regions also show positive trends in total precipitation (Fig. 3), indicating that heavy precipitation events are contributing to the overall increase in precipitation in these areas. By contrast, the annual maximum number of consecutive wet days (CWD) shows a broad area of increase from Svalbard eastward through the Siberian seas to the Chukchi Sea northwest of Alaska. This area of increase in CWD generally coincides with the area of reduced sea ice coverage during the warm season. Correspondingly, the annual maximum number of consecutive dry days (CDD) has decreased over much of the central Arctic as well as the Siberian shelf seas and north-central Siberia.
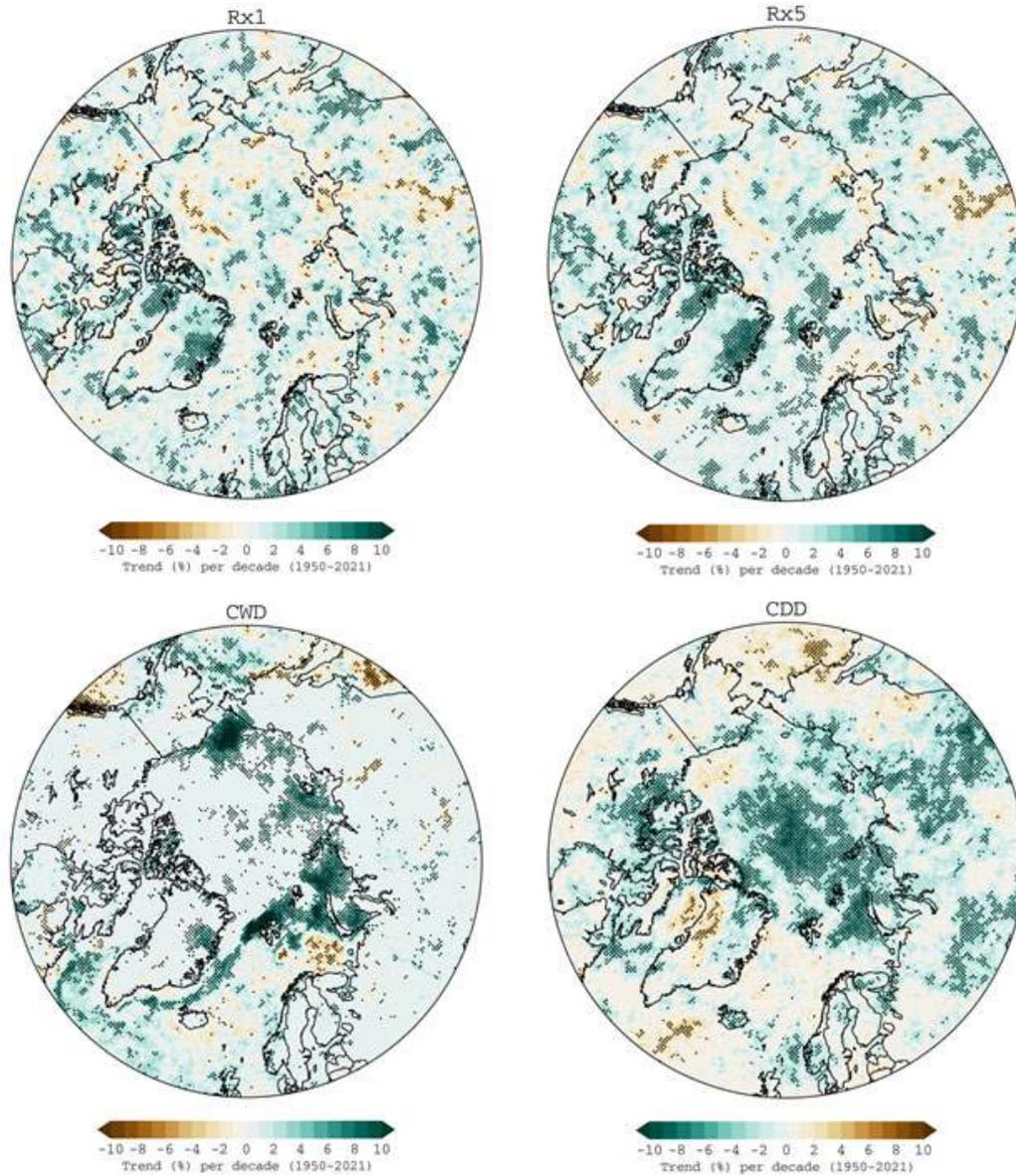
Fig. 4. Trends of daily extreme precipitation indices over the period 1950-2021 from ERA5. Plots are shown for yearly maximum 1-day total precipitation, R×1 (upper left), yearly maximum 5-day amount, R×5 (upper right), yearly maximum number of consecutive wet days, CWD (lower left), and yearly maximum number of consecutive dry days, CDD (lower right). Green shades denote trends toward wetter extremes, brown shades denote trends towards drier extremes. Stippling denotes significance at the 0.05 level.

Methods and data

Because of the challenges of gauge measurements in the Arctic, we make use of gridded precipitation fields from both the ERA5 atmospheric reanalysis of the European Centre for Medium Range Weather Forecasts (ECMWF) (Hersbach at al. 2020) and the Global Precipitation Climatology Centre's GPCC V. 2022 (Becker et al. 2013). ERA5 data are available from January 1950 onwards, but the quality of the output is more reliable starting in 1979 (Hersbach et al. 2020), after which modern satellite data are

assimilated into the analysis and forecast system. ERA5 is the latest atmospheric reanalysis effort and performs slightly better than other atmospheric reanalyses at matching observed precipitation totals from extreme events in the eastern Canadian Arctic (Loeb et al. 2022). We use the entire 1950-2022 record to examine seasonal anomalies of the 2021-2022 water year, linear trends in total precipitation by season, and trends in extreme Arctic precipitation. Given the model-derived nature of ERA5, comparisons are made with the GPCC's Full Data Product, a monthly gridded gauge-based product available from 1891-2020 (Schneider et al. 2022). A merged product that uses satellite retrievals is also available, but retrievals in the Arctic are known to be problematic. Statistical significance of the precipitation trends computed from both sources was evaluated using a Theil-Sen test (Hurtado 2020).

Acknowledgments

References

Becker, A., P. Finger, A. Meyer-Christoffer, B. Rudolf , K. Schamm, U. Schneider, and M. Ziese, 2013: A description of the global land-surface precipitation data products of the Global Precipitation Climatology Centre with sample applications including centennial (trend) analysis from 1901-present. *Earth Syst. Sci. Data*, **5**(1), 71-99, https://doi.org/10.5194/essd-5-71-2013.

Hersbach, H. B., and Coauthors, 2020: The ERA5 global reanalysis. *Q. J. Roy. Meteor. Soc.*, **146**, 1999-2049, https://doi.org/10.1002/qj.3803.

Hurtado, S. I., 2020: RobustLinearReg: Robust Linear Regressions. R package version 1.2.0, https://CRAN.R-project.org/package=RobustLinearReg.

IPCC, 2021: Climate Change 2021: The Physical Science Basis. Contribution of Working Group I to the Sixth Assessment Report of the Intergovernmental Panel on Climate Change [Masson-Delmotte, V., et al. (eds.)]. Cambridge University Press, Cambridge, United Kingdom and New York, NY, USA, pp. 2-6, https://doi.org/10.1017/9781009157896, in press.

Kusunoki, S., R. Mizuta R., and M. Hosaka, 2015: Future changes in precipitation intensity over the Arctic projected by a global atmospheric model with a 60-km grid size. *Polar Sci.*, **9**, 277-292, https://doi.org/10.1016/j.polar.2015.08.001.

Loeb, N. A., A. Crawford, J. C. Stroeve, and J. Hanesiak, 2022: Extreme precipitation in the eastern Canadian Arctic and Greenland: An evaluation of atmospheric reanalyses. *Front. Env. Sci.*, **10**, 866929, https://doi.org/10.3389/fenvs.2022.866929.

McCrystall, M., J. Stroeve, M. C. Serreze, B. C. Forbes, and J. Screen, 2021: New climate models reveal faster and larger increases in Arctic precipitation than previously projected. *Nat. Commun.*, **12**(1), 6765, https://doi.org/10.1038/s41467-021-27031-y.

Schneider, U., P. Finger, E. Rustemeier, M. Ziese, and S. Hänsel, 2022: Global precipitation analysis products of the GPCC, https://opendata.dwd.de/climate_environment/GPCC/PDF/GPCC_intro_products_v2022.pdf.

Sillmann J., V. V. Kharin, F. W. Zwiers, X. Zhang, and D. Bronaugh, 2013: Climate extremes indices in the CMIP5 multimodel ensemble: Part 2. Future climate projections. *J. Geophys. Res.-Atmos.*, **118**, 2473-2493, https://doi.org/10.1002/jgrd.50188.

Walsh, J. E., T. J. Ballinger, E. S. Euskirchen, E. Hanna, J. Mård, J. E. Overland, H. Tangen, and T. Vihma, 2020: Extreme weather and climate events in northern areas: A review. *Earth-Sci. Rev.*, **209**, 103324, https://doi.org/10.1016/j.earscirev.2020.103324.

White, J., J. E. Walsh, and R. L. Thoman, Jr., 2021: Using Bayesian statistics to detect trends in Alaskan precipitation. *Int. J. Climatol.*, **41**(3), 2045-2059, https://doi.org/10.1002/joc.6946.

Ye, H., D. Yang, A. Behrangi, S. L. Stuefer, X. Pan, E. Mekis, Y. Dibike, and J. E. Walsh, 2021: Precipitation Characteristics and Changes. Chapter 2 in Arctic Hydrology, Permafrost and Ecosystems (D. Yang and D.L. Kane, Eds.), Springer Nature Switzerland, 914 pp., https://doi.org/10.1007/978-3-030-50930-9_2.

Yu, L., and S. Zhong, 2021: Trends in Arctic seasonal and extreme precipitation in recent decades. *Theor. Appl. Climatol.*, **145**, 1541-1559, https://doi.org/10.1007/s00704-021-03717-7.

January 6, 2023

Greenland Ice Sheet

**T. A. Moon[1,2], K. D. Mankoff[1,2], R. S. Fausto[3], X. Fettweis[4], B. D. Loomis[5],
T. L. Mote[6], K. Poinar[7], M. Tedesco[8,9], A. Wehrlé[10], and C. D. Jensen[11]**

[1]National Snow and Ice Data Center, University of Colorado Boulder, Boulder, CO, USA
[2]Cooperative Institute for Research in Environmental Sciences, University of Colorado Boulder, Boulder, CO, USA
[3]Geological Survey of Denmark and Greenland, Copenhagen, Denmark
[4]SPHERES Research Unit, University of Liège, Liège, Belgium
[5]Goddard Space Flight Center, NASA, Greenbelt, MD, USA
[6]Department of Geography, University of Georgia, Athens, GA, USA
[7]Department of Geology, University at Buffalo, Buffalo, NY, USA
[8]Lamont-Doherty Earth Observatory, Columbia University, Palisades, NY, USA
[9]Goddard Institute of Space Studies, NASA, New York, NY, USA
[10]Department of Geography, University of Zurich, Zurich, Switzerland
[11]Danish Meteorological Institute, Copenhagen, Denmark

Highlights

- The Greenland Ice Sheet total mass change for 1 September 2021 through mid-August 2022 was -146 ± 64 Gt, equivalent to ~0.4 mm of sea level rise and representing the 25th consecutive year of ice loss.
- Cold temperatures delayed summer ice loss, yet the ice sheet still experienced unprecedented melt events during 2022.
- During September 2022, the Greenland Ice Sheet experienced unprecedented late-season melt events, including surface melt conditions across 36% of the ice sheet surface on 3 September, including at Summit Station (3216 m above sea level in the ice sheet interior).

Introduction

Ice loss from the Greenland Ice Sheet has immediate and global influence on sea level rise, with impacts including coastal erosion, saltwater inundation of freshwater resources, and increased flooding frequency. In addition, ice loss freshens ocean waters and alters ecosystems (Morlighem et al. 2017; Hopwood et al. 2020). The ice sheet has now lost mass every year since 1998 (Mouginot et al. 2019). Annual *total mass change* determines the ice sheet's contribution to global sea level for each mass balance year (1 September through 31 August). The 2021/22 mass balance year (including data through mid-August) recorded -146 ± 64 Gt ice loss as measured by the GRACE-FO satellite (Fig. 1; see Methods and data), equivalent to ~0.4 mm of sea level rise, not including ongoing thermal expansion. The 2021/22 mass balance year had ~115 Gt less loss than the April 2002-August 2022 average of -261 ± 11 Gt/yr.
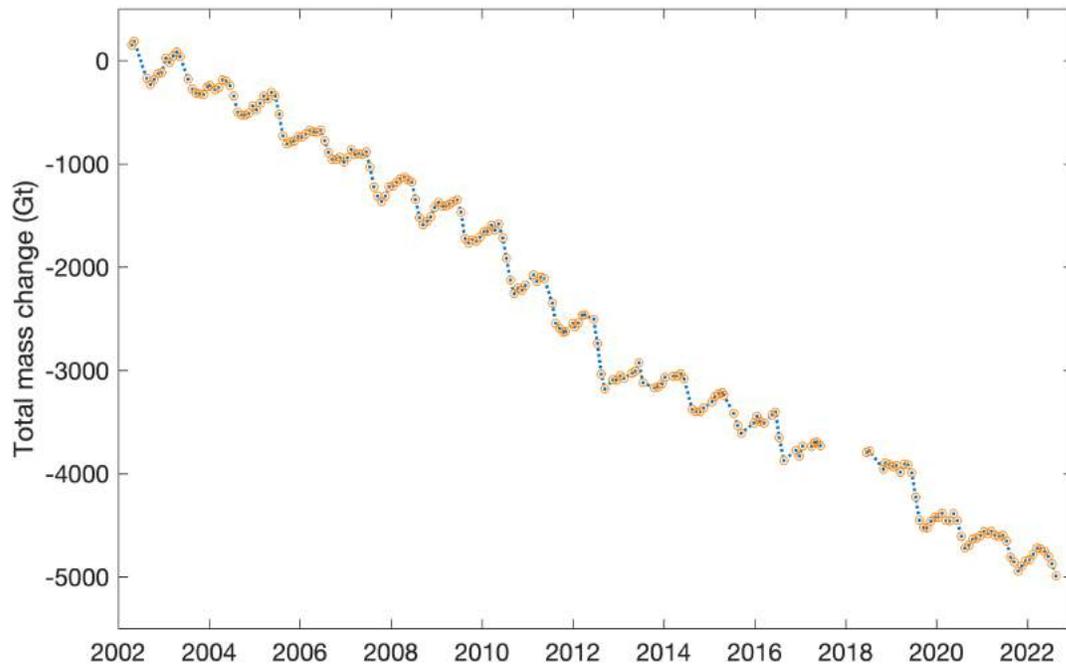
Fig. 1. Total mass change (Gt) of the Greenland ice sheet from April 2002 to mid-August 2022 determined from GRACE (2002-17) and GRACE-FO (2018-Present) satellite data.

The total mass change of the Greenland Ice Sheet is the sum of the *surface mass balance*, which sums the gains from accumulated snow and the losses via surface melt and runoff, and the *solid ice discharge*, which is the loss of solid ice at the ice sheet edges via iceberg calving. Below, we provide details on surface mass balance and solid ice discharge for the 2021/22 mass balance year and highlight unusual September 2022 melt events.

Surface mass balance

The total surface mass balance of the ice sheet is determined through interactions between weather events (e.g., temperature and precipitation) and ice sheet surface condition. Here, we focus on in-situ and satellite observations that give insight into total surface mass balance: surface temperatures and melt, ice sheet surface character, and in-situ ice loss (ablation) measurements.

Surface temperature observations at 15 terrestrial DMI weather stations (see Methods and data) recorded near or above average temperatures throughout the balance year. Temperature anomalies equaled or exceeded one standard deviation at all stations in autumn 2021 (September-November) and winter 2021/2022 (December-February), while spring 2022 (March-May) anomalies were mixed. The 2022 summer began cold, postponing the start of the ablation season. On-ice PROMICE automated weather stations recorded surface temperatures below one standard deviation for June for the whole ice sheet, while July and August were within ±1 standard deviation.

The moderate overall temperatures were associated with mostly moderate surface melt across the ice sheet (Fig. 2). Only one summer melt event extended to an area larger than 600,000 km^2 (37%), with melt conditions on 18 July reaching across 42% (688,000 km^2) of the surface, ranking within the largest

10% of events observed during 1991-2020. Additional anomalous melt events occurred after the end of the mass balance year, in September, and are discussed later. Regionally, the southwest and northeast experienced more melt days as compared to the 1991-2020 average, with fewer melt days for the northwest and southeast (Fig. 2).
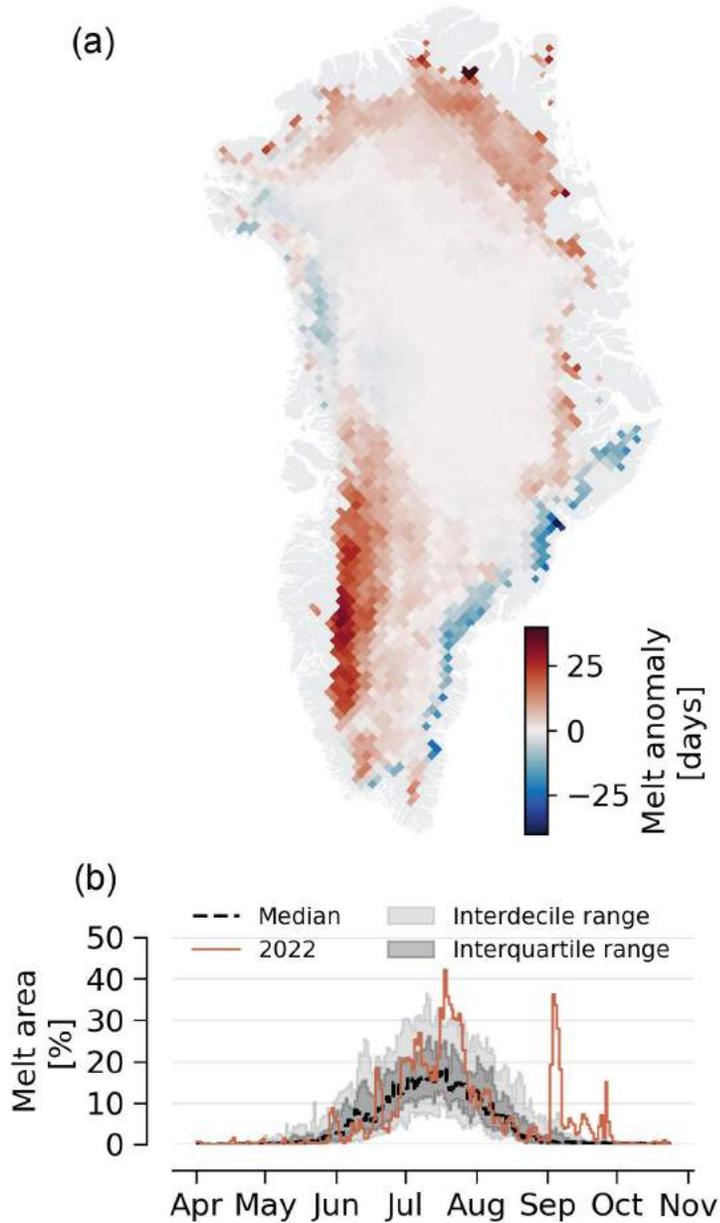
Fig. 2. (a) 2022 melt anomaly (in number of melting days; including data through 24 October 2022) with respect to the 1991-2020 reference period, (b) Surface melt extent as a percentage of the ice sheet area during 2022 (solid red). Data derived from SSMIS satellite data.

One important indicator of the ice sheet surface character is the surface broadband albedo, which is a measure of the relative amount of energy reflected by the surface in all wavelengths. A brighter (higher albedo) surface, such as with fresh snow cover, reduces solar radiation absorption and therefore reduces melt potential. In contrast, a darker (lower albedo) surface absorbs more solar radiation and

may enhance melt. The transition from a snow-covered surface to a bare glacial ice surface creates an especially strong step-change in surface broadband albedo (Ryan et al. 2019; Wehrlé et al. 2021).

Greenland Ice Sheet albedo measurements for June through August 2022 indicate that most of the ice sheet experienced anomalously high albedo (brighter surface) (Fig. 3a,b). The summer bare ice area measurements reflect the unusual melt event in early September, which brought the bare ice area up to its maximum extent of 136,800 km^2 (~8%) on 9 September, a month later than the 2017-21 average (Fig. 3c).
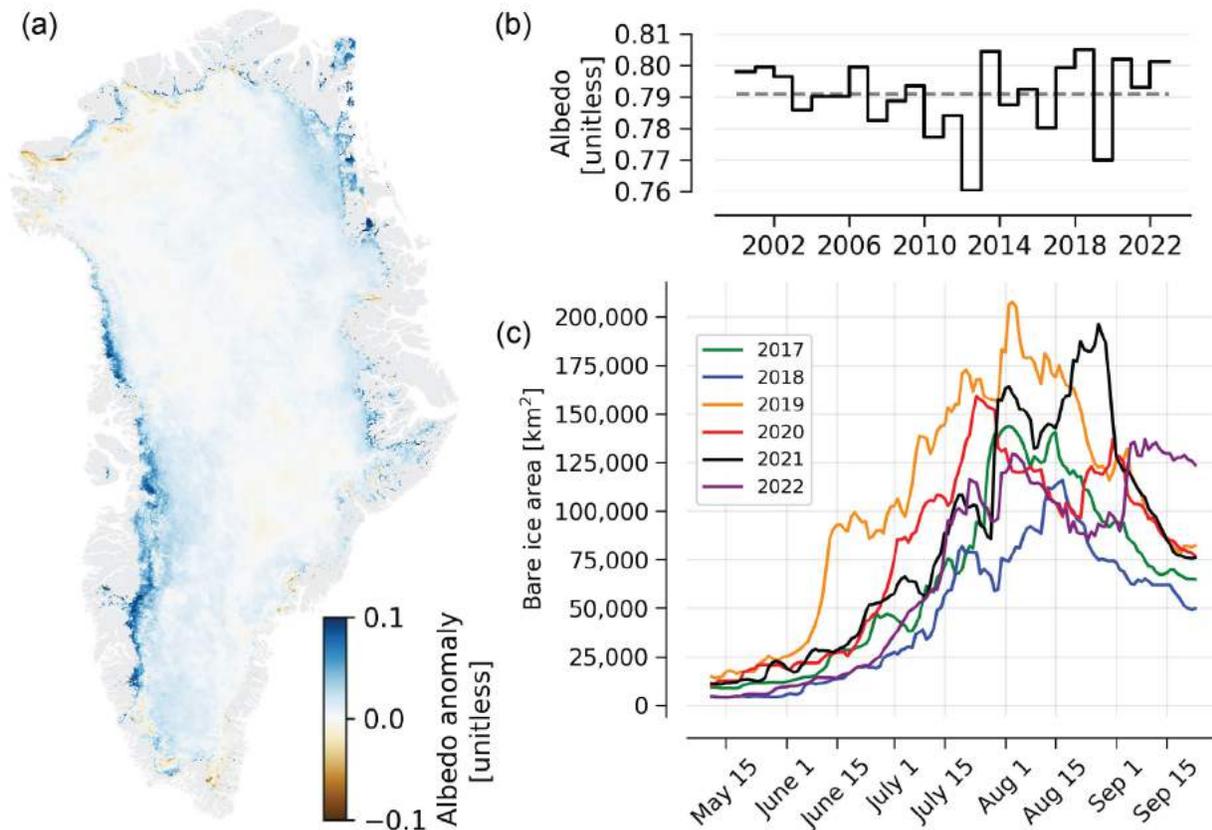
Fig. 3. (a) Albedo anomaly for June through August 2022 from Sentinel-3, relative to a 2017-21 reference period, (b) Time series for average Greenland ice sheet summer albedo from MODIS, (c) Bare ice area from Sentinel-3.

In-situ ablation measurements provide a sense of the integrated outcomes of the season's surface conditions and weather events. For the ablation season measured between 1 January and 25 August 2022, PROMICE measurements around the ice sheet margin indicate substantial positive and negative anomalies, depending on region. Summing across the full ice sheet, however, regional variations broadly offset each other, with average ablation for the ice sheet as a whole (Fig. 4).
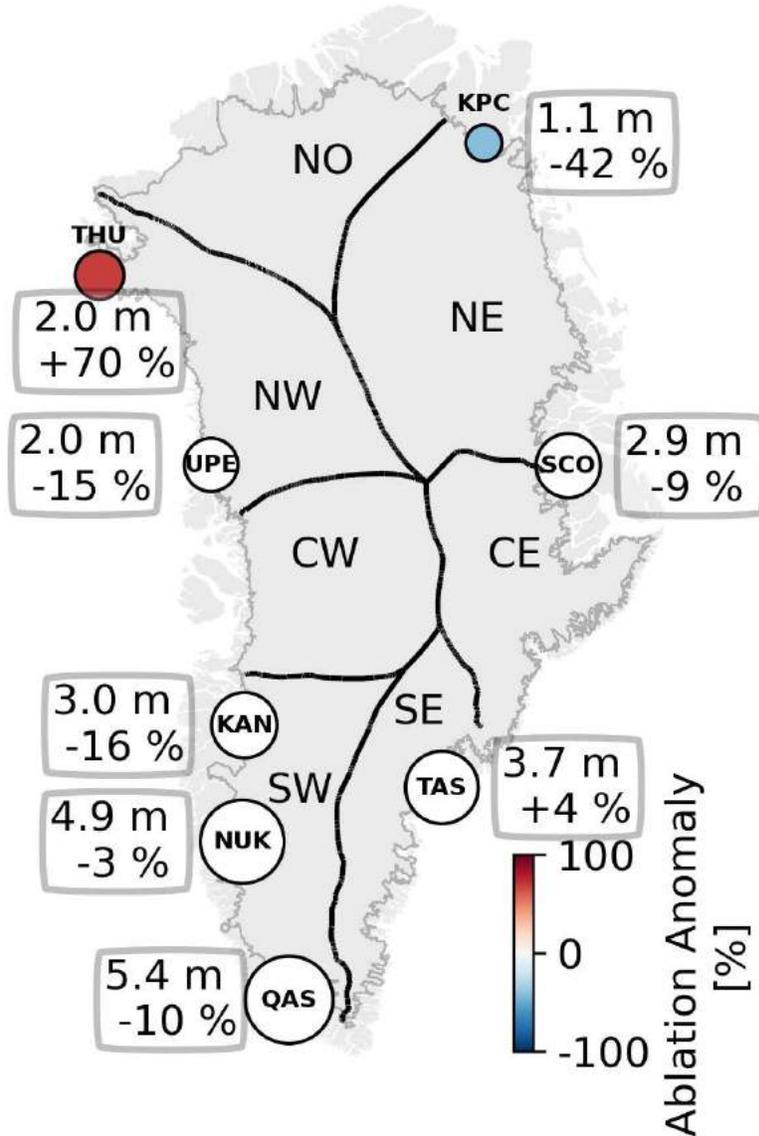
Fig. 4. Net ablation for 1 January through 25 August 2022 measured by PROMICE weather transects and referenced to the 1991-2020 standard period. Circle size is scaled to the ablation in m of ice equivalent, and color scaled with anomaly value. White circles indicate anomaly values not exceeding methodological and measurement uncertainty. Stations are: Thule (THU), Upernavik (UPE), Kangerlussuaq (KAN), Nuuk (NUK), Qassimuit (QAS), Tasiliiq (TAS), Scorebysund (SCO), and Kronprins Christians Land (KPC). The regions North (NO), Northeast (NE), Northwest (NW), Central East (CE), Central West (CW), Southeast (SE), and Southwest (SW) are referenced in Fig. 5.

Solid ice discharge

Along with loss at the ice sheet surface via melt, the Greenland Ice Sheet loses ice through iceberg calving. This *solid ice discharge* occurs year-round from marine-terminating glaciers that act as conveyor belts to move ice from the ice sheet interior to the ocean (see essay *Lessons from Oceans Melting*

Greenland). Measurements of solid ice discharge (see Methods and data) provide information on how ice sheet dynamics may be changing.

For 1991 through 2020, the average total discharge was ~471 ± 44 Gt per year, while average discharge during 2010 through 2019 was ~485 ± 46 Gt per year (Fig. 5). Solid ice discharge through October 2022 averaged 484 ± 45 Gt per year, with the largest contributions from the southeast, followed by the northwest. Ice discharge responds to changes slowly and is therefore a more stable mass balance term, relative to surface mass balance (Mankoff et al. 2021).
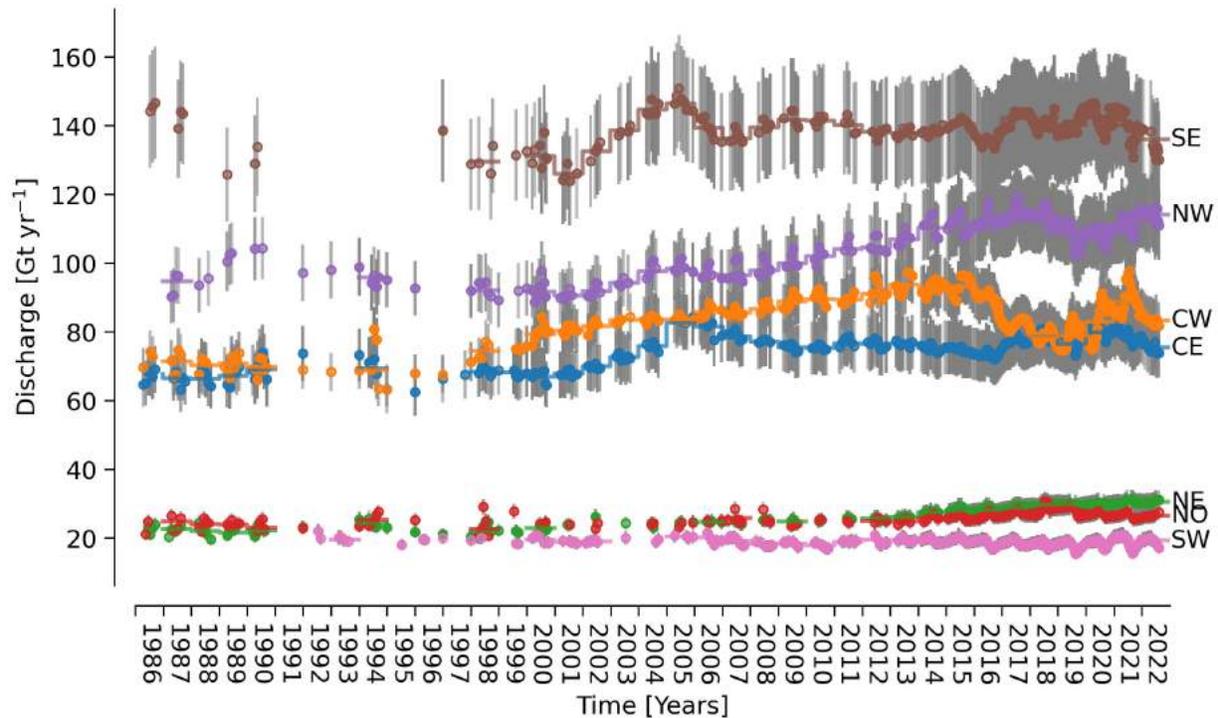
Fig. 5. Solid ice discharge (Gt per year; gray bars show ±10% uncertainty range) based on PROMICE velocity and BedMachine ice thickness (Mankoff et al. 2020). Regions for solid ice discharge shown in Fig. 4.

Unusual September melt events

Throughout this update we focused on the standard mass balance year, September 2021 through August 2022. September 2022, however, was very unusual. PROMICE weather stations recorded monthly temperature anomalies more than +1 standard deviation above the 1991-2020 reference period north of 65° latitude and above +2 standard deviations south of 65° latitude. Six DMI weather stations had record-breaking mean monthly September temperatures, including at Summit Station.

The ice sheet also experienced melt events that are unprecedented in the 44-year observational record. In early September, high pressure that was centered over the south of Greenland on 2 September brought a very warm and wet air mass northward from the central North Atlantic Ocean to along the ice sheet's west side. This pulse of warm air then flowed eastward over the top of the ice sheet on 3 September, when +0.4°C was recorded at Summit Station, 3216 m above sea level, and 36% (592,000 km^2) of the ice sheet experienced melt. The air mass then descended onto the eastern side of the ice sheet on 4-5 September, triggering further surface melt. In addition to bringing a very warm air mass, with daily temperature anomalies reaching +20°C, this event was accompanied by heavy rain and liquid

water clouds (which enhance surface melt) over the western ablation zone. PROMICE weather station measurements detected rainfall at South Dome (2900 m above sea level) and substantial rain in coastal west Greenland (e.g., 32 mm within 24 hours at a QAS transect station, see Fig. 4). Later, on 26 September, the Greenland Ice Sheet experienced record melt extent for the second half of September as a result of the remnants of Hurricane Fiona, when ~15% (245,000 km^2) of the surface experienced melting.

Both melt events were followed by below-freezing temperatures, refreezing meltwater at the top of the snowpack and favoring the formation of ice lenses. By creating a barrier to downward meltwater percolation, ice lenses reduce the snowpack's capacity to retain new meltwater in future summers (MacFerrin et al. 2019). Thus, we must wait to observe the full influence that these September melt events will have on Greenland Ice Sheet mass loss.

Methods and data

Total mass change is measured indirectly by the GRACE (Gravity Recovery and Climate Experiment, 2002-17) and GRACE-FO (Follow On, 2018-present) satellite missions by detecting gravity anomalies (Fig. 1). Technical Notes are hosted at https://podaac-tools.jpl.nasa.gov/drive/files/allData.

Direct weather observations are provided via 15 Danish Meteorological Institute (DMI) weather stations with records beginning from 1784 (Nuuk) to 1991 (Summit) and 8 automatic weather station transects from the Programme for Monitoring of the Greenland Ice Sheet (PROMICE) at the Geological Survey of Greenland and Denmark (GEUS). DMI stations are located on land, with Summit data provided by NOAA GEOSummit. PROMICE transects, located on the ice sheet, also provide surface ablation (following van As et al. 2016; Fig. 4). A high temporal resolution solid ice discharge product is also generated by PROMICE using ice velocity (from MEaSUREs and Sentinel-1), ice thickness (from BedMachine v4), and ice density (following Mankoff et al. 2020; Fig. 5). Surface melt duration and extent measurements are derived from daily Special Sensor Microwave Imager/Sounder (SSMIS) 37 GHz, horizontally polarized passive microwave radiometer satellite data (Mote 2007; Fig. 2).

NASA MODIS satellite data provide multi-decadal albedo monitoring (Box et al. 2017). The Sentinel-3 SICE product is used to monitor bare ice area (Kokhanovsky et al. 2020; Wehrlé et al. 2021; Fig. 3).

Acknowledgments

References

Box, J. E., D. van As, and K. Steffen, 2017: Greenland, Canadian and Icelandic land ice albedo grids (2000-2016). *GEUS Bull.*, **38**, 53-56, https://doi.org/10.34194/geusb.v38.4414.

Hopwood, M. J., and Coauthors, 2020: Review article: How does glacier discharge affect marine biogeochemistry and primary production in the Arctic? *Cryosphere*, **14**, 1347-1383, https://doi.org/10.5194/tc-14-1347-2020.

Kokhanovsky, A., J. E. Box, B. Vandecrux, K. D. Mankoff, M. Lamare, A. Smirnov, and M. Kern, 2020: The determination of snow albedo from satellite measurements using fast atmospheric correction technique. *Remote Sens.*, **12**, 234, https://doi.org/10.3390/rs12020234.

MacFerrin, M., and Coauthors, 2019: Rapid expansion of Greenland's low-permeability ice slabs. *Nature*, **573**, 403-407, https://doi.org/10.1038/s41586-019-1550-3.

Mankoff, K. D., A. Solgaard, W. Colgan, A. P. Ahlstrøm, S. A. Khan, and R. S. Fausto, 2020: Greenland ice sheet solid ice discharge from 1986 through March 2020. *Earth Syst. Sci. Data*, **12**, 1367-1383, https://doi.org/10.5194/essd-12-1367-2020.

Mankoff, K. D., and Coauthors, 2021: Greenland ice sheet mass balance from 1840 through next week. *Earth Syst. Sci. Data*, **13**, 5001-5025, https://doi.org/10.5194/essd-13-5001-2021.

Morlighem, M., and Coauthors, 2017: BedMachine v3: Complete bed topography and ocean bathymetry mapping of Greenland from multibeam echo sounding combined with mass conservation. *Geophys. Res. Lett.*, **44**(21), 11051-11061, https://doi.org/10.1002/2017GL074954.

Mote, T. L., 2007: Greenland surface melt trends 1973-2007: Evidence of a large increase in 2007. *Geophys. Res. Lett.*, **34**, L22507, https://doi.org/10.1029/2007GL031976.

Mouginot, J., and Coauthors, 2019: Forty-six years of Greenland ice sheet mass balance from 1972 to 2018. *P. Natl. Acad. Sci.*, **116**(19), 9239-9244, https://doi.org/10.1073/pnas.1904242116.

Ryan, J. C., L. C. Smith, D. van As, S. W. Cooley, M. G. Cooper, L. H. Pitcher, and A. Hubbard, 2019: Greenland ice sheet surface melt amplified by snowline migration and bare ice exposure. *Sci. Adv.*, **5**, eaav3738, https://doi.org/10.1126/sciadv.aav3738.

van As, D., R. S. Fausto, J. Cappelen, R. S. van de Wa, R. J. Braithwaite, H. Machguth, and PROMICE project team, 2016: Placing Greenland ice sheet ablation measurements in a multi-decadal context. *GEUS Bull.*, **35**, 71-74, https://doi.org/10.34194/geusb.v35.4942.

Wehrlé, A., J. E. Box, A. M. Anesio, and R. S. Fausto, 2021: Greenland bare ice albedo from PROMICE automatic weather station measurements and Sentinel-3 satellite observations. *GEUS Bull.*, **47**, 5284, https://doi.org/10.34194/geusb.v47.5284.

February 14, 2023

Sea Ice

W. N. Meier[1,2], A. Petty[3], S. Hendricks[4], D. Perovich[5], S. Farrell[6], M. Webster[7], D. Divine[8], S. Gerland[8], L. Kaleschke[4], R. Ricker[9], and X. Tian-Kunze[4]

[1]National Snow and Ice Data Center, Boulder, CO, USA
[2]Cooperative Institute for Research in Environmental Sciences, University of Colorado Boulder, Boulder, CO, USA
[3]Goddard Space Flight Center, NASA, Greenbelt, MD, USA
[4]Alfred Wegener Institute, Helmholtz Centre for Polar and Marine Research, Bremerhaven, Germany
[5]Thayer School of Engineering, Dartmouth College, Hanover, NH, USA
[6]Department of Geographical Sciences, University of Maryland, College Park, MD, USA
[7]Geophysical Institute, University of Alaska Fairbanks, Fairbanks, AK, USA
[8]Norwegian Polar Institute, Fram Centre, Tromsø, Norway
[9]NORCE Norwegian Research Centre, Tromsø, Norway

Highlights

- Arctic sea ice extent was similar to 2021 values, higher than many recent years, but much lower than the long-term average.
- Open water areas developed near the North Pole through much of the summer, making the area easier to access for polar class tourist and research vessels; both the Northern Sea Route and Northwest Passage largely opened.
- Multiyear ice extent and sea ice thickness and volume rebounded after near-record low levels in 2021, but were still well-below conditions in the 1980s and 1990s, and the oldest ice continued to be extremely scarce.

Introduction

As the frozen interface between the ocean and atmosphere, sea ice plays a key role in the Earth's climate and polar ecosystems. Over the Arctic Ocean, surface albedo (the fraction of the sun's energy reflected by the surface) is increased by the presence of sea ice and its overlying snow cover, which reduces the absorption of solar radiation and seasonal warming. Sea ice also serves as a platform and interface for marine life and influences the biogeochemical balance of the Arctic. Sea ice in the Arctic has long played a practical and cultural role in Indigenous communities of the north and is increasingly influencing modern commercial transportation, resource extraction, and national security.

After the September 2021 minimum extent, sea ice growth followed a fairly typical pattern, with slower than average freeze-up in the more southerly Hudson and Baffin Bays and near-normal growth elsewhere. Winter and spring near-surface air temperatures over the Central Arctic were well above the 1991-2020 average, particularly in the Beaufort Sea where temperatures were 7°C (13°F) above average in March. However, temperatures reverted back to near-normal values in May. During the June to August summer, temperatures were again higher than average in the Beaufort, but lower than average on the Atlantic side of the Arctic (see essay *Surface Air Temperature*).

Sea ice extent

Sea ice extent, defined as the total area covered by ice of at least 15% concentration, is a common metric to assess seasonal and long-term changes in Arctic sea ice. Starting in 1979, there is now a 44-year record of ice extent derived from a consistent series of satellite-borne passive microwave sensors.

Arctic sea ice undergoes a typical seasonal cycle with an annual maximum extent reached in late February or March and an annual minimum extent reached in September. As in 2021, the March and September 2022 extents were not as extreme as in some recent years (2007-20), but they still ranked as among the lowest in the satellite record (Table 1). We note here that a new 30-year climatology, 1991-2020, is employed for comparison of trends and anomalies (2013-21 Arctic Report Cards used the 1981-2010 baseline period). March and September 2022 continue long-term downward trends in sea ice extent (Fig. 1).
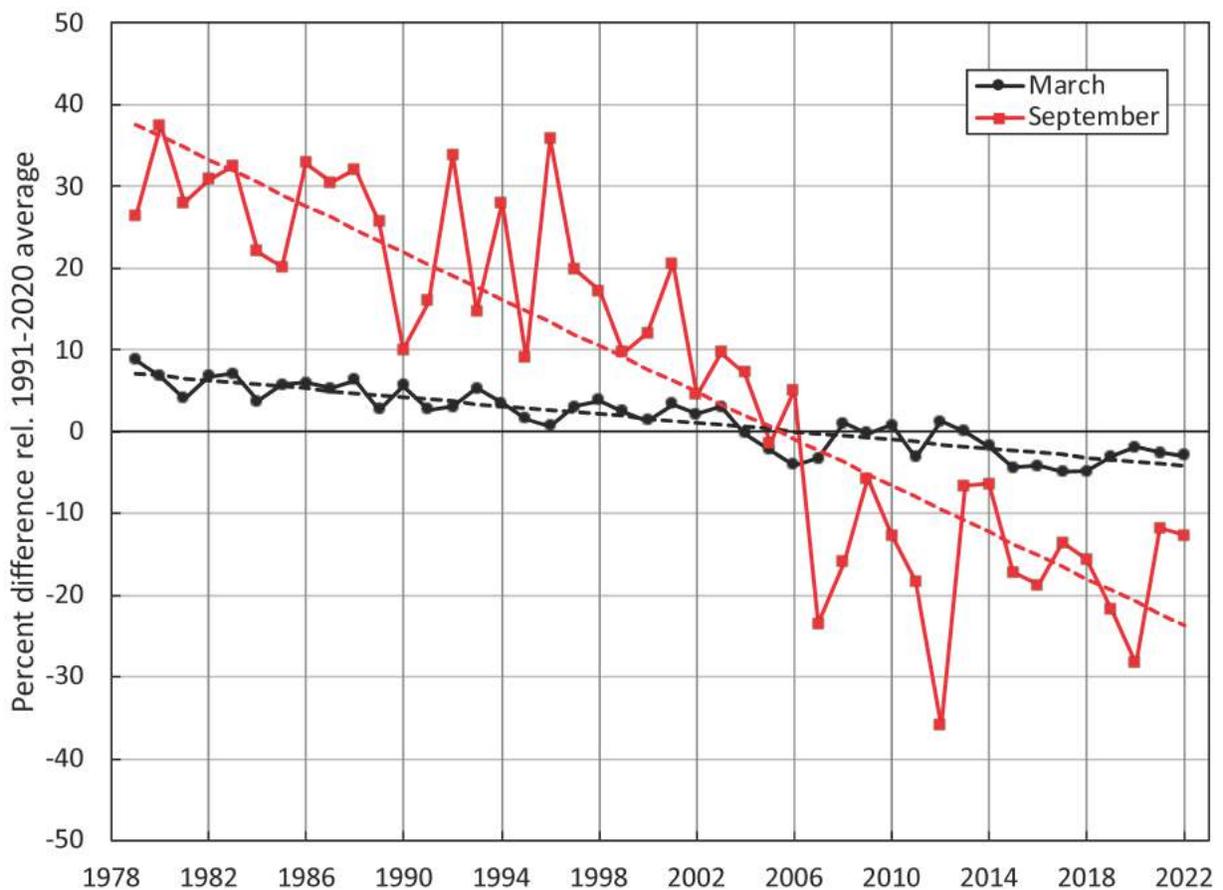
Fig. 1. Monthly sea ice extent anomalies (solid lines) and linear trend lines (dashed lines) for March (black) and September (red) 1979 to 2022. The anomalies are relative to the 1991 to 2020 average for each month (see Table 1); note that this represents a change from 2013-21 reports which used a 1981 to 2010 baseline average.

Table 1. March and September monthly averages and annual daily maximum and minimum extent for 2022 and related statistics. The rank is from least ice to most ice of the 44 years (1 = least, 44 = most).

Values	March Monthly Average	March Daily Maximum	September Monthly Average	September Daily Minimum
Extent (10^6 km^2)	14.59	14.88	4.87	4.67
Rank (out of 44 years)	9	9	13	10
1991-2020 average (10^6 km^2)	15.03	15.26	5.58	5.37
1981-2010 average (10^6 km^2)	15.43	15.70	6.41	6.19
Anomaly rel. **1991-2020** average (10^6 km^2)	-0.44	-0.38	-0.71	-0.70
Trend, 1979-2022 (km^2 per yr)	-39,200	-40,800	-79,400	-78,500
% change from 1979 linear trend value	-9.3	-9.1	-36.5	-37.2

March 2022 was most notable for low ice extent across the Sea of Okhotsk and part of the Barents Sea (Fig. 2). The ice was slightly more extensive than average in Baffin Bay and the Bering Sea. Through the summer, a tongue of ice between the East Siberian and Laptev Seas delayed the opening of the Northern Sea Route, though it did eventually open in August. Ice also remained along the coast in the Chukchi Sea well into summer due to cool temperatures and low winds (see essay *Sea Surface Temperature*). By the end of the summer, extent was well below normal throughout most of the Arctic except for the Barents and East Greenland Seas, where the ice edge was near normal. Notably, the Northwest Passage routes were largely open, including the wide, deep route through the Parry Channel (see essay *Arctic Shipping*). Another unusual feature was low sea ice concentration at high latitudes near the North Pole during July and August. Satellite imagery showed patches of open water near 87° N latitude, within ~300 km of the pole.
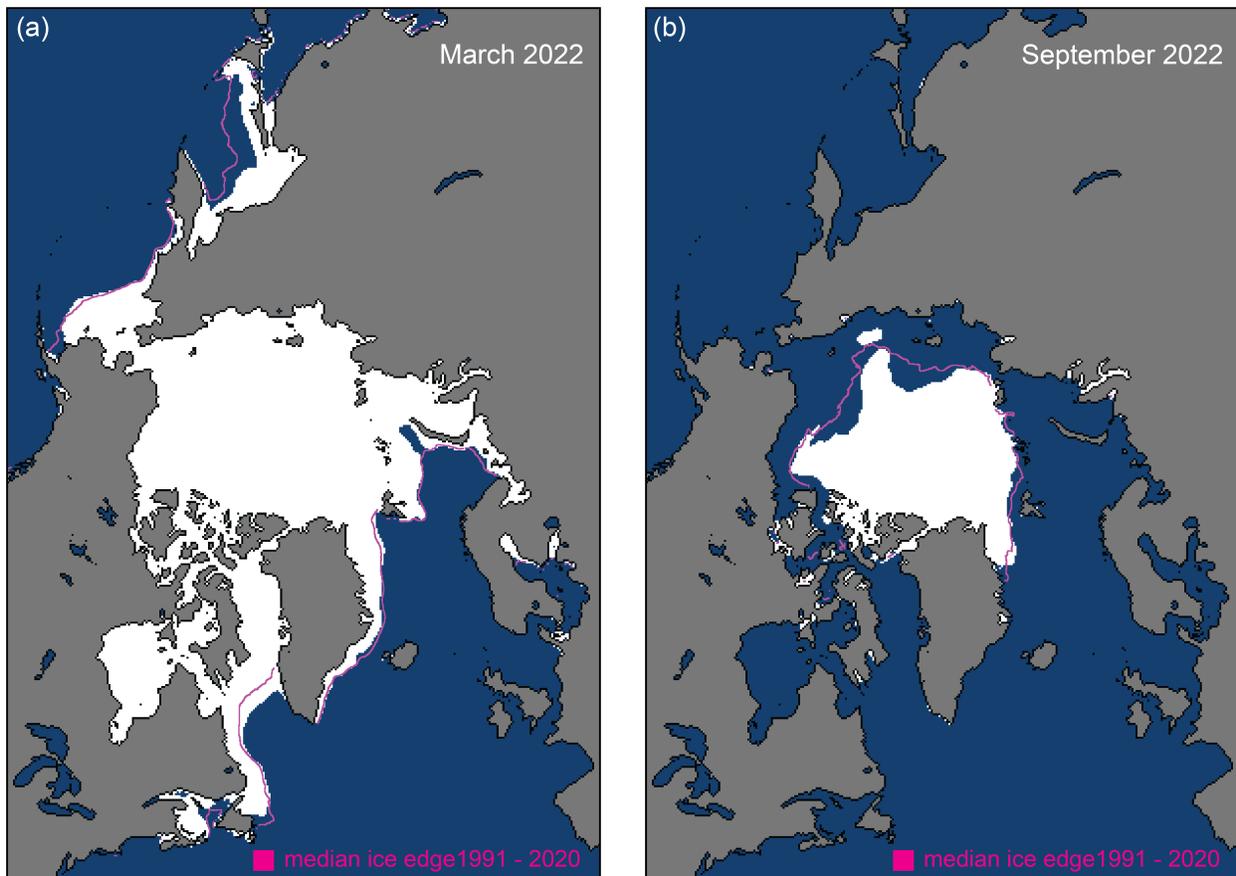
Fig. 2. Monthly average sea ice extent for (a) March 2022, and (b) September 2022. The median extent for 1991-2020 is shown by the magenta contour.

Sea ice age

Sea ice age is a proxy for ice thickness because multiyear ice thermodynamically grows thicker through successive winter periods. The multiyear ice has shown an interannual oscillation since 2007, reflecting variability in the summer transport and melt of sea ice. After a year when substantial multiyear ice is lost, a much larger area of first-year ice takes its place. Some of that first-year ice may survive the next summer, which can replenish the multiyear extent. However, old ice (which we define here as >4 years old) has remained consistently low since 2012. Thus, unlike in earlier decades, multiyear ice does not remain in the Arctic for many years. At the end of the summer 2022 melt season, multiyear ice showed a rebound from near-record low 2021 values, though still far below multiyear extents in the 1980s and 1990s (Fig. 3).
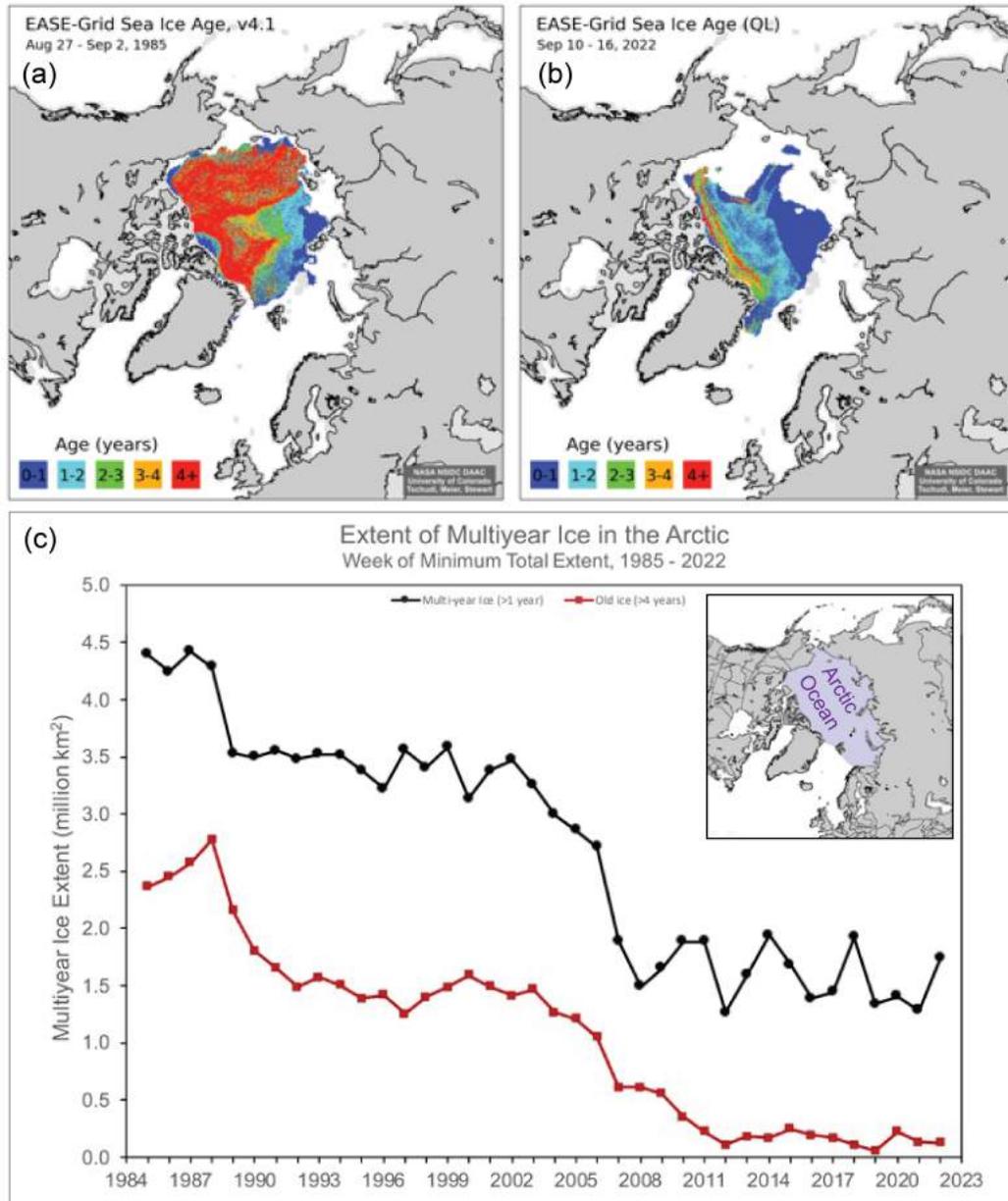
Fig. 3. Sea ice age coverage map for the week before minimum total extent (when age values are incremented to one year older) in (a) 1985, and (b) 2022; (c) extent of multiyear ice (black) and ice >4 years old (red) within the Arctic Ocean for the week of the minimum total extent.

Sea ice thickness and volume

Estimates of sea ice thickness from satellite altimetry can be used to estimate the crucial third dimension of sea ice conditions. The ICESat-2 and CryoSat-2/SMOS satellite products tracked the seasonal October to April growth over the past four years during which all missions were in operation (Fig. 4a) (ICESat-2 data were missing in April 2022 due to a safehold event). The 2021/22 winter Inner Arctic mean thickness time series shows notably thicker ice than the previous winter, which was the lowest in the ICESat-2 (since winter 2018/19) and CryoSat-2/SMOS (since winter 2010/11) records. This is in line with surface air temperatures that were generally cooler as ice began to form and advance

during autumn 2021 compared to autumn 2020 (see essay *Surface Air Temperature*); advection and ridging also likely contributed to the thickness difference between the years. April 2022 thickness (Fig. 4b) from CryoSat-2/SMOS was higher than the 2010-21 April mean (Fig. 4c) across much of the Beaufort Sea and into the Laptev Sea. Thickness was lower than normal in the rest of the Laptev and Kara Seas. CryoSat-2/SMOS sea ice thicknesses were also notably thinner along the northern Canadian Archipelago and Greenland.
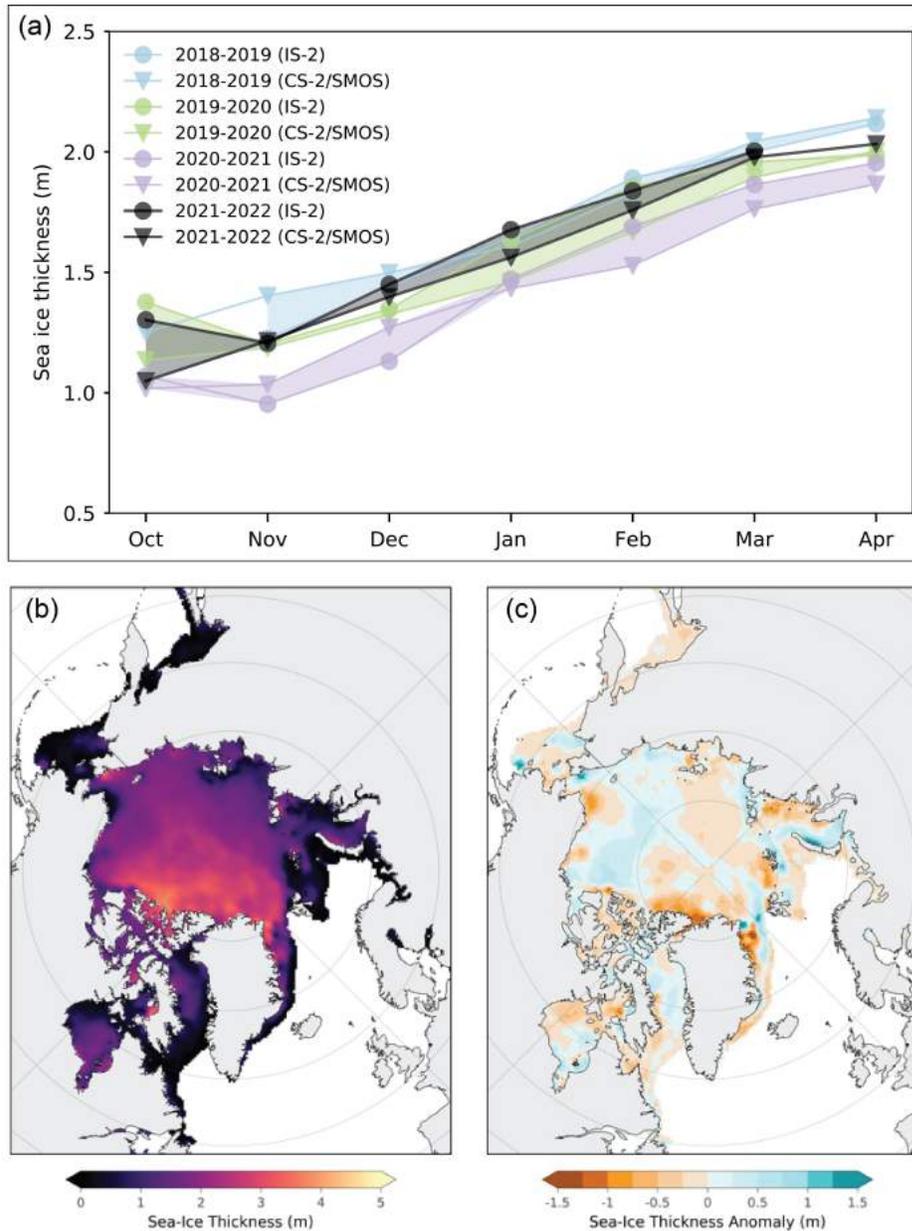
Fig. 4. (a) October through April monthly average sea ice thickness, calculated over an Inner Arctic Ocean Domain (see Methods and data section), from ICESat-2 (circles) and CryoSat-2/SMOS (triangles) for 2018-19 (blue), 2019-20 (green), 2020-21 (lilac), and 2021-22 (black); (b) average April 2022 sea ice thickness map from CryoSat-2/SMOS; (c) CryoSat-2/SMOS thickness anomaly map (relative to the 2010-21 average).

Sea ice thickness is integrated with ice concentration to provide winter volume estimates for the CryoSat-2/SMOS measurement time period. Seasonal change, from winter maximum to summer

minimum and back, shows the strong seasonal cycle and interannual variability (Fig. 5). There is little indication of a trend through the relatively short 11-year time series. After a record low maximum volume in April 2021, there was a relatively small summer loss followed by a strong increase through the October 2021 to April 2022 winter. This resulted in a notable increase in volume compared to April 2021, as was indicated also in the average thickness (Fig. 4a). However, new upward-looking sonar sea ice thickness data from moorings in Fram Strait from 1990 to 2018 (Sumata et al. 2022) also illustrate the changed conditions of recent decades compared to the 1990s and early 2000s. Fram Strait is the region where the largest export of sea ice out of the central Arctic Ocean occurs and is thus representative of ice from the central Arctic.
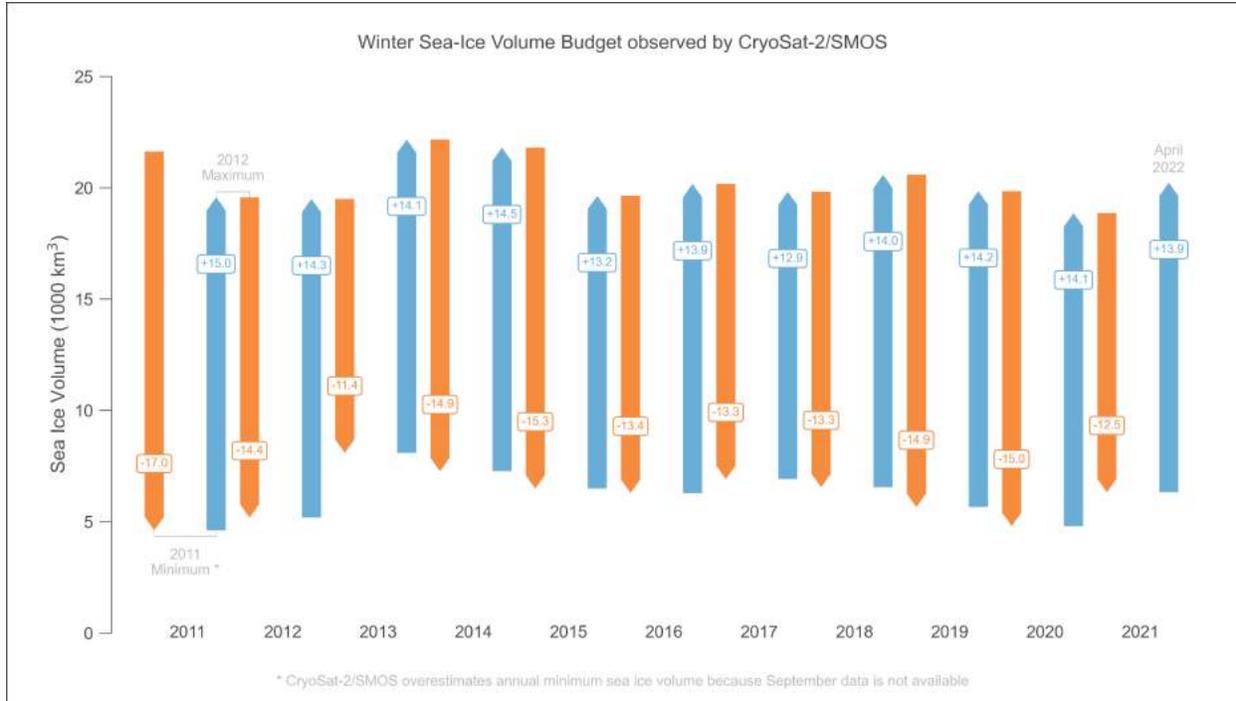
Fig. 5. Annual sea ice volume loss (orange) and gain (blue) between annual maximum and minimum from CryoSat-2/SMOS. Values are in 1000 km^3.

Methods and data

Sea ice extent values are from the NSIDC Sea Ice Index (Fetterer et al. 2017), based on passive microwave derived sea ice concentrations from the NASA Team algorithm (Cavalieri et al. 1996; Meier et al. 2021). There are several other passive microwave derived products available (e.g., Ivanova et al. 2014), including the EUMETSAT OSI-SAF CCI climate data record (Lavergne et al. 2019). All products have some limitations and uncertainties (e.g., Kern et al. 2019), but overall, the trends agree well (Comiso et al. 2017).

Sea ice age data are from the EASE-Grid Sea Ice Age, Version 4 (Tschudi et al. 2019a) and Quicklook Arctic Weekly EASE-Grid Sea Ice Age, Version 1 (Tschudi et al. 2019b) archived at the NASA Snow and Ice Distributed Active Archive Center (DAAC) at NSIDC. Age is calculated via Lagrangian tracking of ice parcels using weekly sea ice motion vectors (Tschudi et al. 2020). Age is generally a proxy for thickness because older ice is typically thicker, via thermodynamic growth and potential dynamic thickening (i.e., ridging and rafting). Only the oldest age category is preserved for each grid cell.

Satellite altimetry has enabled the continuous retrieval of sea ice thickness and volume during the freezing season from ESA CryoSat-2 radar altimeter, launched in 2010 and the NASA Ice, Cloud, and land Elevation 2 (ICESat-2) laser altimeter, launched in 2018.

Weekly CryoSat-2 estimates have been combined with thin ice (<1 m) estimates from the ESA Soil Moisture Ocean Salinity (SMOS) instrument, launched in 2009, to obtain an optimal estimate across thin and thick ice regimes (Ricker et al. 2017) on a 25 km resolution EASE2 grid. Optimal interpolation is used to fill in data gaps in the weekly CryoSat-2 fields and to merge the CryoSat-2 and SMOS estimates. The uncertainty in estimates varies with thickness and other factors, but much of the uncertainty is due to systematic biases that largely cancel out when calculating anomaly fields. When combined with sea ice concentration, the CryoSat-2/SMOS record of ice thickness is used to compute sea ice volume; data are available at ftp://ftp.awi.de/sea_ice/product/cryosat2_smos/v204/.

ICESat-2 estimates here focus on an Inner Arctic Domain (Central Arctic, Beaufort, Chukchi, Laptev, East Siberian Seas—the same domain as for Fig. 3 except without the Barents and Kara Seas) due to poorer knowledge of snow conditions in the more peripheral seas. The data used here are the gridded 25 km x 25 km monthly data (Petty et al. 2021) originally presented in Petty et al. (2020), now using Version 5 ATL10 freeboards from the three strong beams of ICESat-2 and v1.1 NESOSIM snow loading (depth and density) as described in Petty et al. (2022). Data are available at: https://nsidc.org/data/IS2SITMOGR4/versions/2.

Acknowledgments

References

Cavalieri, D. J., C. L. Parkinson, P. Gloersen, and H. J. Zwally, 1996 (updated yearly): Sea Ice Concentrations from Nimbus-7 SMMR and DMSP SSM/I-SSMIS Passive Microwave Data, Version 1. NASA National Snow and Ice Data Center Distributed Active Archive Center, Boulder, CO, USA, accessed 27 August 2022, https://doi.org/10.5067/8GQ8LZQVL0VL.

Comiso, J. C., W. N. Meier, and R. Gersten, 2017: Variability and trends in the Arctic sea ice cover: Results from different techniques. *J. Geophys. Res.*, **122**, 6883-6900, https://doi.org/10.1002/2017JC012768.

Fetterer, F., K. Knowles, W. N. Meier, M. Savoie, and A. K. Windnagel, 2017 (updated daily): Sea Ice Index, Version 3. NSIDC: National Snow and Ice Data Center, Boulder, CO, USA, accessed 2 October 2022, https://doi.org/10.7265/N5K072F8.

Ivanova, N., O. M. Johannessen, L. T. Pedersen, and R. T. Tonboe, 2014: Retrieval of Arctic sea ice parameters by satellite passive microwave sensors: A comparison of eleven sea ice concentration algorithms. *IEEE Trans. Geosci. Rem. Sens.*, **52**(11), 7233-7246, https://doi.org/10.1109/TGRS.2014.2310136.

Kern, S., T. Lavergne, D. Notz, L. T. Pedersen, R. T. Tonboe, R. Saldo, and A. M.Sørensen, 2019: Satellite passive microwave sea-ice concentration data set intercomparison: closed ice and ship-based observations. *Cryosphere*, **13**, 3261-3307, https://doi.org/10.5194/tc-13-3261-2019.

Lavergne, T., and Coauthors, 2019: Version 2 of the EUMETSAT OSI SAF and ESA CCI sea-ice concentration climate data records. *Cryosphere*, **13**, 49-78, https://doi.org/10.5194/tc-13-49-2019.

Meier, W. N., J. S. Stewart, H. Wilcox, M. A. Hardman, and D. J. Scott, 2021: Near-Real-Time DMSP SSMIS Daily Polar Gridded Sea Ice Concentrations, Version 2 [Data Set]. NASA National Snow and Ice Data Center Distributed Active Archive Center, Boulder, CO, USA, accessed 2 October 2022, https://doi.org/10.5067/YTTHO2FJQ97K.

Petty, A. A., N. T. Kurtz, R. Kwok, T. Markus, and T. A. Neumann, 2020: Winter Arctic sea ice thickness from ICESat-2 freeboards. *J. Geophys. Res.-Oceans*, **125**, e2019JC015764, https://doi.org/10.1029/2019JC015764.

Petty, A. A., N. Kurtz, R. Kwok, T. Markus, and T. A. Neumann, 2021: ICESat-2 L4 Monthly Gridded Sea Ice Thickness, Version 1. NASA National Snow and Ice Data Center Distributed Active Archive Center, Boulder, CO, USA, accessed 9 September 2022, https://doi.org/10.5067/CV6JEXEE31HF.

Petty, A. A., N. Keeney, A. Cabaj, P. Kushner, and M. Bagnardi, 2022: Winter Arctic sea ice thickness from ICESat-2: upgrades to freeboard and snow loading estimates and an assessment of the first three winters of data collection. *Cryosphere Discuss*, https://doi.org/10.5194/tc-2022-39, in review.

Ricker, R., S. Hendricks, L. Kaleschke, X. Tian-Kunze, J. King, and C. Haas, 2017: A weekly Arctic sea-ice thickness data record from merged CryoSat-2 and SMOS satellite data. *Cryosphere*, **11**, 1607-1623, https://doi.org/10.5194/tc-11-1607-2017.

Sumata, H., L. de Steur, S. Gerland, D. V. Divine, and O. Pavlova, 2022: Unprecedented decline of Arctic sea ice outflow in 2018. *Nat. Comm.*, **13**, 1747, https://doi.org/10.1038/s41467-022-29470-7.

Tschudi, M., W. N. Meier, J. S. Stewart, C. Fowler, and J. Maslanik, 2019a: EASE-Grid Sea Ice Age, Version 4. [March, 1984-2020]. NASA National Snow and Ice Data Center Distributed Active Archive Center, Boulder, CO, USA, accessed 1 September 2022, https://doi.org/10.5067/UTAV7490FEPB.

Tschudi, M., W. N. Meier, and J. S. Stewart, 2019b: Quicklook Arctic Weekly EASE-Grid Sea Ice Age, Version 1. [March, 2021]. NASA National Snow and Ice Data Center Distributed Active Archive Center, Boulder, CO, USA, accessed 3 October 2022, https://doi.org/10.5067/2XXGZY3DUGNQ.

Tschudi, M. A., W. N. Meier, and J.S. Stewart, 2020: An enhancement to sea ice motion and age products at the National Snow and Ice Data Center (NSIDC). *Cryosphere*, **14**, 1519-1536, https://doi.org/10.5194/tc-14-1519-2020.

November 28, 2022

Sea Surface Temperature

https://doi.org/10.25923/p493-2548

M. -L. Timmermans[1] and Z. Labe[2,3]

[1]Yale University, New Haven, CT, USA
[2]Atmospheric and Oceanic Sciences Program, Princeton University, Princeton, NJ, USA
[3]Geophysical Fluid Dynamics Laboratory, NOAA, Princeton, NJ, USA

Highlights

- August 2022 mean sea surface temperatures (SSTs) were ~2-3°C warmer than 1991-2020 August mean values in the Barents and Laptev Seas.
- Anomalously cool August 2022 SSTs (~3°C cooler) were observed in the Chukchi Sea.
- August mean SSTs show warming trends for 1982-2022 in most regions of the Arctic Ocean that are ice-free in August, with the northern Barents Sea being a notable exception.

Arctic Ocean sea surface temperatures (SSTs) in the summer (June-August) are driven by the amount of incoming solar radiation absorbed by the sea surface and by the flow of warm waters into the Arctic from the North Atlantic and North Pacific Oceans. Solar warming of the Arctic Ocean surface is influenced by the distribution of sea ice (with greater warming occurring in ice-free regions), cloud cover, and upper-ocean stratification. Discharge of relatively warm Arctic river waters can provide an additional source of heat to the surface of marginal seas.

Arctic SST is an essential indicator of the role of the ice-albedo feedback cycle in any given summer sea ice melt season. As the area of sea ice cover decreases, more incoming solar radiation is absorbed by the darker ocean surface and, in turn, the warmer ocean melts more sea ice. In addition, higher SSTs are associated with delayed autumn freeze-up and increased ocean heat storage throughout the year. Marine ecosystems are also influenced by SSTs, which affect the timing and development of production cycles (see essay *Primary Productivity*), as well as available habitat.

The SST data presented here are monthly mean values for August (1982-2022) (see Reynolds et al. 2002, 2007), and comparisons are made to the 1991-2020 baseline period. August mean SSTs provide the most appropriate representation of Arctic Ocean summer SSTs because sea-ice extent is near a seasonal low at this time of year, and there is not the influence of surface cooling and subsequent sea-ice growth that takes place in the latter half of September.

August 2022 mean SSTs were as warm as ~12°C in the southern Barents Sea and reached values as warm as ~6°C in other marginal regions of the Arctic basin (northern Barents, Chukchi, Beaufort, East Siberian, Kara, and Laptev Seas, Fig. 1a). August 2022 mean SSTs were notably warm (around 2-3°C warmer than the 1991-2020 August mean) in the Barents and Laptev Seas, and cool in the Chukchi Sea (around 3°C cooler than the 1991-2020 mean, Fig. 1b). In assessing these regional differences, it is important to note that SSTs exhibit significant variability from year to year. For example, there were considerably warmer SSTs in the Barents Sea and cooler SSTs in the waters off eastern Greenland in August 2022 compared to August 2021, with differences of up to 3°C in each case (Fig. 1c) (see also Timmermans and Labe 2021).
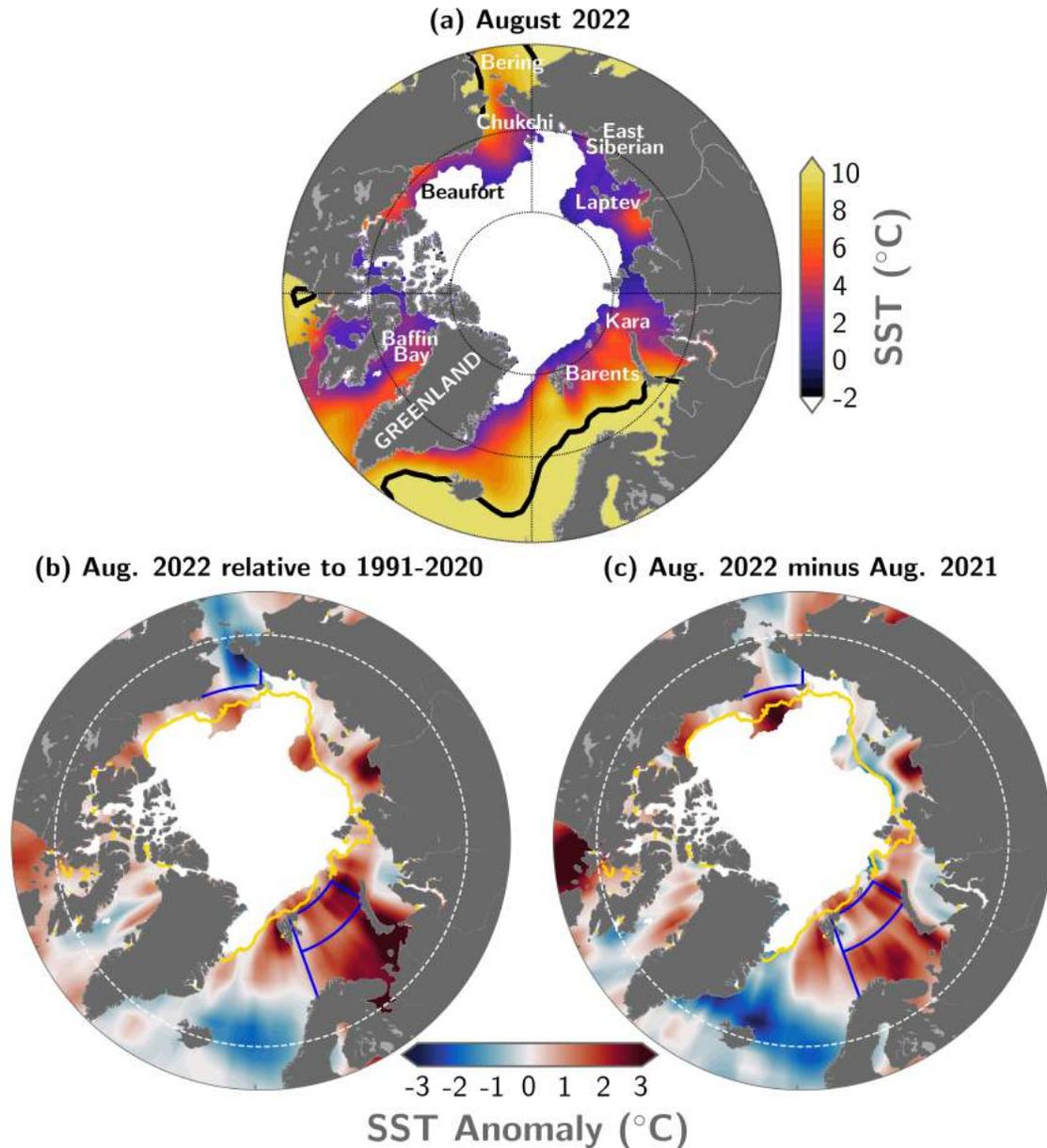
Fig. 1. (a) Mean sea surface temperature (SST; °C) in Aug 2022. Black contours indicate the 10°C SST isotherm, (b) SST anomalies (°C) in Aug 2022 relative to the Aug 1991-2020 mean, (c) Difference between Aug 2022 SSTs and Aug 2021 SSTs (negative values indicate where 2022 was cooler). White shading in all panels is the Aug 2022 mean sea ice extent. Yellow lines in (b) and (c) indicate the median ice edge for Aug 1991-2020. The regions marked by blue boundaries and the white dashed lines indicating 65° N in (b) and (c) relate to data presented in Fig. 3. See Methods and data for source information.

The August 2022 anomalously warm SSTs in the Barents Sea, which were also observed in June and July (Fig. 2), aligned with anomalously warm June-August 2022 surface air temperatures over northern Eurasia (see essay *Surface Air Temperature*). The early timing of seasonal sea-ice retreat from the Barents Sea, with sea ice almost entirely absent from the region by June 2022 (Fig. 2a), also links to warm SSTs via the ice-albedo feedback (see essay *Sea Ice*).
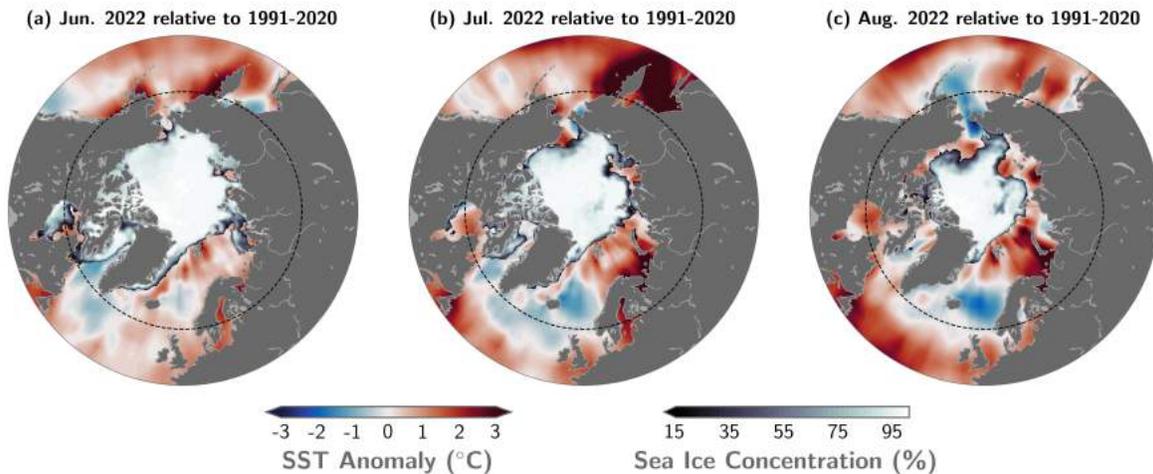
Fig. 2. SST anomalies (°C) for (a) June 2022, (b) July 2022, and (c) August 2022 relative to the 1991-2020 mean for the respective month. The sea-ice concentration for the corresponding month is also shown. The evolution of sea-ice concentration over the months of June to August illustrates why it is not appropriate to evaluate long-term SST trends in June and July over most of the Arctic marginal seas, which still have significant sea-ice cover in those months. The dashed circle indicates the latitudinal bound of the map images shown in Figs. 1 and 3. See Methods and data for source information.

The August 2022 anomalously cool SSTs in the Chukchi Sea are commensurate with below normal surface air temperatures in the region in June-August 2022 (see essay *Surface Air Temperature*). The persistence of a tongue of late-season sea ice near the coast where the East Siberian Sea meets the Chukchi Sea is further consistent with these anomalously cool SSTs (Fig. 2 and see essay on *Sea Ice*). Conversely, to the north of this region of cool SSTs, sea-ice extent was below normal and SSTs were anomalously warm (Fig. 2b).

Mean August SST warming trends from 1982 to 2022 persist over much of the Arctic Ocean, with statistically significant (at the 95% confidence interval) linear warming trends in most regions, except the Laptev, East Siberian, and northern Barents Seas (Fig. 3a). Mean August SSTs for the entire Arctic (the Arctic Ocean and marginal seas north of 65° N) exhibit a linear warming trend of +0.03 ± 0.01°C/yr (Fig. 3b). Even while anomalously cool SSTs in the Chukchi Sea were prominent in the August 2022 SST field (Fig. 1b), SSTs show a linear warming trend over 1982-2022 of +0.05 ± 0.03°C/yr (Fig. 3c) for this region. The cooling trend in mean August SSTs in the northern Barents Sea (Fig. 3d) remains an exception. This cooling trend has been notably influenced by anomalously warm SSTs in that sector of the Barents Sea in the 1980s and 90s (Fig. 3d), although anomalously warm SSTs in recent years in the region continue to have an influence on reversing the overall trend.
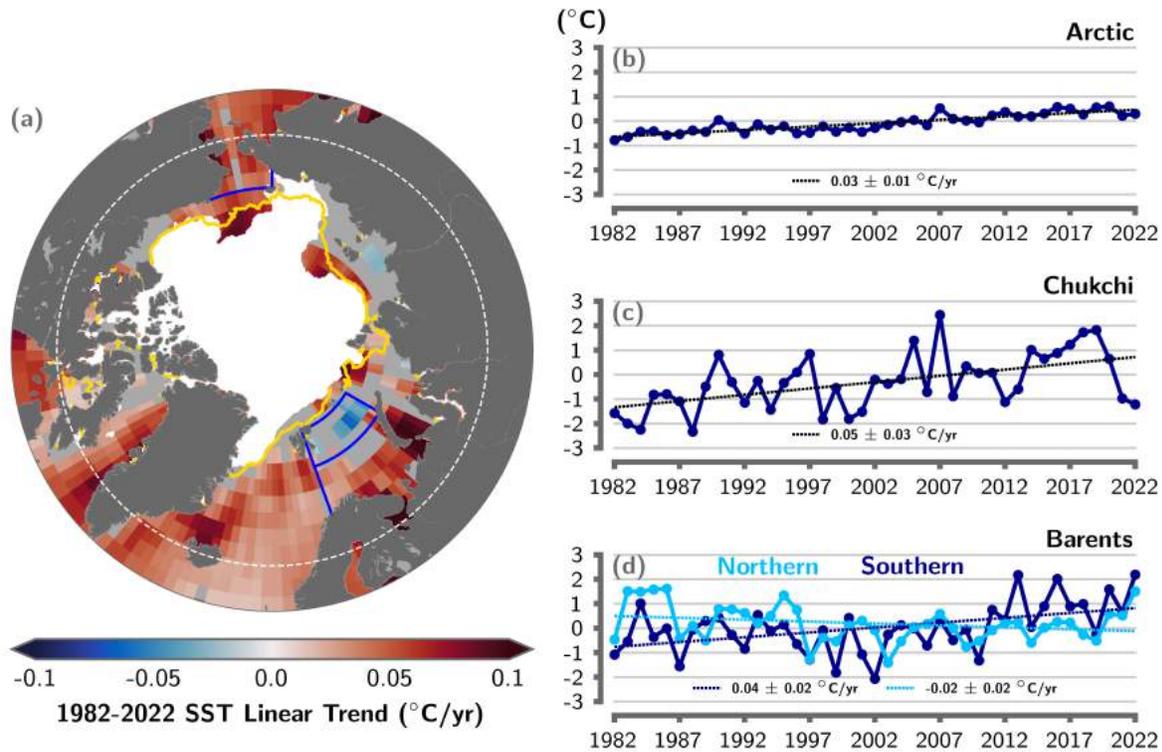
Fig. 3. (a) Linear SST trend (°C/yr) for August of each year from 1982 to 2022. The trend is only shown for values that are statistically significant at the 95% confidence interval; the region is shaded gray otherwise. White shading is the August 2022 mean sea ice extent, and the yellow line indicates the median ice edge for August 1991-2020, (b,c,d) Area-averaged SST anomalies (°C) for August of each year (1982-2022) relative to the 1991-2020 August mean for (b) the entire Arctic Ocean north of 65° N (indicated by the dashed white circle in (a)), (c) the Chukchi Sea, and (d) the Northern and Southern Barents Sea indicated by smaller blue boxes (intersecting with land boundaries) in (a). The dotted lines show the linear SST anomaly trends over the period shown and trends in °C/yr (with 95% confidence intervals) are indicated on the plots. See Methods and data for source information.

Methods and data

The SST data presented here are a blend of in situ and satellite measurements from August 1982 to August 2022, taken from the monthly mean NOAA Optimum Interpolation (OI) SST Version 2 product (OISSTv2; Reynolds et al. 2002, 2007). NOAA OISSTv2 data are provided by the NOAA PSL, Boulder, Colorado, USA, from their website at https://psl.noaa.gov [accessed 6 September 2022], which can be retrieved at https://downloads.psl.noaa.gov/Datasets/noaa.oisst.v2/ (Reynolds et al. 2007). In the Arctic Ocean overall, the OISSTv2 product has been found to exhibit a cold bias (i.e., underestimate SST) of up to 0.5°C compared to in situ measurements (Stroh et al. 2015). The OISSTv2 product uses a simplified linear relationship with sea-ice concentration to infer SST under sea ice (Reynolds et al. 2007), which means SSTs may be too cool by up to 0.2°C where there is sea-ice cover. We focus primarily on waters that are ice free in August, although this uncertainty can be reflected in trends and variability in the vicinity of the sea-ice edge. The period 1991-2020 is used as the climatological reference for the June, July, and August means. We note here that there is an update to the OISSTv2 product. This updated version 2.1 employs a different method than version 2 for setting a proxy SST in sea-ice covered regions, applied only after January 2016 (in addition to some other differences that are not specific to the polar regions). See Huang et al. (2021) for a description. In our examination of trends in the Arctic Ocean

(based on monthly means), we require a product that estimates SST in the presence of sea ice in the same way over the full duration of the record. Otherwise, estimated trends might be artifacts of the change in methodology part way through the record. For this reason, we choose to continue to use the monthly OISSTv2.

Sea ice concentration data are the NOAA/NSIDC Climate Data Record of Passive Microwave Sea Ice Concentration, Version 4 and Near-Real-Time NOAA/NSIDC Climate Data Record of Passive Microwave Sea Ice Concentration, Version 2 (Peng et al. 2013; Meier et al. 2021a,b), where a threshold of 15% concentration is used to calculate sea ice extent.

Acknowledgments

References

Huang, B., C. Liu, V. Banzon, E. Freeman, G. Graham, B. Hankins, T. Smith, and H. Zhang, 2021: Improvements of the Daily Optimum Interpolation Sea Surface Temperature (DOISST) Version 2.1. *J. Climate*, **34**(8), 2923-2939, https://doi.org/10.1175/JCLI-D-20-0166.1.

Meier, W. N., F. Fetterer, A. K. Windnagel, and J. S. Stewart, 2021a: NOAA/NSIDC Climate Data Record of Passive Microwave Sea Ice Concentration, Version 4. [1982-2021]. Boulder, Colorado USA. NSIDC: National Snow and Ice Data Center, accessed 10 September 2022, https://doi.org/10.7265/efmz-2t65.

Meier, W. N., F. Fetterer, A. K. Windnagel, and J. S. Stewart, 2021b: Near-Real-Time NOAA/NSIDC Climate Data Record of Passive Microwave Sea Ice Concentration, Version 2. [1982-2021], accessed 10 September 2022, https://doi.org/10.7265/tgam-yv28.

Peng, G., W. N. Meier, D. J. Scott, and M. H. Savoie, 2013: A long-term and reproducible passive microwave sea ice concentration data record for climate studies and monitoring. *Earth Syst. Sci. Data*, **5**, 311-318, https://doi.org/10.5194/essd-5-311-2013.

Reynolds, R. W., N. A. Rayner, T. M. Smith, D. C. Stokes, and W. Wang, 2002: An improved in situ and satellite SST analysis for climate. *J. Climate*, **15**, 1609-1625, https://doi.org/10.1175/1520-0442(2002)015<1609:AIISAS>2.0.CO;2.

Reynolds, R. W., T. M. Smith, C. Liu, D. B. Chelton, K. S. Casey, and M. G. Schlax, 2007: Daily high-resolution-blended analyses for sea surface temperature. *J. Climate*, **20**, 5473-5496, https://doi.org/10.1175/2007JCLI1824.1, and see http://www.esrl.noaa.gov/psd/data/gridded/data.noaa.oisst.v2.html.

Stroh, J. N., G. Panteleev, S. Kirillov, M. Makhotin, and N. Shakhova, 2015: Sea-surface temperature and salinity product comparison against external in situ data in the Arctic Ocean. *J. Geophys. Res.-Oceans*, **120**, 7223-7236, https://doi.org/10.1002/2015JC011005.

Timmermans, M. -L., and Z. M. Labe, 2021: Sea surface temperature. *Arctic Report Card 2021*, T. A. Moon, M. L. Druckenmiller, and R. L. Thoman, Eds., https://doi.org/10.25923/2y8r-0e49.

November 22, 2022

Arctic Ocean Primary Productivity:
The Response of Marine Algae to Climate Warming and Sea Ice Decline

K. E. Frey[1], J. C. Comiso[2], L. W. Cooper[3], C. Garcia-Eidell[4],
J. M. Grebmeier[3], and L. V. Stock[2]

[1]Graduate School of Geography, Clark University, Worcester, MA, USA
[2]Cryospheric Sciences Laboratory, Goddard Space Flight Center, NASA, Greenbelt, MD, USA
[3]Chesapeake Biological Laboratory, University of Maryland Center for Environmental Science, University of Maryland, Solomons, MD, USA
[4]Global Ocean Monitoring and Observing Program, NOAA, Silver Spring, MD, USA

Highlights

- Satellite estimates of ocean primary productivity (i.e., the rate at which marine algae transform dissolved inorganic carbon into organic material) showed higher values for 2022 (relative to the 2003-21 mean) for five of the nine regions investigated across the Arctic.
- All regions continue to exhibit positive trends in primary productivity over the 2003-22 period, with the strongest trends in the Eurasian Arctic and Barents Sea.
- Broad regions of lower-than-average primary productivity during 2022, particularly for the Beaufort Sea, East Siberian Sea, Greenland Sea, and Baffin Bay (associated with higher-than-average sea ice cover in these regions), contributed to the high variability of primary productivity over both space and time across the Arctic.

Introduction

Primary production by single-celled phytoplankton and sea ice algae forms the foundation of the Arctic Ocean's unique ecosystems and the fisheries they support. Controlled by a complex interplay of light and nutrients, primary producers transform dissolved inorganic carbon into organic material. Light regimes and nutrient supplies in turn are both affected by seasonal melting and retreat of sea ice, water mass structure, and ocean circulation (Popova et al. 2010; Ardyna et al. 2017). Light availability is strongly influenced by the extreme seasonality (continuous sunlight in summer and darkness during winter), spring snow thickness on sea ice, as well as the number of open water days in areas with seasonal sea ice cover. In terms of nutrients, the open ocean regions of the Arctic are typically characterized by a well-stratified surface layer with low nutrient levels. Subsurface waters, however, are nutrient rich and the upwelling of these nutrients at the sea ice edge may support episodic phytoplankton blooms that account for half of the regional production within a season (Mundy et al. 2009). In addition to the upwelling of nutrients, high winds, glacial runoff, and efficient recycling of land-derived nutrients are also regionally important in helping to drive Arctic marine productivity (Crawford et al. 2020; Hopwood et al. 2020; Terhaar et al. 2021). Increasing ice-free conditions, nutrient availability, and warming across the Arctic can all result in increased primary productivity. At the same

time, freshening caused by sea ice melt and increased riverine fresh-water input increases stratification, which restricts nutrient supply to surface layers (von Appen et al. 2021). Increased CO_2 concentrations are also expected to have a fertilization effect on marine autotrophs, but this is highly temperature-dependent (Holding et al. 2015). These observations among others show that underlying drivers of marine primary productivity in a rapidly changing Arctic are not straightforward and depend on various processes, events, and features across different spatial and temporal scales. Satellite-based observations of ocean color are used to calculate marine chlorophyll concentrations that are then incorporated into more complex models that estimate ocean primary productivity, providing a synoptic view of the rates at which plant material is generated through photosynthesis across the Arctic Ocean. *For further references, see Frey et al. (2021) and earlier Arctic Report Card essays.*

Chlorophyll-*a*

We present satellite-based estimates of algal chlorophyll-*a* (occurring in all species of phytoplankton), based on ocean color, and subsequently provide calculated primary production estimates (below). The data presented in Fig. 1 show mean monthly ratios of chlorophyll-*a* concentrations for 2022 as percentages of the multiyear average from 2003 to 2021. Observed patterns, which are spatially and temporally heterogeneous across the Arctic Ocean, are often associated with the timing of the seasonal break-up and retreat of the sea ice cover (Fig. 2) (see essay *Sea Ice*): high percentages tend to occur in regions where the break-up is relatively early, while low percentages tend to occur in regions where the break-up is delayed. Some of the most notable patterns in 2022 are found in the western Barents and northern Norwegian Seas, with widespread higher-than-average concentrations of chlorophyll-*a* in May (Fig. 1a) and subsequent declines in June, July, and August (Figs. 1b-d). Higher-than-average chlorophyll-*a* concentrations are also notable in the central Barents Sea during June and July (Figs. 1b,c) and the northern Laptev Sea during July and August (Figs. 1c,d). In the Greenland Sea and Baffin Bay, broad areas of lower-than-average chlorophyll-*a* concentrations occur during all four months shown. A notable split of chlorophyll-*a* concentration departures from average exists in the Bering Sea, where lower-than-average values are found in the western Bering Sea and higher-than-average values are found in the eastern Bering Sea during all four months (Figs. 1a-d) and are consistent with patterns in sea ice cover observed during May (Fig. 2a).
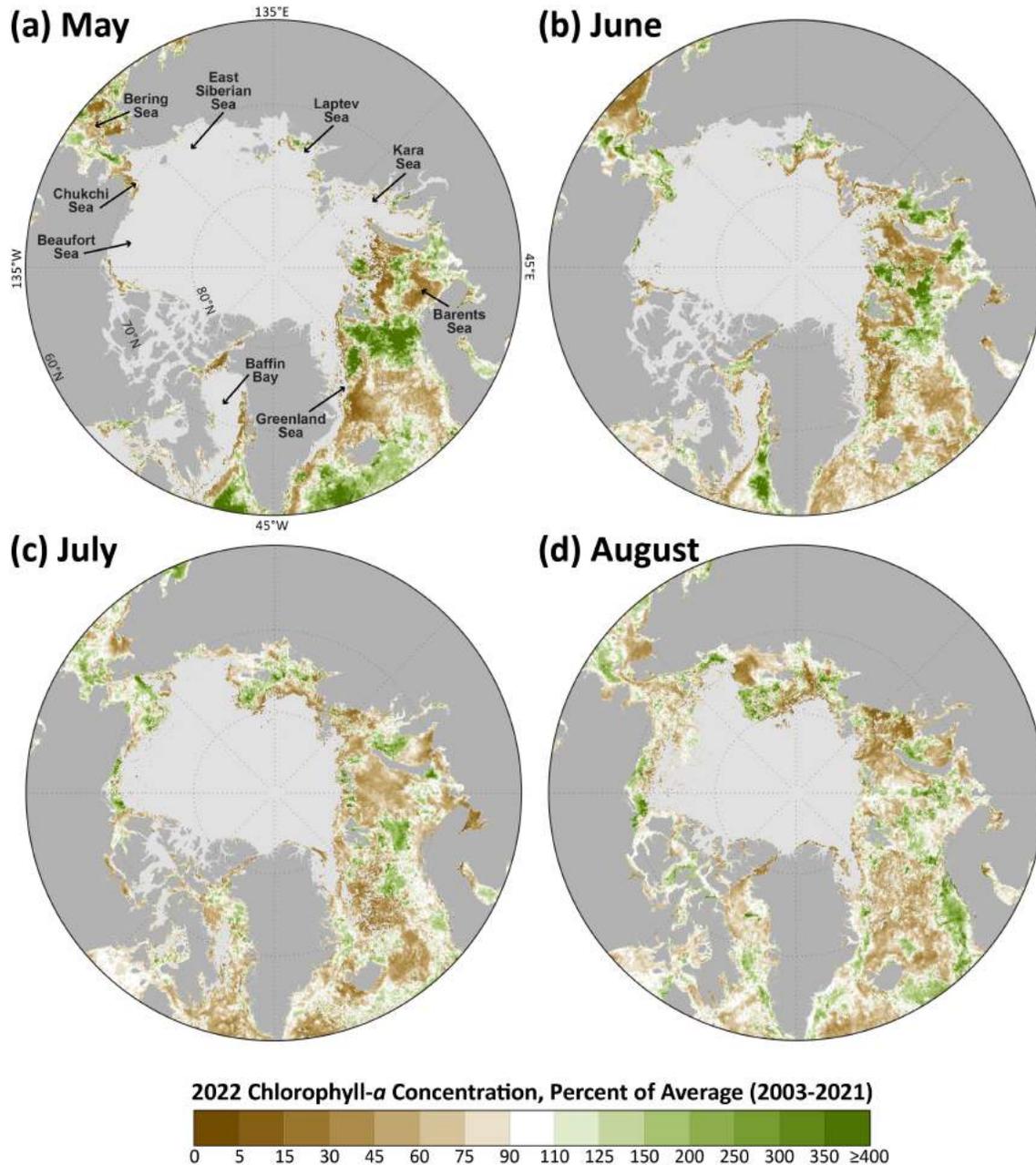
Fig. 1. Mean monthly chlorophyll-*a* concentrations during 2022, shown as a percent of the 2003-21 average for (a) May, (b) June, (c) July, and (d) August. The light gray regions represent areas where no data are available (owing to either the presence of sea ice or cloud cover). The color scale bar uses unequal intervals ranging from 5 to 50 percentage units, including the largest intervals for values greater than 125%. Data source: MODIS-Aqua Reprocessing 2022.0, chlor_a algorithm: https://oceancolor.gsfc.nasa.gov/.
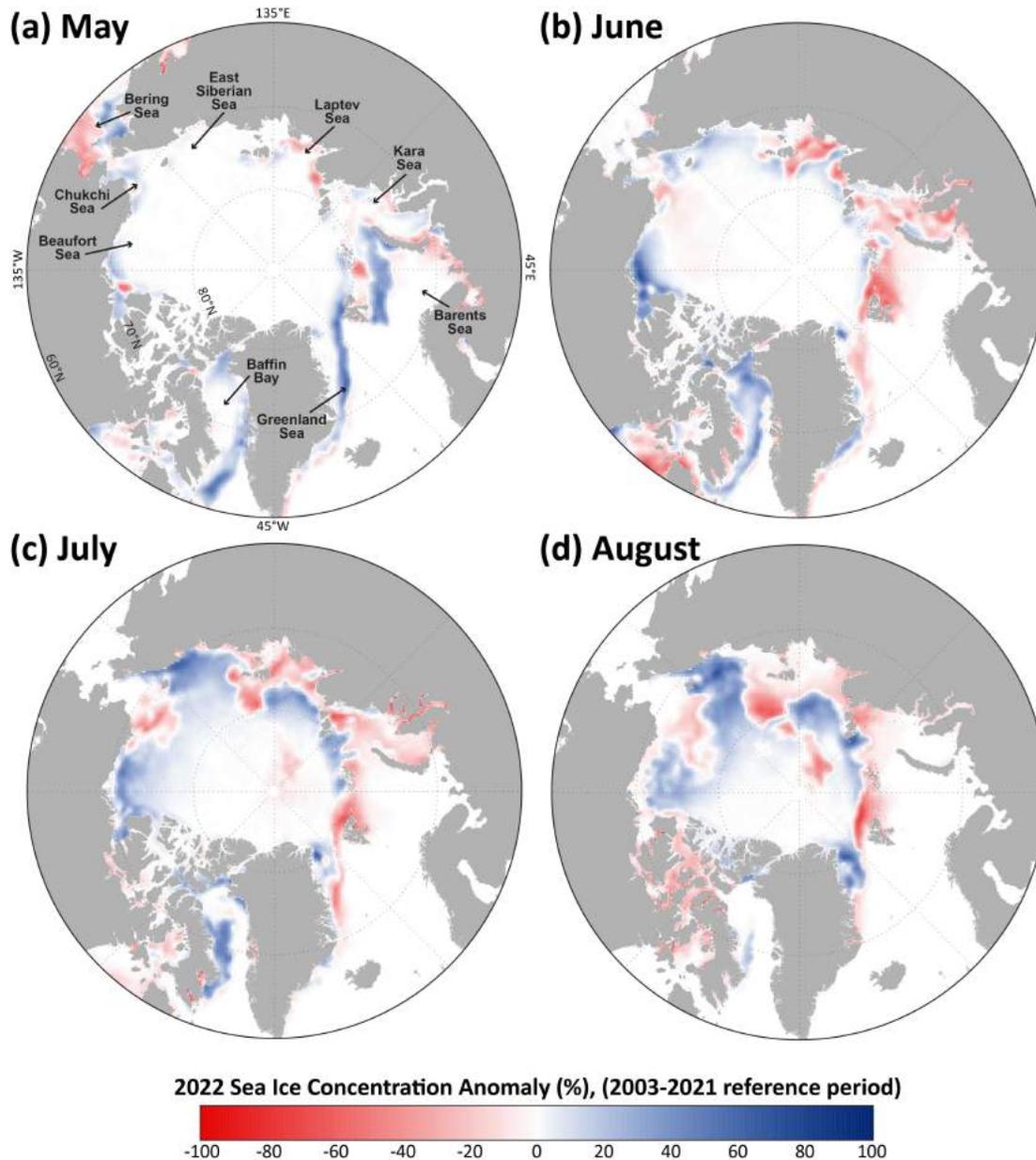
Fig. 2. Sea ice concentration anomalies (%) in 2022 (compared to a 2003-21 mean reference period) for (a) May, (b) June, (c) July, and (d) August. Data source: SSM/I and SSMIS passive microwave, calculated using the Goddard Bootstrap (SB2) algorithm (Comiso et al. 2017).

Primary production

Chlorophyll-*a* concentrations give an estimate of the total standing stock of algal biomass. However, rates of primary production (i.e., the production of organic carbon via photosynthesis) provide a different perspective since not all algae present in the water column are necessarily actively producing. The mean annual primary productivity across the Arctic shows important spatial patterns, most notably the overall decreases moving northward as sea ice cover is present for a greater fraction of the year (Fig. 3a). Spatial trends in annual primary productivity (Fig. 3b) are a particularly useful tool for understanding hotspots of change. Those trends that are positive and largest are located in the Laptev

Sea, reaching rates of ~100 g C/m^2/yr/decade and higher (Fig. 3b). This is consistent with the Eurasian Arctic region as a whole, which exhibits the greatest increases in primary productivity compared to all other Arctic regions (Fig. 4, Table 1). Additional clustered statistically significant increasing trends in primary productivity appear in the eastern Bering Strait/eastern Chukchi Sea region, Barents Sea, and eastern Greenland Sea (Fig. 3b). Trends adjacent to the Eurasian coastline may be associated with variability in river-derived chromophoric (light absorbing) dissolved organic matter (CDOM) as well (e.g., Lewis and Arrigo 2020). Using this primary productivity product, nearly no evidence of significant decreasing trends in primary productivity across the Arctic exists (only isolated locations in the southern Barents Sea and Norwegian Sea; Fig. 3b). Investigations of 2022 annual primary productivity (Fig. 3c), as well as 2022 compared to the 2003-21 average (Fig. 3d), show greater-than-average annual productivity in the central Chukchi Sea, northern Laptev Sea, Kara Sea, and Barents Sea, but lower-than-average annual productivity in the Beaufort Sea, East Siberian Sea, Baffin Bay, and Greenland Sea. Many of these spatial patterns in productivity are reflective of 2022 sea ice conditions (Fig. 2; e.g., higher-than-average sea ice concentrations in the Beaufort Sea, East Siberian Sea, and Baffin Bay vs. lower-than-average sea ice concentrations in the northern Laptev Sea, Kara Sea, and northern Barents Sea).
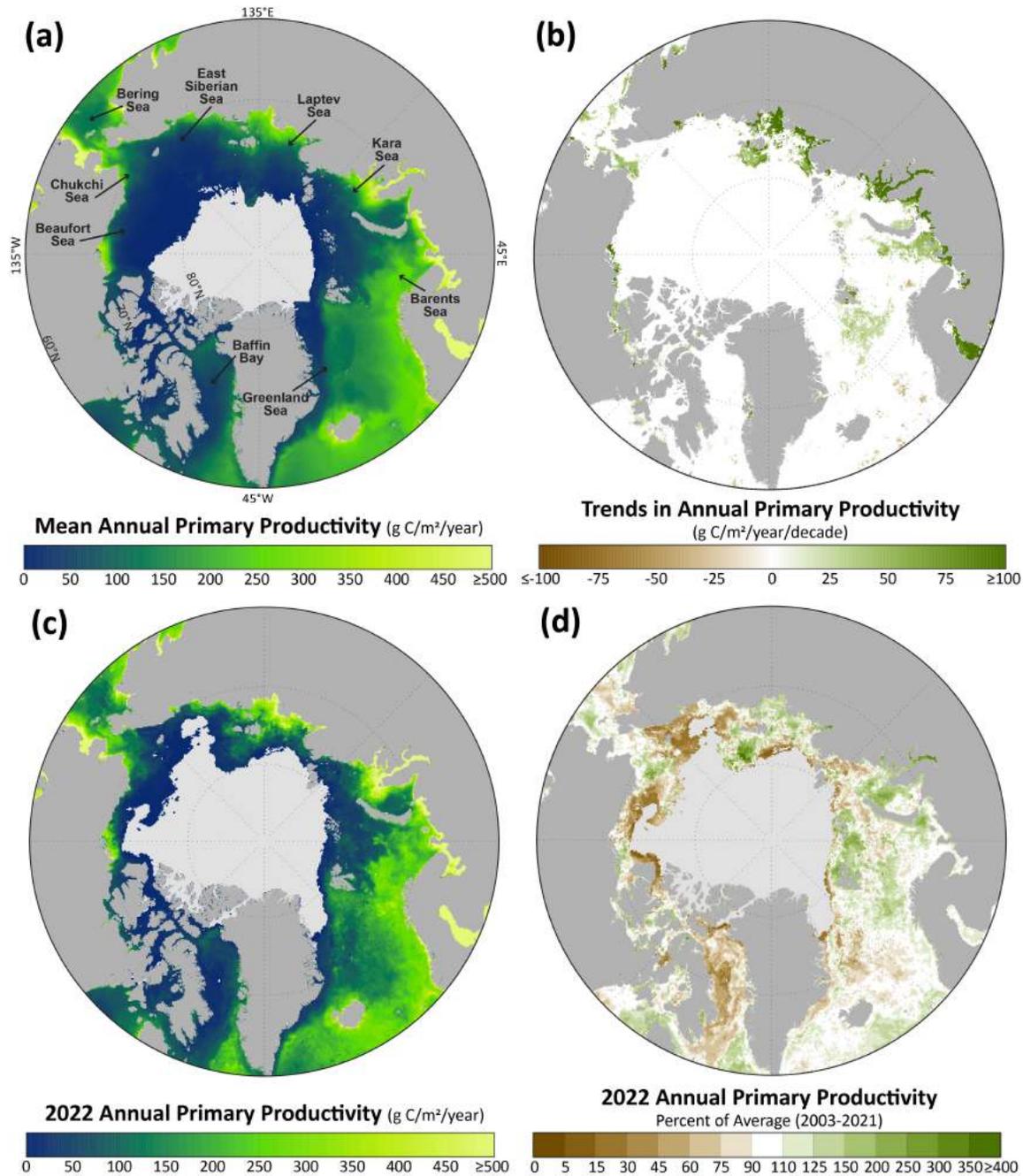
Fig. 3. For the pan-Arctic region: (a) mean annual (March-September only) primary productivity (2003-22); (b) trends in annual productivity (over 2003-22) where only those trends that are statistically significant (*p*<0.05) are shown; (c) annual primary productivity for 2022 only; and (d) 2022 annual primary productivity anomalies (shown as a percent of the 2003-21 average). In a, c, and d, light gray indicates no data owing to the presence of sea ice. Additional information regarding these data can be found in Table 1. See Methods and data section for details of how primary productivity was calculated.
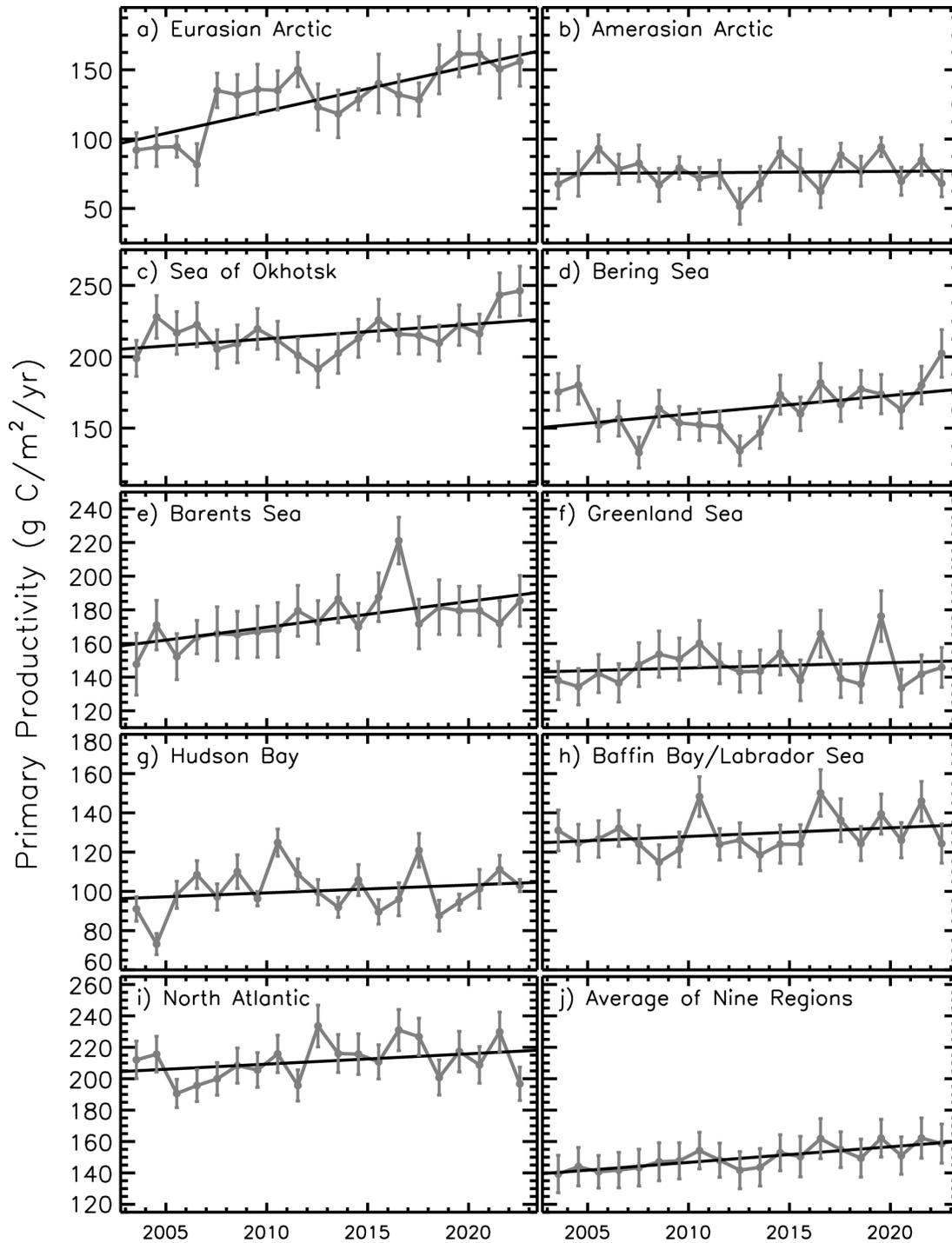
Fig. 4. Primary productivity (2003-22, March-September only) in nine different regions of the Northern Hemisphere (for a definition of the regions see Comiso 2015), as well as the average of these nine regions. The statistical significance of the trends (based on the Mann-Kendall test), *p*-values, and additional information regarding these data can be found in Table 1. See Methods and data section for details of how primary productivity was calculated.

Table 1. Linear trends, statistical significance, and percent change in primary productivity (2003-22) and primary productivity anomalies for 2022 (March-September) in the nine regions (and overall average) as shown in Fig. 4. Values in bold are statistically significant ($p<0.05$) using the Mann-Kendall test for trend. The percent change was estimated from the linear regression of the 20-year time series.

Region	2003-22 Trend (g C/m^2/yr/ decade)	2003-22 Mann-Kendall p-value	2003-22 % Change	2022 Anomaly (g C/m^2/yr) from the 2003-21 reference period	2022 Primary Productivity (% of the 2003-21 average)
Eurasian Arctic	**32.18**	0.001	61.5	27.35	121.3
Amerasian Arctic	1.01	0.871	2.6	-8.37	89.0
Sea of Okhotsk	10.09	0.127	9.3	32.11	115.0
Bering Sea	12.98	0.074	16.3	40.50	125.0
Barents Sea	**15.34**	0.000	18.2	11.56	106.7
Greenland Sea	3.17	0.626	4.2	-0.66	99.6
Hudson Bay	4.02	0.581	7.9	2.64	102.6
Baffin Bay/Labrador Sea	4.41	0.496	6.7	-5.23	96.0
North Atlantic	6.58	0.144	6.1	-15.33	92.8
Average of Nine Regions	**9.98**	0.000	13.5	9.40	106.3

Estimates of ocean primary productivity in 2022 for nine regions and across the Northern Hemisphere (relative to the 2003-21 reference period) were assessed (Fig. 4, Table 1). The Eurasian Arctic designation includes the Kara Sea, Laptev Sea, and East Siberian Sea. The Amerasian Arctic designation includes the Chukchi Sea, Beaufort Sea, and Canadian Archipelago region. The North Atlantic region in this categorization is south of 60° N and east of 45° W, and as such is not inclusive of the Labrador or Greenland Seas. Our results show above-average primary productivity for 2022 in five of the nine regions investigated, while the Amerasian Arctic, Greenland Sea, Baffin Bay/Labrador Sea, and North Atlantic exhibit lower-than-average values (Fig. 4, Table 1). Across the whole time series, however, positive trends in primary productivity remain in all regions during the 2003-22 period. Statistically significant positive trends occurred in the Eurasian Arctic and Barents Sea, as well as on average for the nine regions. In particular, trends over the 2003-22 period have increased by ~61.5% in the Eurasian Arctic and ~18.2% in the Barents Sea. In summary, while observations of primary productivity show complex interannual and spatial patterns over the 2003-22 period, we continue to observe overall increasing trends across all sectors of the Arctic Ocean.

Methods and data

Measurements of the algal pigment chlorophyll (specifically, chlorophyll-*a*) serve as a proxy for the amount of algal biomass present in the ocean as well as overall plant health. The complete, updated Moderate Resolution Imaging Spectroradiometer (MODIS)-Aqua satellite record of chlorophyll-*a* concentrations within northern polar waters for the years 2003-22 serves as a time series against which individual years are compared. Satellite-based chlorophyll-*a* data across the pan-Arctic region were derived using the MODIS-Aqua Reprocessing 2022.0, chlor_a algorithm: https://oceancolor.gsfc.nasa.gov/. For this report, we show mean monthly chlorophyll-*a* concentrations calculated as a percentage of the 2003-21 average, which was chosen as the reference period to

maximize the length of the satellite-based time series. Satellite-based sea ice concentrations were derived from the Special Sensor Microwave/Imager (SSM/I) and Special Sensor Microwave Imager/Sounder (SSMIS) passive microwave instruments, calculated using the Goddard Bootstrap (SB2) algorithm (Comiso et al. 2017). Monthly sea ice concentration anomalies were additionally calculated for 2022 (compared to the 2003-21 average) in order to streamline comparisons with the variability in monthly chlorophyll-*a* satellite data. Primary productivity data were derived using chlorophyll-*a* concentrations from MODIS-Aqua data (Reprocessing 2022.0, chlor_a algorithm), the NOAA 1/4° daily Optimum Interpolation Sea Surface Temperature dataset (or daily OISST) that uses satellite sea surface temperatures from AVHRR, incident solar irradiance, mixed layer depths, and additional parameters. Primary productivity values were calculated based on the techniques described by Behrenfeld and Falkowski (1997). Chlorophyll-*a* and primary productivity data only incorporate pixels where sea ice is less than 10%, which is a compromise between potential pixel contamination with sea ice and an attempt to incorporate open water near the ice edge that typically exhibits high rates of primary production. We define annual productivity as productivity over the March-September time period. The 2022 annual primary productivity percent of average (compared to 2003-21) was calculated the same way as for chlorophyll-*a*, as described above. Lastly, Theil-Sen median trends were calculated spatially (Fig. 3b) and for the extracted time series for each geographic region (Table 1), where statistical significance ($p<0.05$) of the trends was determined using the Mann-Kendall trend test.

It is important to note that the chlorophyll-*a* and primary productivity data are shown for ocean areas with less than 10% sea ice concentration and, therefore, do not include production by sea ice algae or under-ice phytoplankton blooms, which can be significant (e.g., Ardyna et al. 2020). Furthermore, it is well known that satellite observations can underestimate production under stratified conditions when a deep chlorophyll maximum is present (Bouman et al. 2020). The variable distribution of sediments and CDOM (owing to riverine delivery, coastal erosion, and sea ice dynamics) can also affect the accuracy of satellite-based estimations of chlorophyll-*a* and primary productivity in Arctic waters (Lewis and Arrigo 2020). As such, in-situ observations (e.g., Cooper and Grebmeier 2022; Gaffey et al. 2022) continue to importantly provide overall context for changes to and drivers of primary productivity across Arctic marine ecosystems. However, barriers to field-based measurements include the presence of Arctic storms (as was the case for multiple ships in the Pacific Arctic region in the summer of 2022; unpublished data), which also drive enhanced marine primary productivity through the vertical mixing of nutrients (Crawford et al. 2020).

Acknowledgments

References

Ardyna, M., M. Babin, E. Devered, A. Forest, M. Gosselin, P. Raimbault, and J. -É. Tremblay, 2017: Shelf-basin gradients shape ecological phytoplankton niches and community composition in the coastal Arctic Ocean (Beaufort Sea). Limnol. Oceanogr., **62**, 2113-2132, https://doi.org/10.1002/lno.10554.

Ardyna M., and Coauthors, 2020: Under-ice phytoplankton blooms: Shedding light on the "invisible" part of Arctic primary production. *Front. Mar. Sci.*, **7**, 608032, https://doi.org/10.3389/fmars.2020.608032.

Behrenfeld, M. J., and P. G. Falkowski, 1997: Photosynthetic rates derived from satellite-based chlorophyll concentration. *Limnol. Oceanogr.*, **42**(1), 1-20, https://doi.org/10.4319/lo.1997.42.1.0001.

Bouman, H. A., T. Jackson, S. Sathyendranath, and T. Platt, 2020: Vertical structure in chlorophyll profiles: influence on primary production in the Arctic Ocean. *Philos. Trans. Roy. Soc. A*, **378**, 20190351, https://doi.org/10.1098/rsta.2019.0351.

Comiso, J. C., 2015: Variability and trends of the global sea ice covers and sea level: Effects on physicochemical parameters. Climate and Fresh Water Toxins, L. M. Botana, M. C. Lauzao, and N. Vilarino, Eds., De Gruyter, Berlin, Germany, https://doi.org/10.1515/9783110333596-003.

Comiso, J. C., W. N. Meier, and R. Gersten, 2017: Variability and trends in the Arctic Sea ice cover: Results from different techniques. *J. Geophys. Res.-Oceans*, **122**, 6883-6900, https://doi.org/10.1002/2017JC012768.

Cooper L. W., and J. M. Grebmeier, 2022: A chlorophyll biomass time-series for the Distributed Biological Observatory in the context of seasonal sea ice declines in the Pacific Arctic region. *Geosciences*, **12**(8), 307, https://doi.org/10.3390/geosciences12080307.

Crawford, A. D., K. M. Krumhardt, N. S. Lovenduski, G. L. Van Dijken, and K. R. Arrigo, 2020: Summer high-wind events and phytoplankton productivity in the Arctic Ocean. *J. Geophys. Res.-Oceans*, **125**, e2020JC016565, https://doi.org/10.1029/2020jc016565.

Frey, K. E., J. C. Comiso, L. W. Cooper, J. M. Grebmeier, and L. V. Stock, 2021: Arctic ocean primary productivity: The response of marine algae to climate warming and sea ice decline. *Arctic Report Card 2021*, T. A. Moon, M. L. Druckenmiller, and R. L. Thoman, Eds., https://doi.org/10.25923/kxhb-dw16.

Gaffey, C. B., K. E. Frey, L. W. Cooper, and J. M. Grebmeier, 2022: Phytoplankton bloom stages estimated from chlorophyll pigment proportions suggest delayed summer production in low sea ice years in the northern Bering Sea. *PLoS ONE*, **17**, e0267586, https://doi.org/10.1371/journal.pone.0267586.

Holding, J. M., and Coauthors, 2015: Temperature dependence of CO_2-enhanced primary production in the European Arctic Ocean. *Nat. Climate Change*, **5**, 1079-1082, https://doi.org/10.1038/nclimate2768.

Hopwood, M. J., and Coauthors, 2020: Review article: How does glacier discharge affect marine biogeochemistry and primary production in the Arctic? *Cryosphere*, **14**, 1347-1383, https://doi.org/10.5194/tc-14-1347-2020.

Lewis, K. M., and K. R. Arrigo, 2020: Ocean color algorithms for estimating chlorophyll *a*, CDOM absorption, and particle backscattering in the Arctic Ocean. *J. Geophys. Res.-Oceans*, **125**, e2019JC015706, https://doi.org/10.1029/2019JC015706.

Mundy, C. J., and Coauthors, 2009: Contribution of under-ice primary production to an ice edge upwelling phytoplankton bloom in the Canadian Beaufort Sea. *Geophys. Res. Lett.*, **36**, L17601, https://doi.org/10.1029/2009GL038837.

Popova, E. E., A. Yool, A. C. Coward, Y. K. Aksenov, S. G. Alderson, A. de Cuevas, and T. R. Anderson, 2010: Control of primary production in the Arctic by nutrients and light: insights from a high-resolution ocean general circulation model. *Biogeosciences*, **7**, 3569-3591, https://doi.org/10.5194/bg-7-3569-2010.

Terhaar, J., R. Lauerwald, P. Regnier, N. Gruber, and L. Bopp, 2021: Around one third of current Arctic Ocean primary production sustained by rivers and coastal erosion. *Nat. Comm.*, **12**, 169, https://doi.org/10.1038/s41467-020-20470-z.

von Appen, W. J., and Coauthors, 2021: Sea-ice derived meltwater stratification slows the biological carbon pump: results from continuous observations. *Nat. Comm.*, **12**, 7309, https://doi.org/10.1038/s41467-021-26943-z.

November 22, 2022

Tundra Greenness

**G. V. Frost[1], M. J. Macander[1], U. S. Bhatt[2], L. T. Berner[3], J. W. Bjerke[4],
H. E. Epstein[5], B. C. Forbes[6], S. J. Goetz[3], M. J. Lara[7,8], G. K. Phoenix[9],
S. P. Serbin[10], H. Tømmervik[4], D. A. Walker[11], and D. Yang[10,12]**

[1]Alaska Biological Research, Inc., Fairbanks, AK, USA
[2]Geophysical Institute, University of Alaska Fairbanks, Fairbanks, AK, USA
[3]School of Informatics, Computing and Cyber Systems, Northern Arizona University, Flagstaff, AZ, USA
[4]Norwegian Institute for Nature Research, FRAM - High North Research Centre for Climate and the Environment, Tromsø, Norway
[5]Department of Environmental Sciences, University of Virginia, Charlottesville, VA, USA
[6]Arctic Centre, University of Lapland, Rovaniemi, Finland
[7]Department of Plant Biology, University of Illinois, Urbana, IL, USA
[8]Department of Geography, University of Illinois, Urbana, IL, USA
[9]School of Biosciences, University of Sheffield, Sheffield, UK
[10]Environmental and Climate Sciences Department, Brookhaven National Laboratory, Upton, NY, USA
[11]Institute of Arctic Biology, University of Alaska Fairbanks, Fairbanks, AK, USA
[12]Department of Ecology and Evolution, Stony Brook University, Stony Brook, NY, USA

Highlights

- The circumpolar average peak tundra greenness value in 2022 declined from the record high values of the previous two years, but still represented the fourth highest value since 2000.
- Tundra greenness in 2022 was high in most of the North American Arctic, but unusually low in northeastern Siberia, consistent with persistent summer sea-ice in the adjacent Chukchi Sea.
- Wildfires, extreme weather events, and other disturbances have become more frequent, highlighting components of Arctic change that drive increased regional variability in tundra greenness.

Introduction

Earth's northernmost continental landmasses and island archipelagos are home to the Arctic tundra biome, a 5.1 million km^2 region characterized by low-growing, treeless vegetation (CAVM Team 2003). The tundra biome forms a "ring" of cold-adapted vegetation atop the globe, bordered by the Arctic Ocean to the north and the boreal forest biome to the south. The biological, physical, and climatic conditions of Arctic tundra ecosystems are changing profoundly, as vegetation and underlying permafrost soils are strongly influenced by warming air temperatures and the rapid decline of sea ice on the nearby Arctic Ocean (Bhatt et al. 2021; see essays *Surface Air Temperature* and *Sea Ice*). In the late 1990s, a sharp increase in the productivity of tundra vegetation became evident in global satellite observations, a phenomenon that has come to be known as "the greening of the Arctic." Arctic greening is dynamically linked with Earth's changing climate, permafrost, seasonal snow, and sea-ice cover, and continues to be a subject of multi-disciplinary scientific research.

Satellite observations of tundra greenness

In 2022, the era of spaceborne global vegetation monitoring entered its fifth decade. Global vegetation has been consistently monitored from space since 1982 by the Advanced Very High Resolution Radiometer (AVHRR) onboard NOAA satellites. In 2000, the Moderate Resolution Imaging Spectroradiometer (MODIS) entered the constellation of Earth-observing satellites and provides a more recent record with higher spatial resolution and improved calibration. Both sensors monitor vegetation greenness using the Normalized Difference Vegetation Index (NDVI), a spectral metric that exploits the unique way in which green vegetation absorbs and reflects light in the visible and infrared wavelengths. The AVHRR and MODIS records both indicate that the yearly maximum tundra greenness (MaxNDVI) has increased across most of the circumpolar Arctic during 1982-2021 and 2000-22, respectively (Figs. 1a,b).
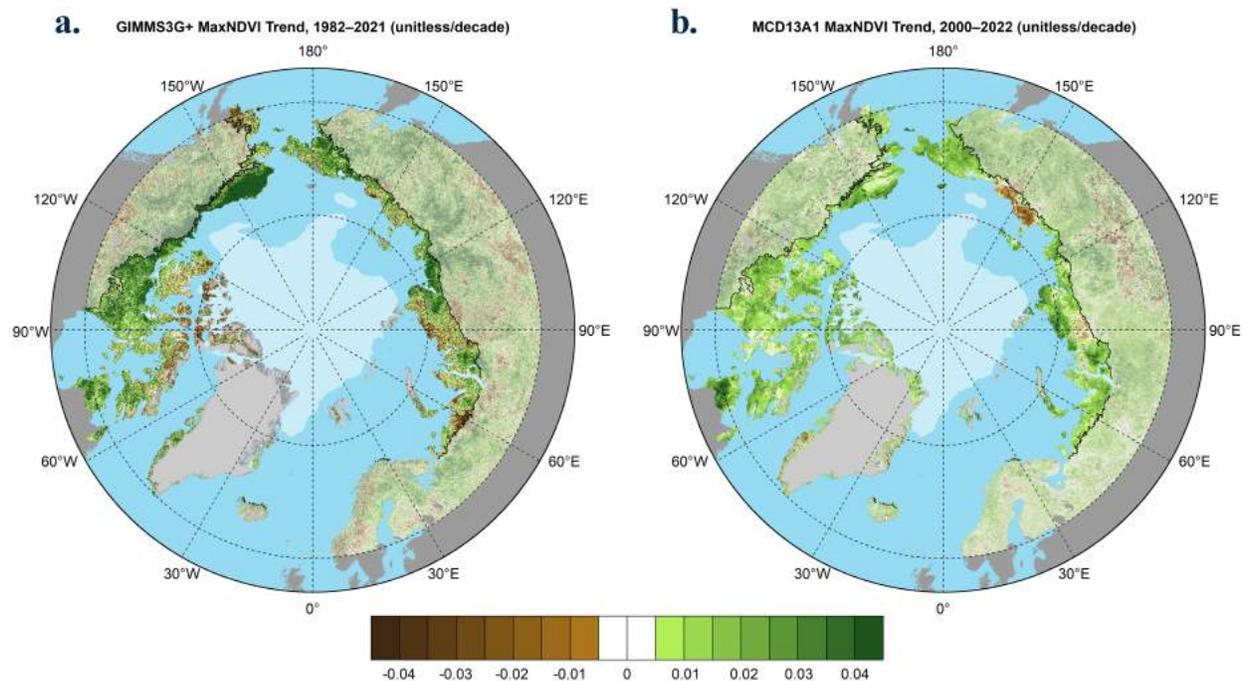
Fig. 1. Magnitude of the MaxNDVI trend calculated as the change per decade using ordinary least squares regression for Arctic tundra (solid colors), and boreal forest north of 60° latitude (muted colors) during (a) 1982-2021 based on the AVHRR GIMMS-3g+ dataset, and (b) 2000-22 based on the MODIS MCD13A1 v6.1 dataset. In each panel, the circumpolar treeline is indicated by a black line, and the 2022 minimum sea-ice extent is indicated by light shading.

Several tundra regions display particularly strong positive (greening) trends in both records. In North America, greening has been strongest on Alaska's North Slope and the Canadian mainland. In Eurasia, strong greening has occurred in the Russian Far East (Chukotka), but browning is evident in the East Siberian Sea region and parts of the Taymyr Peninsula. Trends in northwestern Siberia and the European Arctic provide mixed signals of greening and browning across the two satellite records, which may be partly due to their different observational periods. Regional contrasts in greening highlight the complexity of Arctic change, and the rich web of interactions that exist between tundra ecosystems and the local properties of sea ice, permafrost, seasonal snow, soil composition and moisture, disturbance processes, wildlife (see essays *Terrestrial Snow Cover*, *Arctic Pollinators*, and *Arctic Geese of North America*), and human activities (Heijmans et al. 2022; Jorgenson et al. 2022; Macander et al. 2022). Parsing the underlying drivers of complex Arctic trends is an important step toward improved monitoring of tundra ecosystem function (Rogers et al. 2022).

The boreal forest biome (see Figs. 1a,b), which occupies large portions of continental Eurasia and North America north of the Arctic Circle, has also emerged as a focal point of global environmental change. In this region, greenness trends resemble a patchwork quilt, with areas of interspersed greening and "browning" (i.e., productivity decreases) that are closely linked to complex interactions among climate change, wildfire history, pathogens, human land-use, and other factors (Berner and Goetz 2022; Dial et al. 2022).

In 2021—the most recent year with observations from both AVHRR and MODIS—circumpolar mean MaxNDVI for tundra regions declined from the record high values set in 2020 for both satellite records. AVHRR-observed MaxNDVI declined 8.3% from 2020; nonetheless, the 2021 value still exceeded the 1991-2020 mean value and represented the 15th highest value recorded in the full 40-year record (Fig. 2). Notably, the six highest circumpolar average peak greenness values in the long-term AVHRR record (1982-2021) have all been recorded in the last 10 years. The 2020 to 2021 decline in MaxNDVI was less pronounced for MODIS (2.7%), and the 2021 value was the second highest value in the 22-year record for that sensor. Circumpolar MaxNDVI time-series for the two sensors show virtually identical trends for the period of overlap (2000-21), although the AVHRR record displays higher variability, especially over the last 10 years. This is likely due in part to the lower spatial resolution and less advanced calibration of the AVHRR sensor compared to MODIS.
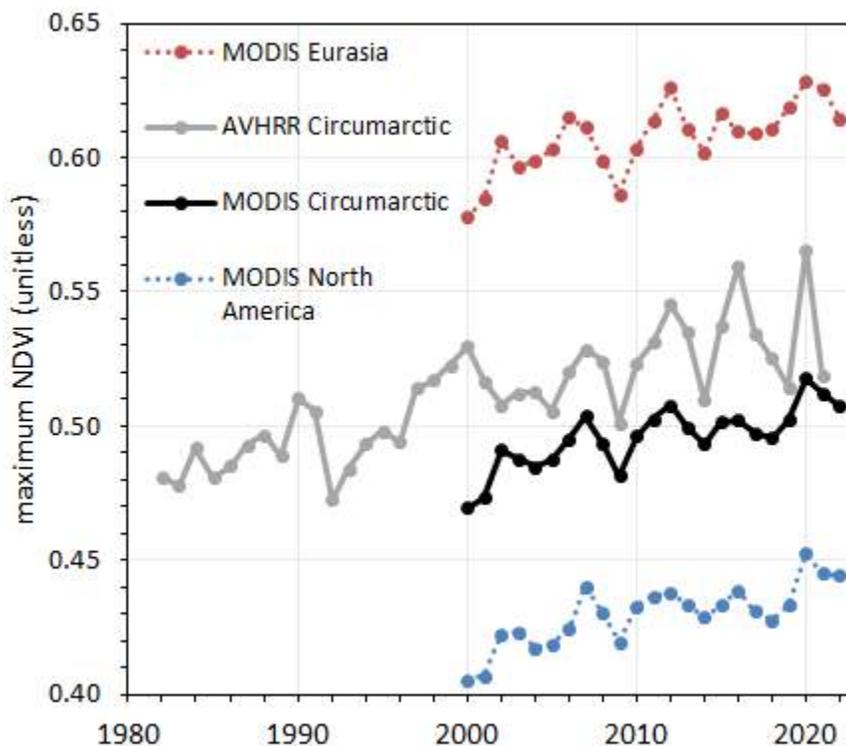
Fig. 2. Time series of mean MaxNDVI for Arctic tundra from the MODIS MCD13A1 v6.1 (2000-22) dataset for the Eurasian Arctic (red), North American Arctic (blue), and the circumpolar Arctic (black), and from the long-term AVHRR GIMMS-3g+ dataset (1982-2021) for the circumpolar Arctic (gray).

In 2022, the circumpolar MODIS-observed MaxNDVI value declined 0.9% from the previous year, but nonetheless represented the 4th highest value in the 23-year MODIS record and continued a series of exceptionally high values that began in 2020 (Fig. 2). Tundra greenness was relatively high in the Canadian Arctic Archipelago, northern Quebec, and central Siberia, but was strikingly low in

northeastern Siberia, which experienced unusually persistent summer sea ice and northerly winds in summer 2022 (Fig. 3; see essays *Sea Ice* and *Surface Air Temperature*). The overall trend in MODIS-observed circumpolar MaxNDVI is strongly positive, and circumpolar values have exceeded the 23-year mean in eleven of the last thirteen growing seasons (Fig. 2).
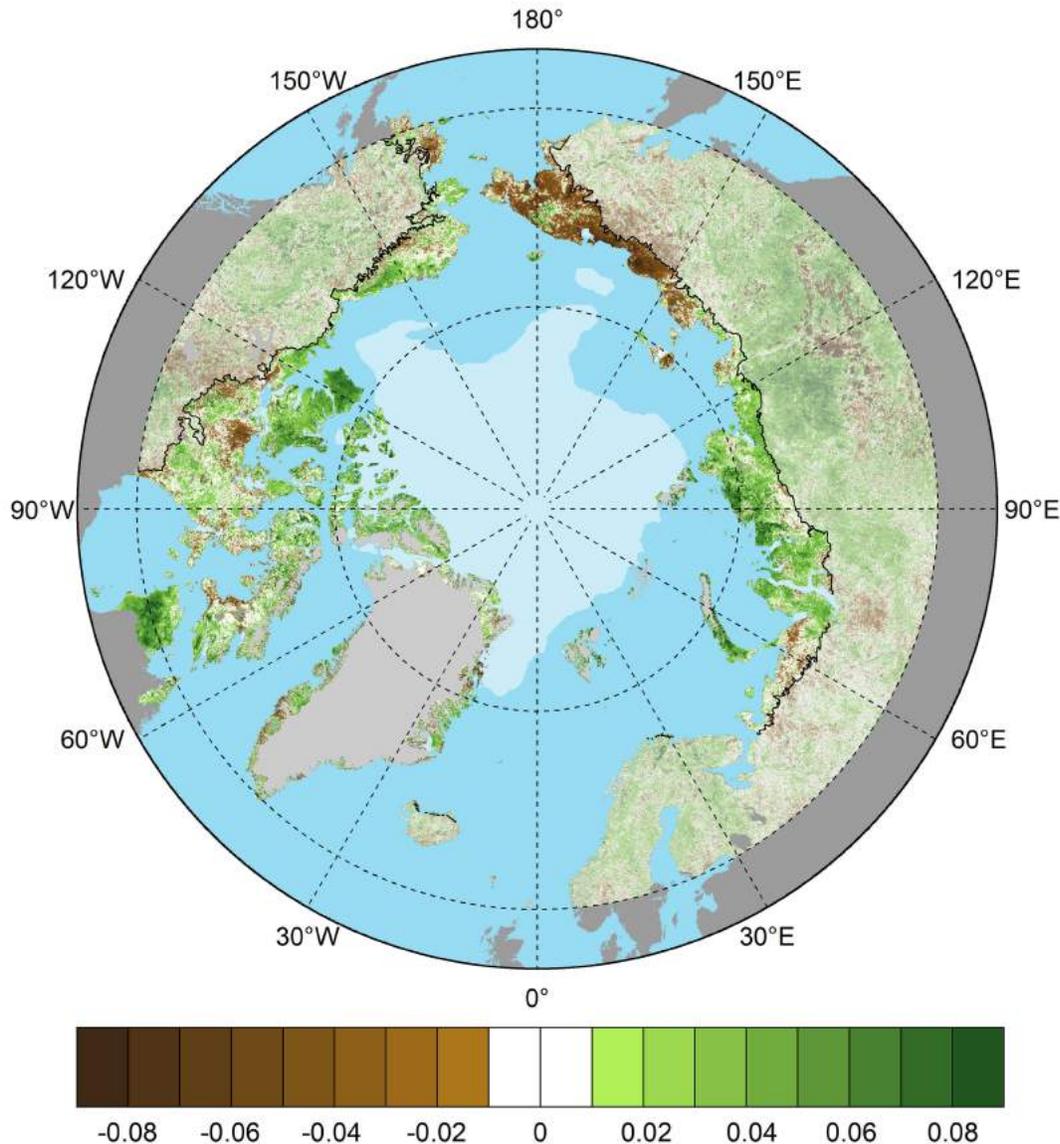
Fig. 3. Circumpolar MaxNDVI anomalies for the 2022 growing season relative to mean values (2000-22) from the MODIS MCD13A1 v6.1 dataset. The 2022 minimum sea-ice extent is indicated by light shading.

Interpretation of greening trends

What are the drivers that underlie tundra greening trends, and what types of change might an observer see on the ground? Recent low-altitude remote sensing and field-based studies provide detail and context for understanding changes in vegetation and landscape features that contribute to the greenness trends observed by satellites (Magnússon et al. 2022; Yang et al. 2022). Increases in the

abundance and height of Arctic shrubs are a key driver of Arctic greening, and have important impacts on biodiversity, surface energy balance, permafrost temperatures, and biogeochemical cycling. However, many Arctic landscapes are a complex mosaic of lakes, ponds, marshes, and upland vegetated terrain, and this heterogeneity presents challenges in quantifying the drivers and impacts of vegetation change and landscape disturbance.

Several Arctic regions experienced widespread disturbance and extreme weather in 2022. For example, western Alaska's Yukon-Kuskokwim Delta experienced extensive wildfires, continuing a series of years with burned areas far exceeding normal historical conditions. Summer heat waves were prevalent across the European, Asian, Greenland-Iceland, and North American Arctic in 2022 (see essay *Surface Air Temperature*).

Although the satellite record provides unequivocal evidence of widespread tundra greening, there is substantial regional variability in trends. Some Arctic regions exhibit little or no trend, and a few, such as the East Siberian Sea sector, exhibit widespread browning, which is likely due in part to ground subsidence and increased surface water triggered by permafrost thaw (Magnússon et al. 2022). In addition, areas of tundra greening and browning can be interspersed even within local landscapes. For example, complex mosaics of greening and browning in northwestern Canada are driven by interactions among tundra vegetation, local soil and permafrost conditions, and topography (Seider et al. 2022). While warming is likely to continue to drive Arctic greening, extreme events and other causes of browning are also increasing in frequency (Christensen et al. 2021), highlighting the emergence of increased variability as a component of Arctic climate change.

Methods and data

The satellite record of Arctic tundra greenness began in 1982 using AVHRR, a sensor that collects daily observations and continues to operate onboard polar-orbiting satellites. As of September 2022, however, processed AVHRR data were only available through the 2021 growing season. Therefore, we also report observations from the Moderate Resolution Imaging Spectroradiometer (MODIS), a more modern sensor with improved calibration and spatial resolution that became operational in 2000. The long-term AVHRR dataset analyzed here for 1982-2021 is the Global Inventory Modeling and Mapping Studies 3g V1.2 dataset (GIMMS-3g+), which is based on corrected and calibrated AVHRR data with a spatial resolution of about 8 km (Pinzon and Tucker 2014). For MODIS, we computed tundra greenness trends for 2000-22 at a much higher spatial resolution of 500 m, combining 16-day Vegetation Index products from Terra (MOD13A1, version 6.1) and Aqua (MYD13A1, version 6.1), referred to as MCD13A1. Circumpolar maps depicting greenness trends cover the full Arctic tundra biome (CAVM Team 2003), as well as boreal forests and non-Arctic tundra north of 60° N latitude. For time series plots, data were masked to include only ice-free land within the extent of the Circumpolar Arctic Vegetation Map. MODIS data were further masked to exclude permanent water based on the 2015 MODIS Terra Land Water Mask (MOD44W, version 6). We summarize the GIMMS-3g+ and MODIS records for Maximum NDVI (MaxNDVI), the peak yearly value that is typically observed during the months of July and August.

Acknowledgments

References

Berner, L. T., and S. J. Goetz, 2022: Satellite observations document trends consistent with a boreal forest biome shift. *Glob. Change Biol.*, **28**(10), 3275-3292, https://doi.org/10.1111/gcb.16121.

Bhatt, U. S., and Coauthors, 2021: Climate drivers of Arctic tundra variability and change using an indicators framework. *Environ. Res. Lett.*, **16**, 055019, https://doi.org/10.1088/1748-9326/abe676.

CAVM Team, 2003: Circumpolar Arctic vegetation map (1:7,500,000 scale). Conservation of Arctic Flora and Fauna (CAFF) Map No. 1 U.S. Fish and Wildlife Service, Anchorage, AK.

Christensen, T. R., and Coauthors, 2021: Multiple ecosystem effects of extreme weather events in the Arctic. *Ecosystems*, **24**, 122-136, https://doi.org/10.1007/s10021-020-00507-6.

Dial, R. J., C. T. Maher, R. E. Hewitt, and P. F. Sullivan, 2022: Sufficient conditions for rapid range expansion of a boreal conifer. *Nature*, **608**, 546-551, https://doi.org/10.1038/s41586-022-05093-2.

Heijmans, M. M. P. D., and Coauthors, 2022: Tundra vegetation change and impacts on permafrost. *Nat. Rev. Earth Environ.*, **3**, 68-84, https://doi.org/10.1038/s43017-021-00233-0.

Jorgenson, M. T., and Coauthors, 2022: Rapid transformation of tundra ecosystems from ice-wedge degradation. *Global Planet. Change*, **216**, 103921, https://doi.org/10.1016/j.gloplacha.2022.103921.

Macander, M. J., P. R. Nelson, T. W. Nawrocki, G. V. Frost, K. M. Orndahl, E. C. Palm, A. F. Wells, and S. J. Goetz, 2022: Time-series maps reveal widespread change in plant functional type cover across Arctic and boreal Alaska and Yukon. *Environ. Res. Lett.*, **17**, 054042, https://doi.org/10.1088/1748-9326/ac6965.

Magnússon, R. Í., A. Hamm, S. V. Karsanaev, J. Limpens, D. Kleijn, A. Frampton, T. C. Maximov, and M. M. P. D. Heijmans, 2022: Extremely wet summer events enhance permafrost thaw for multiple years in Siberian tundra. *Nat. Commun.*, **13**, 1556, https://doi.org/10.1038/s41467-022-29248-x.

Pinzon, J. E., and C. J. Tucker, 2014: A non-stationary 1981-2012 AVHRR NDVI$_{3g}$ time series. *Remote Sens.*, **6**, 6929-6960, https://doi.org/10.3390/rs6086929.

Rogers, A., S. P. Serbin, and D. A. Way, 2022: Reducing model uncertainty of climate change impacts on high latitude carbon assimilation. *Glob. Change Biol.*, **28**, 1222-1247, https://doi.org/10.1111/gcb.15958.

Seider, J. H., T. C. Lantz, T. Hermosilla, M. A. Wulder, and J. A. Wang, 2022: Biophysical determinants of shifting tundra vegetation productivity in the Beaufort Delta region of Canada. *Ecosystems*, https://doi.org/10.1007/s10021-021-00725-6.

Yang, D., and Coauthors, 2022: Remote sensing from unoccupied aerial systems: Opportunities to enhance Arctic plant ecology in a changing climate. *J. Ecol.*, https://doi.org/10.1111/1365-2745.13976.

November 21, 2022

Satellite Record of Pan-Arctic Maritime Ship Traffic

P. A. Berkman[1,2,3], G. J. Fiske[4], D. Lorenzini[5], O. R. Young[6], K. Pletnikoff[7,8], J. M. Grebmeier[9], L. M. Fernandez[10], L. M. Divine[11], D. Causey[12], K. E. Kapsar[13], and L. L. Jørgensen[14]

[1]Science Diplomacy Center™, Falmouth, MA, USA
[2]Program on Negotiation at Harvard Law School, Cambridge, MA, USA
[3]United Nations Institute for Training and Research (UNITAR), Geneva, Switzerland
[4]Woodwell Climate Research Center, Falmouth, MA, USA
[5]AAC SpaceQuest, Fairfax, VA, USA
[6]Bren School of Environmental Science & Management, University of California Santa Barbara, Santa Barbara, CA, USA
[7]Aleutian Pribilof Islands Association, Anchorage, AK, USA
[8]Aleut International Association, Anchorage, AK, USA
[9]Chesapeake Biological Laboratory, University of Maryland Center for Environmental Science, University of Maryland, Solomons, MD, USA
[10]Department of Economics, Center for Environmental Studies, Virginia Commonwealth University, Richmond, VA, USA
[11]Aleut Community of St. Paul Island Tribal Government, St. Paul Island, AK, USA
[12]Arctic Domain Awareness Center, University of Alaska, Anchorage, AK, USA
[13]Center for Systems Integration and Sustainability, Department of Fisheries and Wildlife, Michigan State University, East Lansing, MI, USA
[14]Institute of Marine Research, Tromsø, Norway

Highlights

- Satellite-based records from 1 September 2009 through 31 December 2018 reveal increasing maritime ship traffic, with pronounced seasonality, within all Law of the Sea zones north of the Arctic Circle.
- Arctic maritime ship traffic is increasing as sea ice is diminishing, representing the 'ship-ice hypothesis' to test over diverse time and space scales in view of socioeconomic impacts and the dynamics of natural systems.
- Maritime ship traffic into the Central Arctic Ocean High Seas predominates from the Pacific sector through the Bering Strait and Beaufort Sea, as revealed by ship types, sizes, and flag states from 2009-18 with complementary satellite-observed increases in the Bering Sea from 2015 to 2020.

Introduction

A prominent socioeconomic development in recent years has been an increase in maritime ship traffic (characterized in view of ship movements and attributes of type, size, and flag state) in the Arctic Ocean as the sea ice diminishes with climate warming (see essay *Sea Ice*). Increasing maritime ship traffic has diverse implications for Arctic and non-Arctic communities in view of emergent and projected shipping

routes (Fig. 1). Shipping activities also impact biogeophysical systems, generating environmental and societal risks—especially for Indigenous Peoples, with system impacts in the:

- **Atmosphere:** Greenhouse gas impacts, including heavy fuel-oil burning that produces black carbon with ice-surface darkness impacts (IMO 2021);
- **Ocean:** Pollution impacts (Sheffield et al. 2021) on marine ecosystems (see essay *Primary Productivity*); overharvesting marine living resources; marine species disturbances, including ship strikes on marine mammals and birds; underwater noise (Stafford 2021); and invasive species introductions that change trophic interactions;
- **Communities:** Port development, socioeconomic impacts, and access changes.
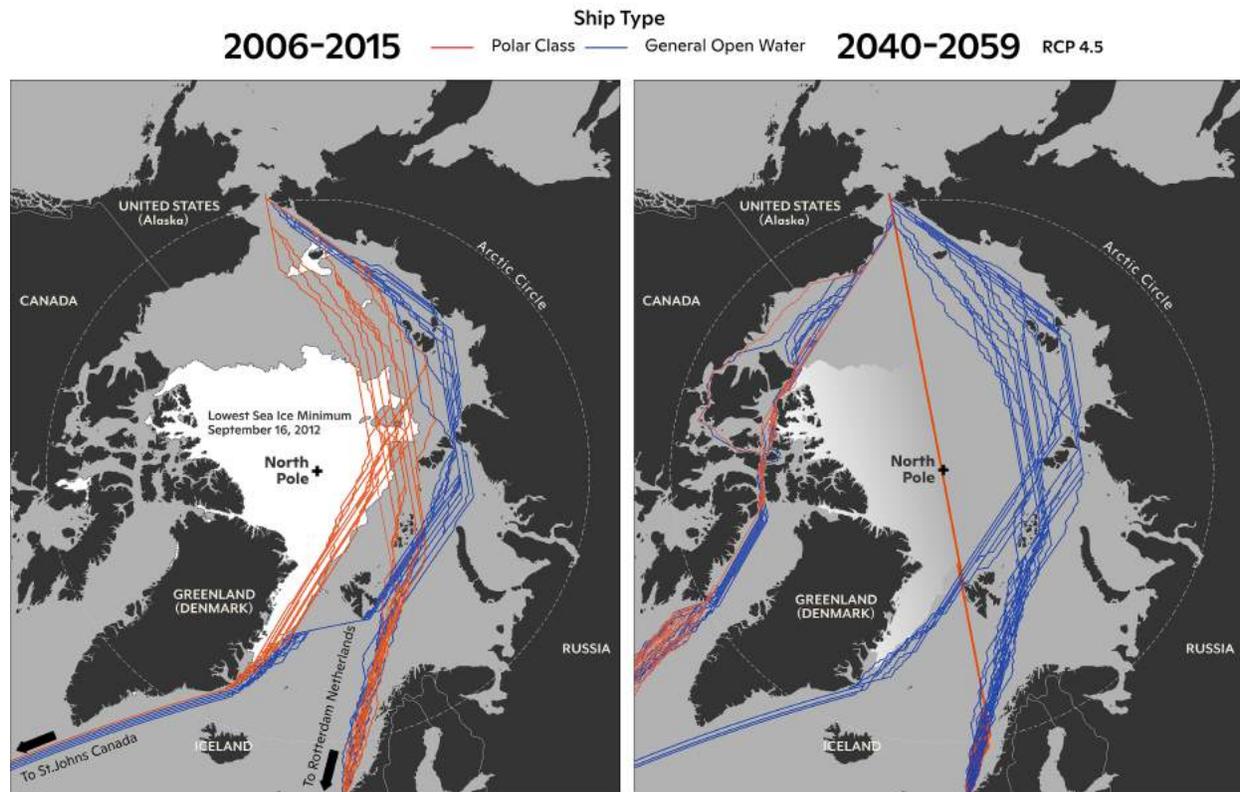
Fig. 1. Model of maritime ship-traffic in the Arctic Ocean (Smith and Stephenson 2013), predicting trade routes that will open as sea ice diminishes through mid-21st century with polar-class ships that are ice-strengthened (orange) according to the International Association of Classification Societies (IACS) and other ship types that are designed for open water (blue).

Indigenous communities are the most vulnerable (Sheffield et al. 2021), respecting they have resided continuously on islands and along the coastlines of Arctic landmasses in a resilient manner in the face of ecosystem changes across millennia. The applications and implications of maritime ship traffic also are cross-cutting with the five binding Arctic agreements that have entered into force during the past decade with Arctic states as well as non-Arctic states (Berkman et al. 2022a).

Maritime ship traffic data across jurisdictions in the Arctic Ocean

Satellite Automatic Identification System (S-AIS) observations north of the Arctic Circle began on 1 September 2009, enabling synoptic coverage of maritime ship traffic in the Arctic Ocean (see Methods

and data). The comprehensive pan-Arctic illustration herein (Fig. 2) is based on the framework of the Law of the Sea, to which the eight Arctic states and six Indigenous Peoples' organizations "*remain committed*" (Arctic Council 2013). The Law of the Sea zones are unambiguous in the superjacent waters above the sea floor and objectively defined with the Exclusive Economic Zones (EEZ) beyond and adjacent to the Territorial Sea, extending a maximum of 200 nautical miles from coastal boundaries into the High Seas of the Arctic Ocean (Berkman and Young 2009). This S-AIS baseline from 2009-18 (Berkman et al. 2022b)—which will be brought current with future funding—reveals pronounced seasonality (Fig. 2). The increasing number of ships over time in all national and international maritime jurisdictions north of the Arctic Circle (Tables 1 and 2) raises diverse questions about relative ship-traffic changes and characteristics within as well as between regions seasonally and interannually in view of socioeconomic impacts and the dynamics of natural systems.
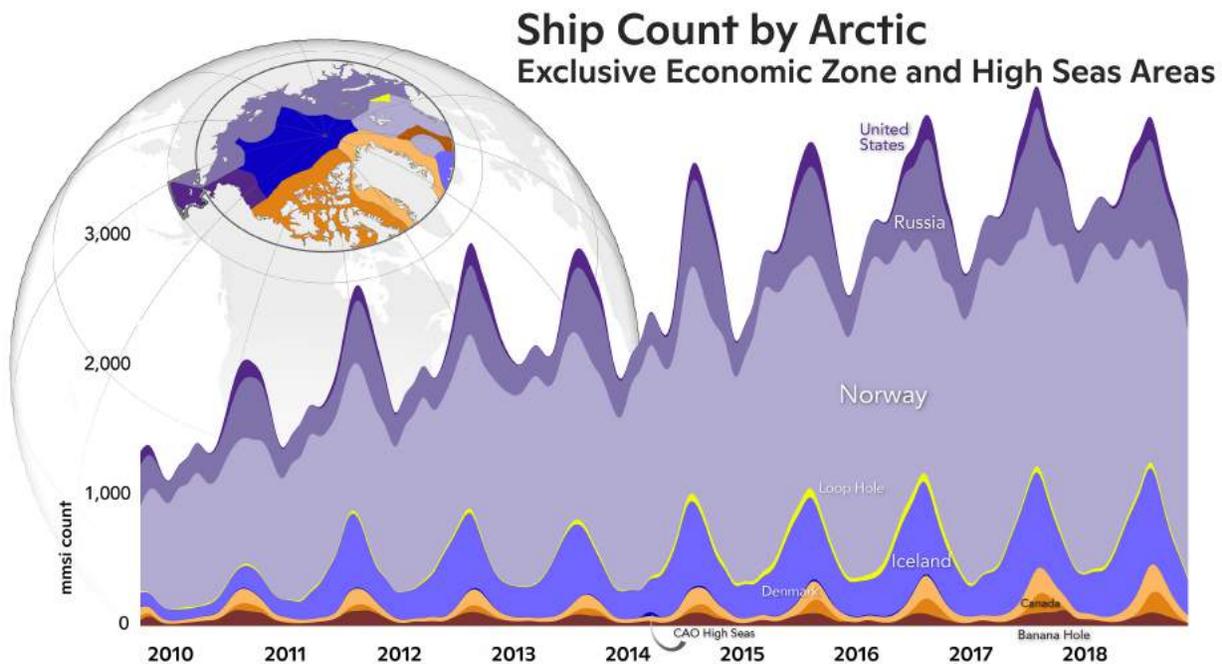
Fig. 2. Oldest continuous S-AIS record of pan-Arctic maritime ship traffic across Law of the Sea zones (United Nations 1982) within and beyond jurisdictions of the six Arctic coastal states north of the Arctic Circle (see Tables 1 and 2), involving more than 173,000,000 S-AIS records from 1 September 2009 to 31 December 2018 (Berkman et al. 2022a,b).

Table 1. Annual and seasonal trends of maritime ship traffic of the Exclusive Economic Zone (EEZ)—areas within national jurisdictions as defined by the international framework of the Law of the Sea for the regions shown in Fig. 2.

Arctic Ocean Area	Total of Monthly Unique Ship Days[1]	Rate of Change[2,3] (2009-18)		
Canada	2,541	Annual: +1.2%	Summer: +2.1%	Winter: -0.1%
Denmark / Greenland	7,563	Annual: +1.7%	**Summer: +2.8%**	**Winter: +0.7%**
Iceland	40,644	**Annual: +10.9%**	**Summer: +15.1%**	**Winter: +5.3%**
Norway	176,048	**Annual: +41.9%**	**Summer: +47.6%**	**Winter: +47.9%**
Russian Federation	43,950	**Annual: +8.8%**	**Summer: +12.5%**	**Winter: +5.0%**
United States	6,836	Annual: +1.0%	**Summer: +1.9%**	Winter: +0.1%

[1]Total number of unique ships derived with S-AIS data in each area north of the Arctic Circle (Fig. 2), summed from 111 monthly totals of ships based on daily observations (Berkman et al. 2022b).
[2]Ship numbers versus time from 2009-18 (statistically significant trends highlighted in bold).
[3]Annual and seasonal trends for summer (June-July-August-September) and winter (December-January-February-March) with shoulder periods unanalyzed.

Table 2. Annual and seasonal trends of maritime ship traffic of the High Seas—areas beyond national jurisdictions (ABNJ) as defined by the international framework of the Law of the Sea for the regions shown in Fig. 2.

Arctic Ocean Area	Total of Monthly Unique Ship Days[1]	Rate of Change[2,3] (2009-18)		
Banana Hole	6,426	Annual: +0.1%	Summer: -0.3%	Winter: +0.5%
Central Arctic Ocean (CAO)	494	Annual: +0.2%	Summer: +0.3%	Winter: +0.3%
Loop Hole	3,275	**Annual: +1.1%**	**Summer: +1.4%**	**Winter: +0.7%**

[1]Total number of unique ships derived with S-AIS data in each area north of the Arctic Circle (Fig. 2), summed from 111 monthly totals of ships based on daily observations (Berkman et al. 2022b).
[2]Ship numbers versus time from 2009-18 (statistically significant trends highlighted in bold).
[3]Annual and seasonal trends for summer (June-July-August-September) and winter (December-January-February-March) with shoulder periods unanalyzed.

The centroid of maritime ship traffic also has shifted hundreds of kilometers to the north and east in the Atlantic sectors (NASA 2018), where maritime ship traffic predominates in the Arctic Ocean (Fig. 2). Complementary analyses of Arctic maritime ship traffic after 2013 are available from the Arctic Ship Traffic Database with redacted S-AIS metadata (Arctic Council 2022) and from other public and private sources (Theocharis et al. 2018).

'Ship-ice hypothesis' testing across the Arctic Ocean

Increasing ship traffic with diminishing sea ice has been framed as the 'ship-ice hypothesis,' (Berkman et al. 2020a) which has been tested comprehensively in a pan-Arctic context with daily satellite observations of ship traffic and sea ice within 4 km^2 grids to reveal 'ship-ice interactions' from 2009-16.

Testing and elaborating this hypothesis leads to useful insights, such as identifying the threshold increase in ship-ice interactions in the Arctic Ocean after 2013 and toward higher latitudes, following the sea-ice minimum observed by satellites in 2012.

The Central Arctic Ocean (CAO) High Seas (Fig. 2, Table 2) offer a unique regional test of the 'ship-ice hypothesis', with diminished sea-ice and open-water seasonally on the Pacific sector adjacent to the 180° EW meridian, in contrast to open water year-round in the Atlantic sectors where the ship traffic predominates (Fig. 2, Table 1). The S-AIS metadata with ship flag state, type, and size attributes (Fig. 3) indicate maritime ship traffic into the CAO High Seas is chiefly originating from the Pacific sector of the Arctic Ocean adjacent to the Bering Strait.
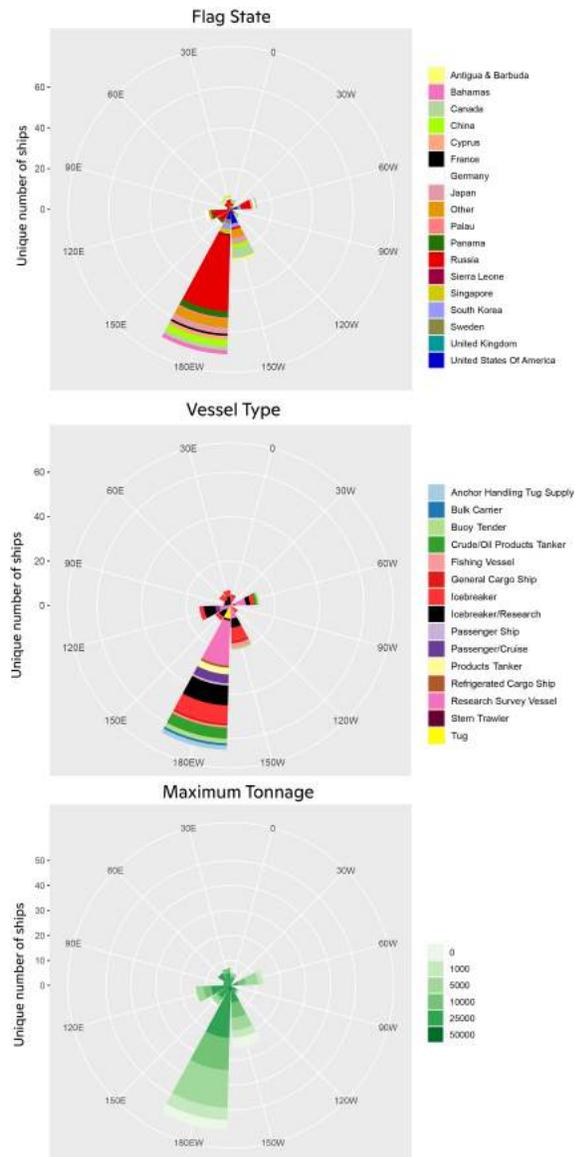
Fig. 3. 'Ship-ice hypothesis' test with the Central Arctic Ocean (CAO) High Seas (Fig. 2), showing predominant directionality of maritime ship traffic from the Pacific sector from the Aleutian Islands northward, in view of: (upper) flag states; (middle) vessel types; and (lower) maximum tonnages, which are recorded in the metadata with S-AIS records of IMO-registered vessels from 2009-18 (Berkman et al. 2022a,b).

Discovery of the primary movement of maritime ship traffic into the CAO High Seas from the Pacific sector (Fig. 3) reveals risks to address among diverse stakeholders, rightsholders, and actors inclusively since the Bering Strait is the narrowest choke point into and out of the Arctic Ocean. This conclusion is reinforced by S-AIS observations of increasing maritime ship traffic in the Bering Sea from 2015-20 (Kapsar et al. 2022), especially considering adjacent Indigenous communities that have inhabited this region for millennia.

Conclusions

From national security interests to continuous considerations among Arctic communities, S-AIS data provide a synoptic pan-Arctic platform (Table 3) to assess patterns, trends, and processes of socioeconomic change with user-defined granularity across the Arctic Ocean. Understanding increasing maritime ship traffic (Figs. 2 and 3, Tables 1 and 2) in relation to the welfare of surrounding coastal communities, dynamics of natural systems with their biogeophysical features, and socioeconomic development of the Arctic as a whole will inform decisions about investments and response capacities across a 'continuum of urgencies' (Berkman et al. 2017) to build resilience in view of Arctic Ocean change.

Methods and data

S-AIS data on a pan-Arctic scale are a technological innovation with distinct advantages, extending the Earth surface observations that had been synthesized from the six Arctic coastal states (Table 1) into the Arctic Marine Shipping Assessment (Arctic Council 2009) and subsequently (Table 3). The baseline S-AIS data herein were collected by AAC SpaceQuest Ltd as part of a public-private partnership supported by the National Science Foundation with Belmont Forum collaborations internationally and deposited in the Arctic Data Center (Berkman et al. 2020b). The key attributes in the S-AIS data are location (latitude and longitude) and timestamp for each unique ship along with metadata about ship characteristics for vessels that are IMO registered.

Table 3. Next-Generation Arctic Marine Shipping Assessments (AMSA)[1]

Attribute	AMSA (Arctic Council 2009)	Next-Generation AMSA[2]
Sampling Period	2004	2009 forward
Data Sources	Arctic States Individually	Diverse Government and Commercial Satellite Automatic Identification System (S-AIS) Receivers
Observation Coverage	Point, Regional	Point, Regional, and Pan-Arctic
Observation Scope	Ground-Based	Ground-Based and Satellite
Observation Frequency	Inconsistent over Space and Time	Synoptic and Continuous (seconds-decades)
Ship-Type Designations	Variable National Designations	Standardized International Designations
Individual Ship Attributes	Inconsistent and Incomplete	Consistent and Comprehensive
Analytical Capacity	Limited Granularity and Questions	Open-Ended Granularity and Questions
Science-Diplomacy Contributions	Scenarios and Negotiated Recommendations	Holistic Evidence and Options (without advocacy)
Informed Decisionmaking	Governance Mechanisms	Operations, Built Infrastructure, and Governance Mechanisms

[1]Modified from Berkman et al. (2020a).
[2]Involves ship transponder data received by polar-orbiting satellites.

Geospatial data were integrated over time with the 'space-time cube' (in the cloud and analyzed with SQL queries of tables through the Google Compute Engine with BigQuery (Berkman et al. 2020a, 2022b). This analytical approach enabled integration with other spatial datasets with time stamps, as demonstrated with sea-ice data on a pan-Arctic scale within 4 km^2 grids to reveal ship-ice interactions. Relational databases in the cloud have a wealth of advantages, including cost-effectiveness, scalability, analytical speed, and n-dimensional dataset integration to 'future-proof' next-generation AMSA with user-defined applications.

Acknowledgments

References

Arctic Council, 2009: *Arctic Marine Shipping Assessment 2009 Report*, 187 pp, https://pame.is/index.php/projects/arctic-marine-shipping/amsa.

Arctic Council, 2013: *Vision for the Arctic*, 6 pp, https://oaarchive.arctic-council.org/handle/11374/287.

Arctic Council, 2022: Arctic Ship Traffic Data. Accessed 27 September 2022, https://pame.is/index.php/projects/arctic-marine-shipping/astd#astd-geographical-scope.

Berkman, P. A., and O. R. Young, 2009: Governance and environmental change in the Arctic Ocean. *Science*, **324**, 339-340, https://doi.org/10.1126/science.1173200.

Berkman, P. A., L. Kullerud, A. Pope, A. N. Vylegzhanin, and O. R. Young, 2017: The Arctic Science Agreement propels science diplomacy. *Science*, **358**, 596-598, https://doi.org/10.1126/science.aaq0890.

Berkman, P. A., G. Fiske, J.-A. Royset, L. W. Brigham, and D. Lorenzini, 2020a: Next-generation Arctic marine shipping assessments. Governing Arctic Seas: Regional Lessons from the Bering Strait and Barents Sea, Vol. 1, O. R. Young, P. A. Berkman, and A. N. Vylegzhanin, Eds., Springer Nature, 241-268.

Berkman, P. A., G. Fiske, and D. Lorenzini, 2020b: Baseline of Next-Generation Arctic Marine Shipping Assessments - Oldest Continuous Pan-Arctic Satellite Automatic Identification System (AIS) Data Record of Maritime Ship Traffic, 2009-2016, https://doi.org/10.18739/A2TD9N89Z.

Berkman, P. A., J. M. Grebmeier, G. Fiske, and L. L. Jørgenson, 2022a: Satellite observations of maritime ship traffic to enhance implementation of binding agreements in the Arctic Ocean, Arctic Observing Summit 2022, Trømso, Norway, 1-5, https://arcticobservingsummit.org/wp-content/uploads/2022/02/2022_013_Berkman_WG5.pdf.

Berkman, P. A., G. Fiske, J. M. Grebmeier, and A. N. Vylegzhanin, 2022b: Maritime ship traffic in the Central Arctic Ocean High Seas as a case study with informed decisionmaking. Building Common Interests in the Arctic Ocean with Global Inclusion, Vol. 2, P. A. Berkman, A. N. Vylegzhanin, O. R. Young, D. A. Balton, and O. R. Øvretveit, Eds., Springer Nature, 321-346.

IMO, 2021. Further shipping GHG emission reduction measures adopted. International Maritime Organization, London. 17 June 2021, https://www.imo.org/en/MediaCentre/PressBriefings/pages/MEPC76.aspx.

Kapsar, K., B. Sullender, J. Liu, and A. Poe, 2022: North Pacific and Arctic marine traffic dataset (2015-2022). *Data in Brief*, **44**, 108531, https://doi.org/10.1016/j.dib.2022.108531.

NASA, 2018: Shipping Responds to Arctic Ice Decline. Accessed 25 September 2022, https://earthobservatory.nasa.gov/images/91981/shipping-responds-to-arctic-ice-decline.

Sheffield, G., A. Ahmasuk, F. Ivanoff, A. Noongwook, and J. Koonooka, 2021: 2020 Foreign Marine Debris Event—Bering Strait. NOAA Technical Report OAR ARC; 21-12, 8 pp, https://doi.org/10.25923/jwag-eg41.

Smith, L. C., and S. R. Stephenson, 2013: New Trans-Arctic shipping routes navigable by midcentury. *P. Natl. Acad. Sci.*, **10**, 6-10, https://doi.org/10.1073/pnas.1214212110.

Stafford, K. M., 2021: The Changing Arctic Marine Soundscape. NOAA Technical Report OAR ARC; 21-14, https://doi.org/10.25923/jagc-4a84.

Theocharis, D., S. Pettit, V. S. Rodrigues, and J. Haider, 2018: Arctic shipping: A systematic literature review of comparative studies. *J. Transp. Geogr.*, **69**, 112-128, https://doi.org/10.1016/j.jtrangeo.2018.04.010.

United Nations, 1982: Convention on the Law of the Sea. (Signed: Montego Bay, 10 December 1982; Entry into Force: 16 November 1994), https://www.refworld.org/docid/3dd8fd1b4.html.

January 11, 2023

Lake Ice

L. C. Brown[1] and C. R. Duguay[2]

[1]Department of Geography, Geomatics and Environment, University of Toronto Mississauga, Mississauga, ON, Canada
[2]Department of Geography and Environmental Management, University of Waterloo, Waterloo, ON, Canada

Highlights

- Striking differences were observed between lake ice durations in Eurasia and North America, with substantially longer than average ice durations in Eurasia and predominantly shorter in North America.
- Freeze-up occurred later than the 2004-20 average for most of North America (except for western Alaska), with notably later freeze in Canada (~10-20 days later), where warmer temperatures and more snow free days were noted in the fall.
- Ice break-up across the Arctic was mainly within ±10 days of the 2004-21 average, except for some lakes in Europe where later break-up was detected.
- Longer ice durations than average in Europe, particularly southern Finland, were due to both earlier freeze-up (~10-30 days) and later break-up (~10-20 days).

Introduction

Lake ice cover is an important component of the cryosphere and changes to the timing of ice freeze-up, break-up, duration, and thickness can have substantial impacts on weather and climate, transportation, and ecology (e.g., Brown and Duguay 2010; Arp et al. 2019). Since lake ice is predominantly influenced by air temperature changes it is a robust indicator of regional climate trends and variability.

Ground-based observations of lake ice have provided valuable information on long-term trends and variability in the timing and duration of ice cover (e.g., Duguay et al. 2006). Satellite data are frequently used to examine lake ice changes over larger regions than are possible with ground-based observations alone (e.g., Du et al. 2017; Dauginis and Brown 2021). Recent satellite-based records (2004-19) show slight trends towards shorter lake ice durations, with notable annual and regional variability across the Arctic (Dauginis and Brown 2021). However, the recent season (2021/22) shows the 6th longest average pan-Arctic lake ice durations since 2004.

We examine the lake ice cover in the Arctic using a satellite data product that can identify areas of water larger than 4 km x 4 km. We examine the 2021/22 lake ice season by ice-on timing (the date when ice cover is detected for the rest of the winter season), ice-off timing (the date when ice is no longer detected at the end of the season) and the ice cover duration (the number of days between the ice-on and ice-off dates). Data are presented relative to the 2004/05 to 2020/21 lake ice season mean.

Ice cover duration

The ice cover duration highlights a marked difference between North America and Eurasia with predominantly shorter durations in North America (71% of all North American pixels) and predominantly longer durations in Eurasia (82% of Eurasian pixels) (Fig. 1). Longer ice durations in Europe and Alaska were due to both the early ice-on and later ice-off, while the shorter durations in the rest of North America were influenced by later ice-on with near-mean ice-off timing.

Fig. 1. Lake ice cover duration anomalies in 2021/22 relative to the 2004/05 to 2020/21 mean from the IMS 4-km product. Focus regions 1 and 2 are highlighted in Figs. 3 and 4.

Focusing on the larger lakes (Fig. 2), the North American lakes were all near-mean for their lake-wide ice duration (except for Great Bear Lake at 6 days shorter), and since 2004 have experienced a range of 25-40 days between their shortest and longest mean durations. On the Eurasian side, Lake Taymyr in the

north had 1 day longer ice duration, while Lakes Onega and Ladoga were notably longer (Onega: +32 days, 2nd longest duration since 2004/05, and Ladoga: +24 days, 5th longest since 2004/05 and first longer-than-mean duration in several years). The ice durations over the last 18 years are more variable for these lower-latitude lakes where milder winters occur.
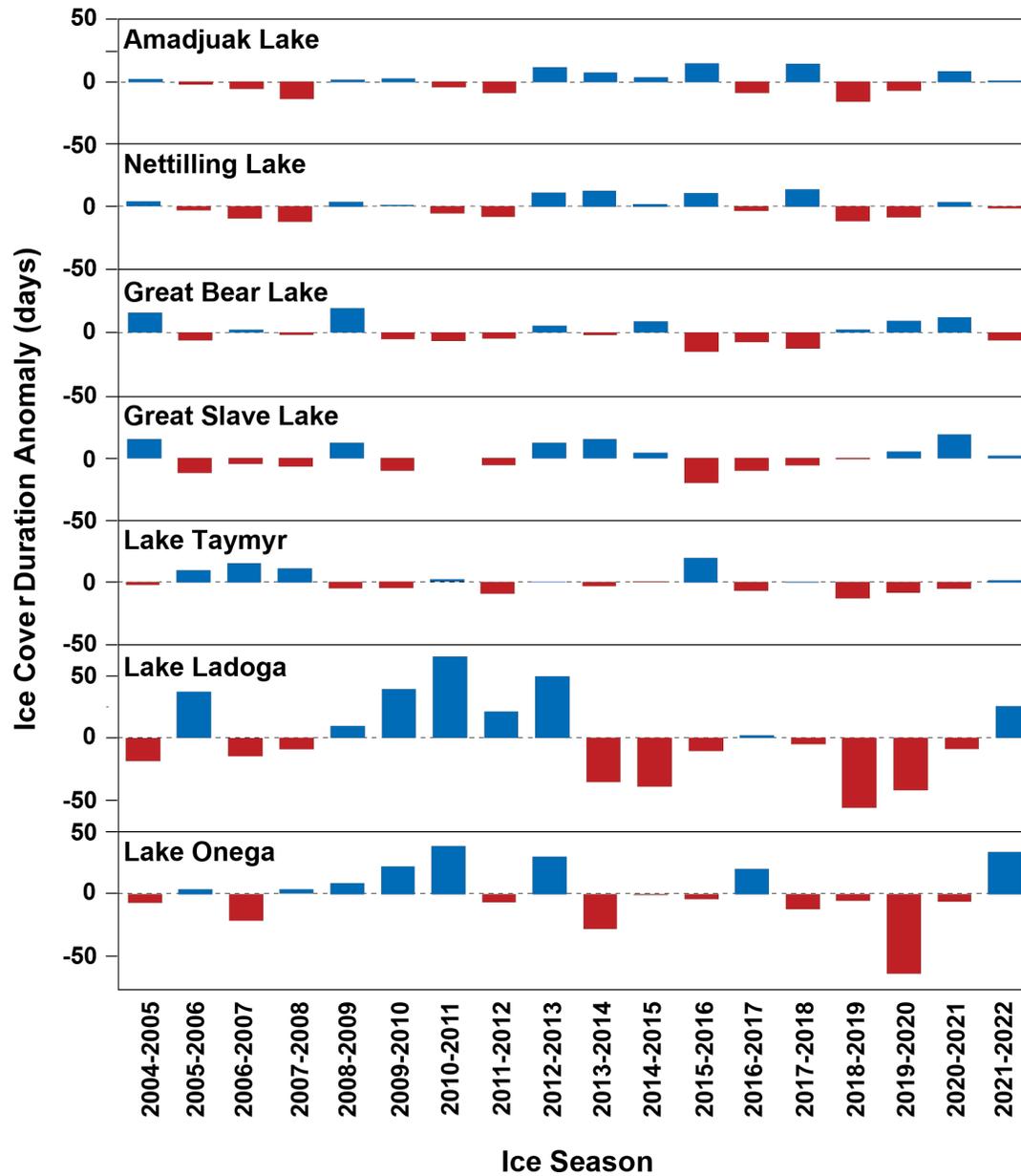
Fig. 2. Lake-wide ice cover duration anomalies for large lakes in Canada (Amadjuak, Nettilling, Great Bear, Great Slave) and Russia (Taymyr, Ladoga, Onega) derived from the full length of the IMS 4-km product (2004/05 to 2022/22).

Ice-on

Substantial regional variability is shown for ice-on in Eurasia compared to North America (Fig. 3). Forty-seven percent of all lake ice pixels were identified as ice covered 0-20 days later than average; primarily located in North America where most lakes experienced a later freeze. Conversely, 51% of the lake ice

pixels experienced an earlier ice-on, with this percentage driven mainly by earlier ice detection in Eurasia and Alaska. Overall, the average ice-on date for the pan-Arctic was 4th earliest since 2004.
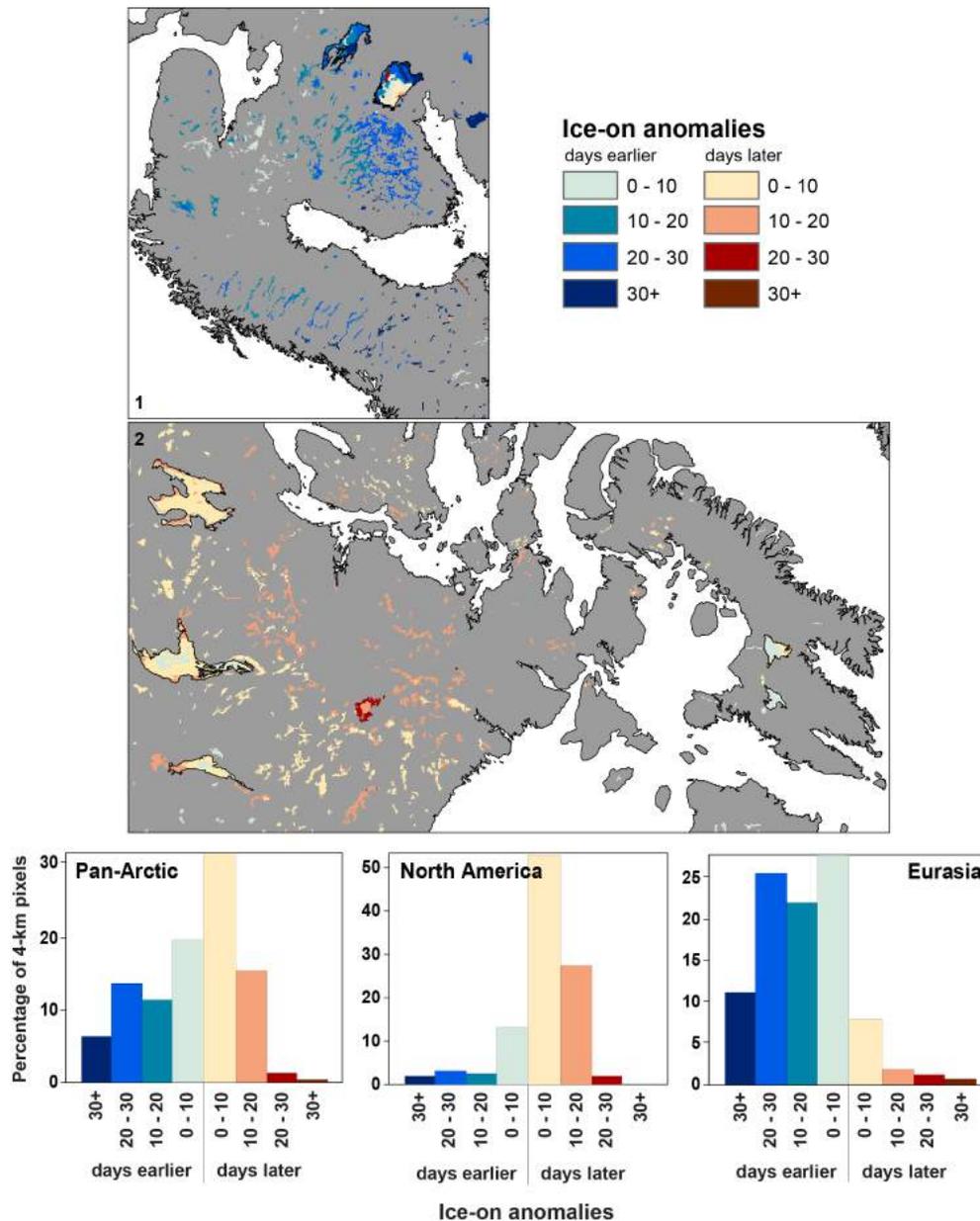
Fig. 3. Lake ice-on anomalies in 2021/22 relative to the 2004/05 to 2020/21 mean from the IMS 4-km product. Focus regions as outlined in Fig. 1.

While lakes across Eurasia predominantly experienced earlier ice-on in 2021, some specific regions of later ice-on are evident in southern Sweden. Lake Onega showed earlier ice-on anomalies ranging from a week to a month earlier, while the larger Lake Ladoga experienced earlier ice-on in the southern extent, but later (mainly in the 10-20 days later category) for the rest of the lake.

A particularly early ice cover was detected in southern Finland with a large cluster of lakes forming ice nearly a month earlier than the mean period; early December, rather than the end of December/early January. While the October-December seasonal temperature there was near the climatological mean

(see essay *Surface Air Temperature*), December 2021 experienced 5-6°C cooler than recent (2004-21) December temperatures. A higher percentage of snow-covered days during the snow-onset period were also noted in this region (see essay *Terrestrial Snow*).

In North America, several Alaskan lakes also showed earlier ice-on dates, ranging up to about a month earlier than average. Earlier freeze in this region corresponds to cooler fall air temperatures, and a longer duration of snow on the ground (see essays *Surface Air Temperature* and *Terrestrial Snow*). While Alaskan lakes saw earlier ice-on dates, most North American lakes experienced a later than average ice-on. Lake Athabasca, Great Bear Lake, and Great Slave Lake were near mean (mostly within ~1 week); however, the region to the east of these lakes (to the west of Hudson Bay) experienced later than usual ice-on, reaching up to a month later than the mean (majority in the 10-20 days later category). A warmer than usual fall in this region resulted in lakes in the northern portion freezing in early November rather than late October, and lakes further south freezing in late, rather than early, November. To the northeast, Nettilling and Amadjuak Lakes were near-mean with ~5 days earlier ice-on.

Ice-off

Across the pan-Arctic, ice-off was detected within ±10 days of the mean for 78% of the lake pixels (Fig. 4), with the overall average ice-off date the 5th latest since 2004. In North America, 90% of the lake pixels were near-mean timing, while 59% of Eurasian lake pixels experienced later than usual ice-off timing.
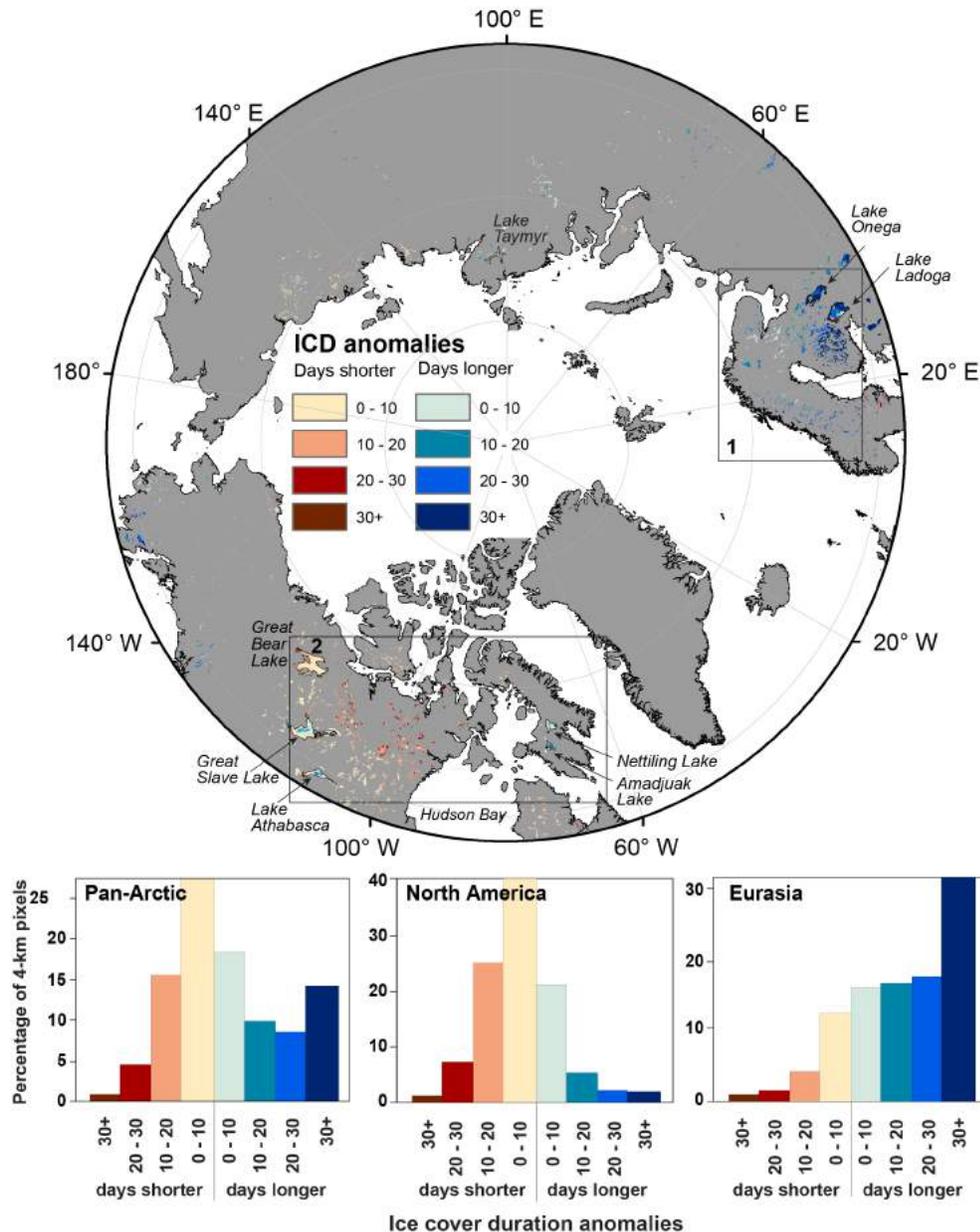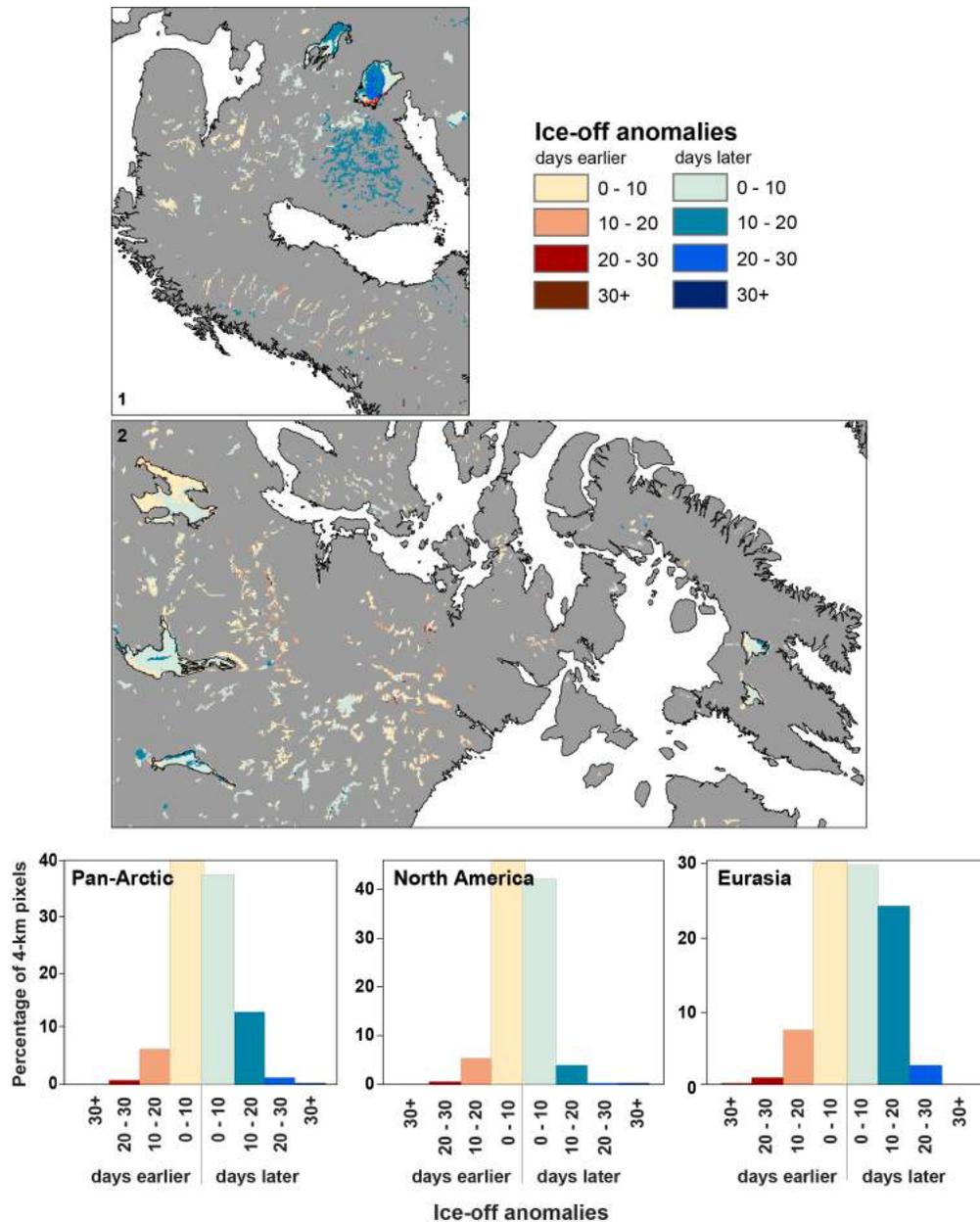
Fig. 4. Lake ice ice-off anomalies in 2022 relative to the 2004/05 to 2020/21 mean from the IMS 4-km product. Focus regions as outlined in Fig. 1.

Most of Siberia/Russia experienced later ice-off, which is in agreement with more snow-covered days during the spring in this region (see essay *Terrestrial Snow*). Southern Finland experienced ice-off ~2 weeks later, with the lakes in this region not becoming fully ice free until mid-May, rather than the typical late April. This later ice-off timing coincided with longer spring snow cover durations (see essay *Terrestrial Snow*) and ~1-2°C cooler than usual April air temperature (2004-21). The five larger North American lakes observed were mostly within 0-10 days later than the mean ice-off timing, except for Great Bear Lake, where a mix of slightly earlier and slightly later ice-off was detected. The smaller lakes in the region to the northwest of Hudson Bay experienced earlier than usual ice-off (mostly within 10 days earlier) becoming ice free in early July. Shorter spring snow cover durations were seen through this

region as well as anomalously warm air temperatures (see essays *Surface Air Temperature* and *Terrestrial Snow*).

Methods and data

For this report, lake ice-on, ice-off, and ice duration are derived from the 4-km (2004-present) National Ice Center Interactive Multisensor Snow and Ice Mapping System (IMS) product (U.S. National Ice Center 2008). The IMS product is an operational dataset used to map daily snow and ice cover with input from a variety of multi-sourced datasets (e.g., AVHRR, GOES, SSMI, Ice Charts; for a complete list of data sources, see National Snow and Ice Data Center) to produce maps that distinguish between land, snow-covered land, water, and ice. Analysis for ice cover relies primarily on AVHRR or MODIS imagery; however, when visible imagery is not available, microwave-based retrievals and/or ice climatology are used (Helfrich et al. 2007).

For each pixel, consecutive days of IMS imagery were compared to determine the first and last changes between ice and water to denote the timing of the change from water to ice, and ice to water (e.g., Duguay and Brown 2018; Dauginis and Brown 2021). As lake ice freeze-up and break-up are processes that typically occur over time there could be multiple changes between water and ice during these processes. For this analysis, the final change from water to ice for each pixel was identified as the ice-on date, and the final change from ice to water was identified as the ice-off date, with ice cover duration the time between these dates. Approximately 25,000 pixels are identified as lakes in the region north of 58° N, slightly south of the more usual 60° N used to delineate Arctic regions: ~14,000 in North America and ~11,000 in Eurasia. MODIS Imagery was used to visually confirm some of the IMS-derived dates. Lake-wide ice cover durations were determined using the mean date of all pixels encompassed by the lake boundary, extracted from the Natural Earth free vector and raster map data (Natural Earth 2022).

Monthly air temperature anomalies for the 2021/22 ice season using ERA-5 reanalysis data (Copernicus Climate Change Service 2017) were calculated relative to the same time frame as the IMS data, 2004-present.

References

Arp, C. M., and Coauthors, 2019: Ice roads through lake-rich Arctic watersheds: Integrating climate uncertainty and freshwater habitat responses into adaptive management. *Arct. Antarct. Alp. Res.*, **51**(1), 9-23, https://doi.org/10.1080/15230430.2018.1560839.

Brown, L. C., and C. R. Duguay, 2010: The response and role of ice cover in lake-climate interactions. *Prog. Phys. Geog.*, **34**, 671-704, https://doi.org/10.1177/0309133310375653.

Copernicus Climate Change Service, 2017: ERA5: Fifth generation of ECMWF atmospheric reanalyses of the global climate, Copernicus Climate Change Service Climate Data Store (CDS), 5 September 2022, https://cds.climate.copernicus.eu/cdsapp#!/home.

Dauginis, A. L., and L. C. Brown, 2021: Recent changes in pan-Arctic sea ice, lake ice, and snow-on/off timing. *Cryosphere*, **15**, 4781-4805, https://doi.org/10.5194/tc-15-4781-2021.

Du, J., J. S. Kimball, C. R. Duguay, Y. Kim, and J. Watts, 2017: Satellite microwave assessment of Northern Hemisphere lake ice phenology from 2002 to 2015. *Cryosphere*, **11**, 47-63, https://doi.org/10.5194/tc-11-47-2017.

Duguay, C. R., and L. Brown, 2018: Lake Ice. *Arctic Report Card 2018*, E. Osborne, J. Richter-Menge, and M. Jeffries, Eds., https://www.arctic.noaa.gov/Report-Card.

Duguay, C. R., T. D. Prowse, B. R. Bonsal, R. D. Brown, M. P. Lacroix, and P. Ménard, 2006: Recent trends in Canadian lake ice cover. *Hydrol. Process.*, **20**, 781-801, https://doi.org/10.1002/hyp.6131.

Helfrich, S. R., D. McNamara, B. H. Ramsay, T. Baldwin, and T. Kasheta, 2007: Enhancements to, and forthcoming developments in the Interactive Multisensor Snow and Ice Mapping System (IMS). *Hydrol. Process.*, **21**, 1576-1586, https://doi.org/10.1002/hyp.6720.

Natural Earth , 2022: Free vector and raster map data @ naturalearthdata.com. Accessed: 18 Aug 2022, https://www.naturalearthdata.com/

U.S. National Ice Center, 2008: IMS daily Northern Hemisphere snow and ice analysis at 1 km, 4 km, and 24 km resolutions, version 3. Boulder, Colorado, USA. NSIDC: National Snow and Ice Data Center, accessed: 18 Aug 2022, https://doi.org/10.7265/N52R3PMC.

November 9, 2022

Arctic Geese of North America

J. M. Pearce[1], J. Dooley[2], V. Patil[1], T. L. Sformo[3,4],
B. L. Daniels[5], A. Greene[6], and J. Leafloor[7]

[1]Alaska Science Center, U.S. Geological Survey, Anchorage, AK, USA
[2]Division of Migratory Bird Management, U.S. Fish & Wildlife Service, Vancouver, WA, USA
[3]Department of Wildlife Management, North Slope Borough, Utqiaġvik (Barrow), AK, USA
[4]Institute of Arctic Biology, University of Alaska Fairbanks, Fairbanks, AK, USA
[5]Yukon Delta National Wildlife Refuge, U.S. Fish & Wildlife Service, Bethel, AK, USA
[6]Kotzebue, AK, USA
[7]Aquatic Unit, Environment and Climate Change Canada, Winnipeg, MB, Canada

Highlights

- Multiple species of geese spend part of their annual cycle in the circumpolar Arctic and serve as a source of nutrition and cultural affirmation for many peoples.
- Arctic geese function as important indicators of environmental changes and some species also have the potential to alter ecosystem processes when they become overabundant.
- In 2022, despite an outbreak of highly pathogenic avian influenza in North America and variable spring weather conditions, the population sizes of most Arctic geese remained at or above historical levels.

Introduction

Most species of geese in the Northern Hemisphere are long-distance migrants, moving between lower-latitude wintering areas and summer breeding areas in the Arctic and sub-Arctic (Fig. 1). Arctic geese (Fig. 2) are keystone herbivores and their numbers and distributions are influenced by summer and winter environmental conditions and changes in forage quality and quantity. Geese are one of the first avian species to return to northern regions in early spring and these birds and their eggs are highly valued as a source of nutrition and cultural affirmation for Indigenous Peoples and Arctic residents.

Fig. 1. Important goose nesting areas in Arctic and sub-Arctic North America [Credit: Sarah Battle, NOAA/PMEL; Map is modified from Fig. 7, U.S. Fish and Wildlife Service (2022). Waterfowl population status, 2022. U.S. Department of the Interior, Washington, D.C., USA.].

Fig. 2. Arctic geese of North America. (a) emperor goose (*A. canagica*), (b) black brant (*B. bernicla nigricans*), (c) cackling goose (*Branta hutchinsii*), (d) greater white-fronted goose (*Anser albifrons*), (e) lesser snow goose (*A. caerulescens caerulescens*), and (f) Ross's goose (*A. rossii*). Not shown: greater snow goose (*A. caerulescens atlantica*), Canada goose (*B. canadensis*), and Atlantic brant (*B. bernicla hrota*), which are very similar to lesser snow goose, Cackling goose, and black brant, respectively. Photo credits: (a) Brian Uher-Koch, USGS; (b through e) Ryan Askren, USGS; (f) Andrea Mott, USGS.

This essay focuses on the status of North American goose populations that breed within areas of the Arctic and sub-Arctic (Fig. 1). Within North America, the status and trends of waterfowl species and their breeding habitats are of significant interest to federal, state, and tribal entities and are primarily assessed through standardized ground and aerial surveys and the marking of individuals (U.S. Fish and Wildlife Service 2022). Additionally, the Arctic Goose Joint Venture (AGJV) publishes a strategic plan that summarizes information needs across North America (https://www.agjv.ca) and provides links to current species and population management plans. These efforts, along with annual coordination among agencies and co-management councils, documentation of Inuit Knowledge of Arctic geese (e.g., www.kangut.ca), and involvement of Indigenous Peoples and Arctic residents, help to provide the most up-to-date status information, ensure sustainable harvest regulations, and improve our collective knowledge of these birds. An in-depth review of the abundance, status, and distribution of circumpolar Arctic geese can be found in Fox and Leafloor (2018).

Spring conditions in 2022

An outbreak of highly pathogenic avian influenza (HPAI) that began in both eastern Canada and British Columbia and quickly spread across North America (U.S. Geological Survey 2022) affected many Arctic geese in 2022. This outbreak, only the second ever detected in North America, has already resulted in more losses of wild and domestic birds than the previous outbreak during 2014-16. HPAI mortality events in 2022 occurred across all migratory flyways during the spring migration period and involved notable die-offs of Canada geese and lesser snow geese in some staging areas where they rest and feed along their migration. HPAI was also detected in several species of migratory geese in breeding areas of Alaska from early May 2022 to August 2022 (Alaska Division of Environmental Health 2022). Live geese

were swabbed during banding in the Canadian Arctic in 2022 as part of national HPAI surveillance activities, and no active mortality events were observed at that time; further analysis of these samples is currently underway.

In Canada, biologists noted favorable spring 2022 conditions that led to average to above-average goose productivity (i.e., young geese observed) on Banks Island, Southampton Island, Baffin Island, the Ungava Peninsula, and along western Hudson Bay (Fig. 1). However, low production was noted for geese in some areas of the central Arctic and on Bylot Island. Spring phenology was later than average on Bylot Island but appeared to be early or average in many areas of the Canadian Arctic and sub-Arctic. Many areas in these regions also experienced above-average temperatures during late May or June (U.S. Fish and Wildlife Service 2022; see similar observations in essay *Surface Air Temperature*, Figs. 2c and 2d, and essay *Terrestrial Snow Cover*, Fig. 2d), which likely improved habitat and breeding conditions.

In northwestern Alaska, large numbers of snow geese were observed along with cold spring conditions that would have been considered "normal" spring weather 30 years ago. Geese were present but food availability was limited by persistent snow and ice cover. The coast of the Yukon-Kuskokwim Delta (YKD; Fig. 1) was mostly snow free by mid-April, but lakes (see essay *Lake Ice*) and rivers were still frozen until mid-May. Migrating birds bypassed Bethel, Alaska, and arrived on the coast in early to mid-May. Warm and dry weather conditions during the nesting period (mid-May to June) may have negatively affected productivity. Decreased nesting effort (i.e., lower number of nests found) was observed on the YKD in 2022 for black brant, emperor geese, and cackling geese, with multiple research crews reporting loafing behavior and lack of nesting.

Local spring weather conditions and migratory bird observations are used each year by entities such as the Alaska Migratory Bird Co-Management Council (AMBCC; https://www.alaskamigratorybirds.com) to determine when to initiate spring harvest closures to protect birds and eggs during the primary nesting period (see Methods and data). Harvest dates were fixed prior to 2021, despite increasing variability in the phenology of spring weather and goose nesting behavior. The shift towards flexible start dates based on local observations is recent, representing widespread efforts to provide more effective evidence-based wildlife management through collaboration between management agencies and Indigenous community members in Alaska and Canada.

Population status of Arctic geese

Almost all North American populations of geese have been stable or have increased over the long-term, but about half of all Arctic and sub-Arctic populations have declined over the most recent 10-year period (Table 1). Population trends often determine management actions. For example, increased abundance of emperor geese allowed for an open harvest season in 2017 following a 30-year closure due to previously lower population numbers and Aleutian cackling geese were removed from the 'endangered' category of the Endangered Species List in 2001 in response to a dramatic increase in abundance (the 2022 population estimate was the highest on record). In contrast, Atlantic Population Canada geese, which breed primarily on the Ungava Peninsula (Fig. 1), have had restrictive harvest regulations in recent years due to declining abundance and low productivity, primarily due to multiple years of lower-than-average May temperatures. However, surveys in 2022 indicated improved breeding conditions and the first notable increase in the breeding population in almost a decade. For most northern-nesting goose populations, short-term declines have not led to management actions, because overall, most populations remain at or above historical levels.

Table 1. Species and populations of Arctic and sub-Arctic nesting geese and associated growth rates (percentage change in abundance per year; 0 = no change) from primary North American monitoring surveys, given for the entire survey range period and for the most recent 10 years of survey data (see Methods and data). Populations and trends shown in bold are those with recent changes explained in the text (see also Fig. 3).

Species	Population	Survey Range	Growth Rate (% change/yr; All Survey Years)	Growth Rate (% change/yr; Most Recent 10 Survey Years)
Brant	Atlantic	1970-2022	+1	0
	Pacific	1970-2022	0	0
Cackling Goose	Midcontinent	1987-2019	+3	-5
	Cackling	1985-2022	+4	-6
	Taverner's	2007-2022	-1	+4
	Aleutian	**1975-2022**	**+12**	**+1**
Canada	North Atlantic	1990-2022	0	-1
	Atlantic	1993-2022	+4	-3
	Southern Hudson Bay	2016-2021	0	0
	W. Prairie/Great Plains	1970-2022	+6	+4
	Dusky	1986-2022	0	-2
	Lesser	1970-2022	-1	+4
Emperor Goose	**Yukon-Kuskokwim Delta**	**1985-2022**	**+2**	**-2**
Snow Goose	Greater	1970-2022	+5	-2
	Midcontinent Lesser	1970-2019	+6	-6
	Western Arctic Lesser	**2000-2018**	**+3**	**+11**
	Wrangel Island Lesser	**1975-2021**	**+4**	**+17**
Ross's	Western and Central Arctic	1989-2019	+9	-2
Greater white-fronted Goose	Pacific	1985-2022	+6	-2
	Midcontinent	1976-2020	+4	-3
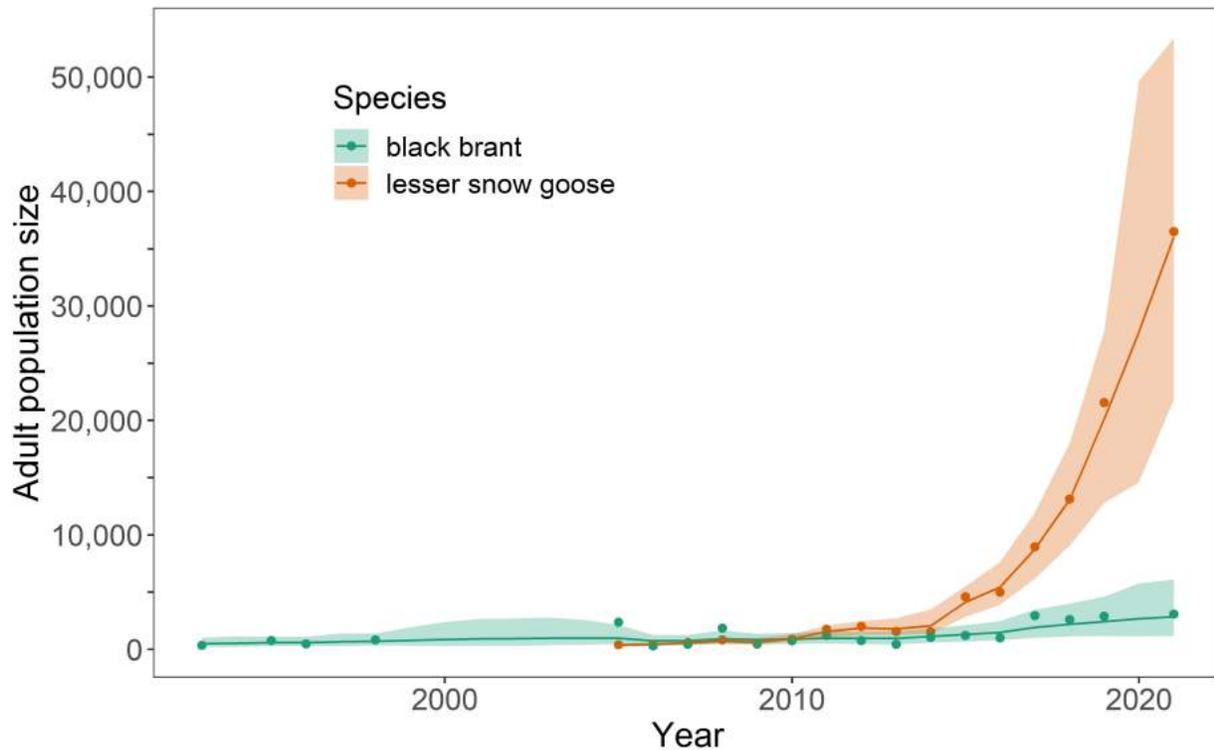
Fig. 3. Example of difference in population sizes and growth rates of adult Western Arctic lesser snow geese (2005-22) and Pacific black brant (1993-2022) on the Colville River Delta, Alaska, based on aerial surveys during the brood-rearing period (Parrett et al. 2021; see Methods and data). Western Arctic lesser snow geese breed primarily on Banks Island, Canada, with smaller colonies in coastal areas of Northwest Territories, and along the North Slope of Alaska, including the Colville River Delta.

Abundance of Ross's and greater and lesser snow geese in the midcontinent and eastern regions of North America has stabilized or declined in recent years. This recent change follows decades of exponential growth since the 1970s, which prompted overabundance designations and liberal harvest regulations beginning in 1999. Harvest probabilities (the proportion of the population likely harvested by hunters) have remained low with minimal impacts on population dynamics of Ross's and midcontinent lesser snow geese (Alisauskas et al. 2022), but greater harvest probabilities were achieved on the smaller population of greater snow geese, which contributed to curtailing population growth (Lefebvre et al. 2017). Despite low harvest rates, biologists have documented declines in abundance at major snow goose breeding colonies in the midcontinent region, multiple years of poor productivity, high rates of emigration, and shifts in wintering and breeding distribution (Alisauskas et al. 2022; Weegman et al. 2022). These changes have been linked to resource limitations caused by climate change and negative feedbacks associated with high goose abundance. As a result, the midcontinent population of lesser snow geese has declined by approximately 60% since reaching peak abundance in 2007. In contrast, populations of lesser snow geese in the Western North American Arctic are exhibiting rapid growth due to improved climatic and habitat conditions in that region.

Observations from the Colville River Delta in Arctic Alaska distinctly highlight the effects of a rapidly warming Arctic on goose species. Both black brant and lesser snow geese have adjusted their behavior in tandem with phenological shifts, arriving earlier each spring and initiating nesting earlier in years with warmer springs and earlier snowmelt (Ruthrauff et al. 2021). Increasing goose populations on the Colville River Delta (Fig. 3), and elsewhere in Arctic Alaska, may also have benefited indirectly from

permafrost thaw and coastal erosion, which have allowed nitrogen-rich salt-tolerant vegetation to replace less digestible freshwater meadows (Tape et al. 2013). Unlike black brant, however, snow geese can dig for belowground food when aboveground plant growth is delayed by cold weather. They also have a flexible breeding strategy, which allows them to be more successful breeders across years with variable spring conditions (Hupp et al. 2018). These traits may account for their explosive growth in the Western Arctic and on Wrangel Island (Table 1 and Fig. 3).

Climate and habitat changes in recent years have also altered distributions of geese during the non-breeding season. For example, large numbers of midcontinent greater-white-fronted, cackling, lesser snow, and Ross's geese have moved eastward and northward from traditional wintering areas in coastal Texas and Louisiana, as agricultural production in those areas has decreased and winter temperatures have increased (VonBank et al. 2021). Black brant, which are a maritime goose, have substantially shifted their wintering distribution northward, with greater numbers overwintering at Izembek Lagoon and adjacent estuaries on the Alaska Peninsula, instead of at traditional wintering areas in Mexico (Olson 2021; Dave Safine, U.S. Fish and Wildlife Service, 2022, personal communication). Expansive drought in California and other western states is also altering goose distribution and migration patterns (Overton et al. 2021).

Methods and data

On the YKD and North Slope of Alaska, local observations are used to set a 30-day closure period of spring harvest, mandatory under the Migratory Bird Treaty Act (U.S. Fish and Wildlife Service 2020). As birds start arriving in spring, local observations are collected and communicated among hunters, tribal organizations, and observers, and the U.S. Fish and Wildlife Service (USFWS) contributes information about harvest and nest initiation that determine a range of likely closure dates. The final start date of the 30-day closure for the core nesting period is then communicated through radio, press release, and other methods.

Trends in Table 1 were calculated by regressing the natural logarithms of survey results on year. Estimates in Fig. 3 were derived using a Bayesian state-space model with lognormal process variation and log-normal observation errors. Points are observed counts, solid lines are the posterior mean estimates for each species, and shading represents the 95% posterior credible intervals.

Acknowledgments

References

Alaska Division of Environmental Health, 2022: Highly pathogenic avian influenza (HPAI) outbreaks and biosecurity toolkit from USDA APHIS. Accessed 26 September 2022, https://dec.alaska.gov/eh/vet/announcements/avian-influenza-outbreaks/#resources.

Alisauskas, R. T., and Coauthors, 2022: Subpopulation contributions to a breeding metapopulation of migratory arctic herbivores: survival, fecundity and asymmetric dispersal. *Ecography*, **2022**(7), e05653, https://doi.org/10.1111/ecog.05653.

Fox, A. D., and J. O. Leafloor (eds.), 2018: A global audit of the status and trends of Arctic and Northern Hemisphere goose populations. Conservation of Arctic Flora and Fauna International Secretariat: Akureyri, Iceland. ISBN 978-9935-431-66-0.

Hupp, J. W., D. H. Ward, D. X. Soto, and K. A. Hobson, 2018: Spring temperature, migration chronology, and nutrient allocation to eggs in three species of arctic-nesting geese: Implications for resilience to climate warming. *Glob. Change Biol.*, **24**, 5056-5071, https://doi.org/10.1111/gcb.14418.

Lefebvre, J., G., Gauthier, J. F., Giroux, A. Reed, E. T. Reed, and L. Bélanger, 2017: The greater snow goose *Anser caerulescens atlanticus*: Managing an overabundant population. *Ambio*, **46**, 262-274, https://doi.org/10.1007/s13280-016-0887-1.

Olson, S. J., 2021: Pacific Flyway Data Book, 2021: U.S. Department of the Interior, Fish and Wildlife Service, Division of Migratory Bird Management, Vancouver, Washington.

Overton, C. T., and Coauthors, 2022: Megafires and thick smoke portend big problems for migratory birds. *Ecology*, **103**(1), e03552, https://doi.org/10.1002/ecy.3552.

Parrett, J. P., T. Obritschkewitsch, and R. W. McNown, 2021: Avian studies for the Alpine Satellite Development Project, 2021, ABR, Inc. Available at: https://catalog.northslopescience.org/gl/dataset/2321.

Ruthrauff, D. R., V. P. Patil, J. W. Hupp, and D. H. Ward, 2021: Life-history attributes of Arctic-breeding birds drive uneven responses to environmental variability across different phases of the reproductive cycle. *Ecol. Evol.*, **11**, 18514-18530, https://doi.org/10.1002/ece3.8448.

Tape, K. D., P. L. Flint, B. W. Meixell, and B. V. Gaglioti, 2013: Inundation, sedimentation, and subsidence creates goose habitat along the Arctic coast of Alaska. *Environ. Res. Lett.*, **8**, 045031, https://doi.org/10.1088/1748-9326/8/4/045031.

U.S. Fish and Wildlife Service, 2020: Migratory bird subsistence harvest in Alaska; updates to the regulations: Federal Register, 85 FR 73233, FWS-R7-MB-2-2-0022.

U.S. Fish and Wildlife Service, 2022: Waterfowl population status, 2022. U.S. Department of the Interior, Washington, D.C. USA. https://www.fws.gov/library/collections/waterfowl-population-status-reports.

U.S. Geological Survey, 2022: Distribution of highly pathogenic avian influenza H5 and H5N1 in North America, 2021/2022. https://www.usgs.gov/media/images/distribution-highly-pathogenic-avian-influenza-h5-and-h5n1-north-america-20212022. Accessed 26 September 2022.

VonBank, J. A., M. D. Weegman, P. T. Link, S. A. Cunningham, K. J. Kraai, D. P. Collins, and B. M. Ballard, 2021: Winter fidelity, movements, and energy expenditure of midcontinent greater white-fronted geese. *Mov. Ecol.*, **9**, 2, https://doi.org/10.1186/s40462-020-00236-4.

Weegman, M. D., R. T. Alisauskas, D. K. Kellett, Q. Zhao, S. Wilson, and T. Telenský, 2022: Local population collapse of Ross's and lesser snow geese driven by failing recruitment and diminished philopatry. *Oikos*, **2022**(5), e09184, https://doi.org/10.1111/oik.09184.

November 22, 2022

Arctic Pollinators

**C. T. Burns[1], M. L. Burns[2], S. Cannings[3], M. L. Carlson[4], S. Coulson[5],
M. A. K. Gillespie[6], T. T. Høye[7], D. MacNearney[8], E. Oberndorfer[9],
J. J. Rykken[4], and D. S. Sikes[10]**

[1]Bureau of Land Management, U.S. Department of the Interior, Anchorage, AK, USA
[2]U.S. Fish & Wildlife Service, Anchorage, AK, USA
[3]Canadian Wildlife Service, Environment and Climate Change Canada, Whitehorse, YT, Canada
[4]Alaska Center for Conservation Science, University of Alaska Anchorage, Anchorage, AK, USA
[5]University Centre in Svalbard, Longyearbyen, Svalbard, Norway
[6]Department of Environmental Sciences, Western Norway University of Applied Sciences, Sogndal,
Vestland, Norway
[7]Department of Ecoscience and Arctic Research Center, Aarhus University, Aarhus, Denmark
[8]Wildlife Research Division, Environment and Climate Change Canada, Ottawa, ON, Canada
[9]Agriculture and Agri-Food Canada, Goose Bay, NL, Canada
[10]University of Alaska Museum, University of Alaska Fairbanks, Fairbanks, AK, USA

Highlights

- Pollinating insects are critical to the function of Arctic ecosystems and to the food systems of
  Arctic Indigenous Peoples and Arctic residents. The distribution, conservation status, and
  ecology of most Arctic pollinators are poorly known due to few long-term research and
  monitoring sites and geographically limited inventory sampling.
- In the high Arctic, there are 14 known bee species and 17 known butterfly species; in the low
  Arctic, there are 58 known bee species and 95 known butterfly species. The number of
  pollinating fly species is unknown.
- Coordinated long-term monitoring, strategic inventories, emerging technologies, engagement
  with Indigenous Peoples, and resources to support these efforts can improve our understanding
  of the status of pollinators and their habitats, and inform effective conservation strategies.

Introduction

Knowledge of Arctic pollinators is deficient, despite their important functional roles in terrestrial
ecosystems and contribution to the food systems of Arctic Indigenous Peoples and Arctic residents. As is
the case in non-Arctic ecosystems, some Arctic flowering plants are highly dependent on particular
pollinator taxa for fruit and seed production. However, there are also unique features of Arctic
pollination, such as the increasingly important roles at higher latitudes of nectar- and pollen-feeding fly
species as pollinators (Hodkinson 2018; Tiusanen et al. 2016; Koch et al. 2020).

Arctic insects are sensitive indicators of ecological responses to climate change (Høye 2020). Some Arctic
pollinators are responding strongly to changing conditions, but a full understanding of their responses is
lacking. Coordinated monitoring to track changes in the distribution and abundance of Arctic insects is
required to understand the capabilities and limits of Arctic pollinators under ongoing climate change

(Gillespie et al. 2020a,b). Here, we provide an inventory and monitoring summary across the Arctic and describe recent initiatives to advance further data collection and synthesis.

Inventory, monitoring, and research summary

North America: Pollinator data are particularly limited in the North American Arctic; from a total area of approximately two million km^2, there are less than 8,000 curated bee specimens. Specimens are primarily associated with larger communities and research stations (Fig. 1) while other areas are nearly devoid of data (Fig. 2). In Canada, the Northern Insect Survey (1947-62) sampled 39 sites across high and low Arctic zones; in 2010-11, twelve of these sites were resampled by the Northern Biodiversity Program using a standardized protocol. Recent targeted pollinator surveys in some of Alaska's Arctic National Parks have provided numerous records of solitary bee and syrphid fly species. In 2020, federal, state, university, and community scientists launched the Alaska Bee Atlas to increase species distribution and habitat data, especially in poorly sampled ecoregions. The Arctic BIOSCAN project is developing capacity for community and DNA-based biodiversity monitoring in the Canadian Arctic.
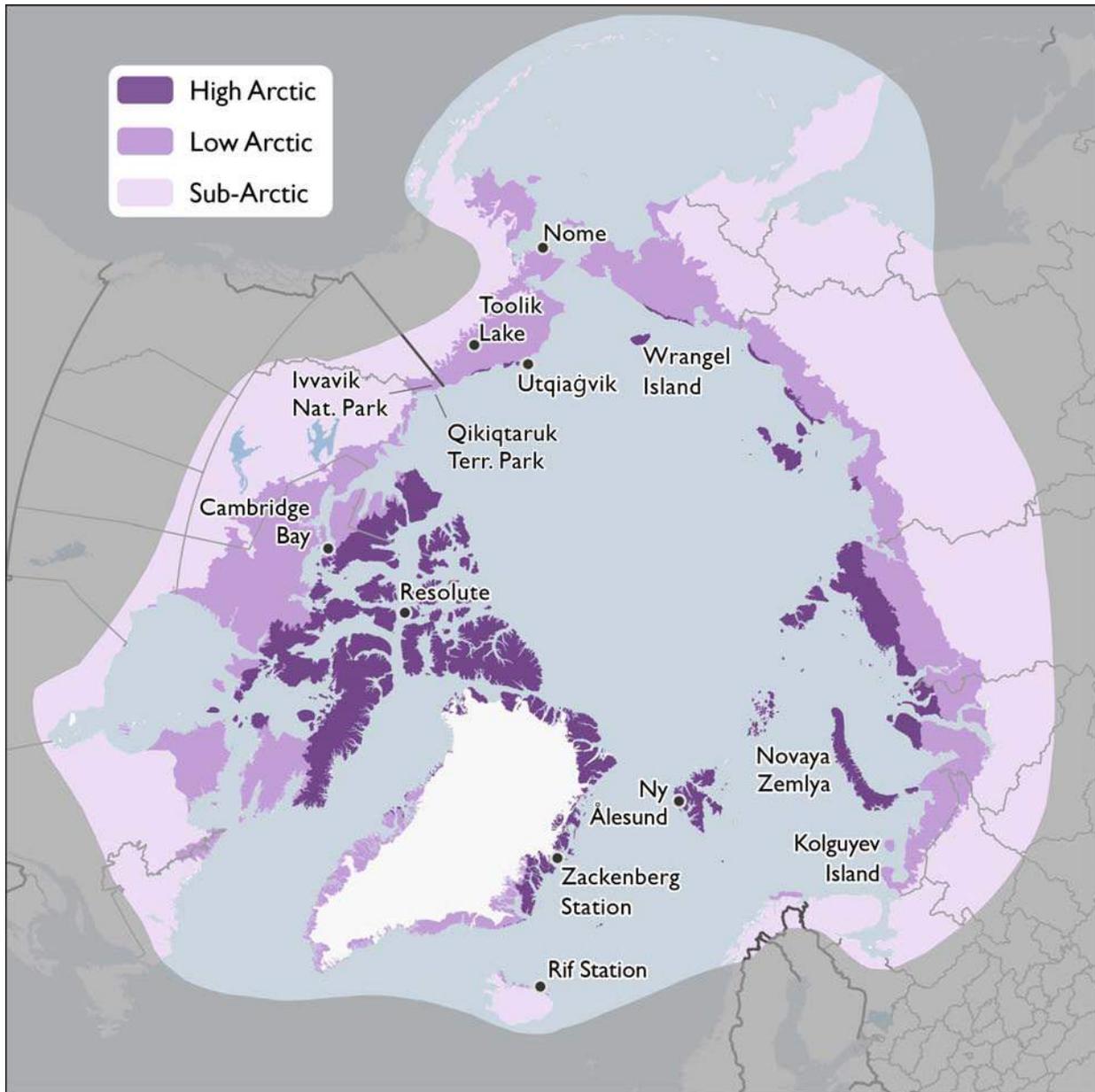
Fig. 1. Distribution of pollinator data collection sites in the high, low, and sub-Arctic regions, as delineated by the Circumpolar Arctic Vegetation Map. High Arctic is characterized by summer temperatures of 5-7°C and prostrate shrubs, low graminoids, and forbs; low Arctic by summer temperatures of 7-9°C and erect shrubs; and sub-Arctic by summer temperatures of 9-12°C and typically below treeline. Geographic areas and research stations associated with significant pollinator data are labeled.
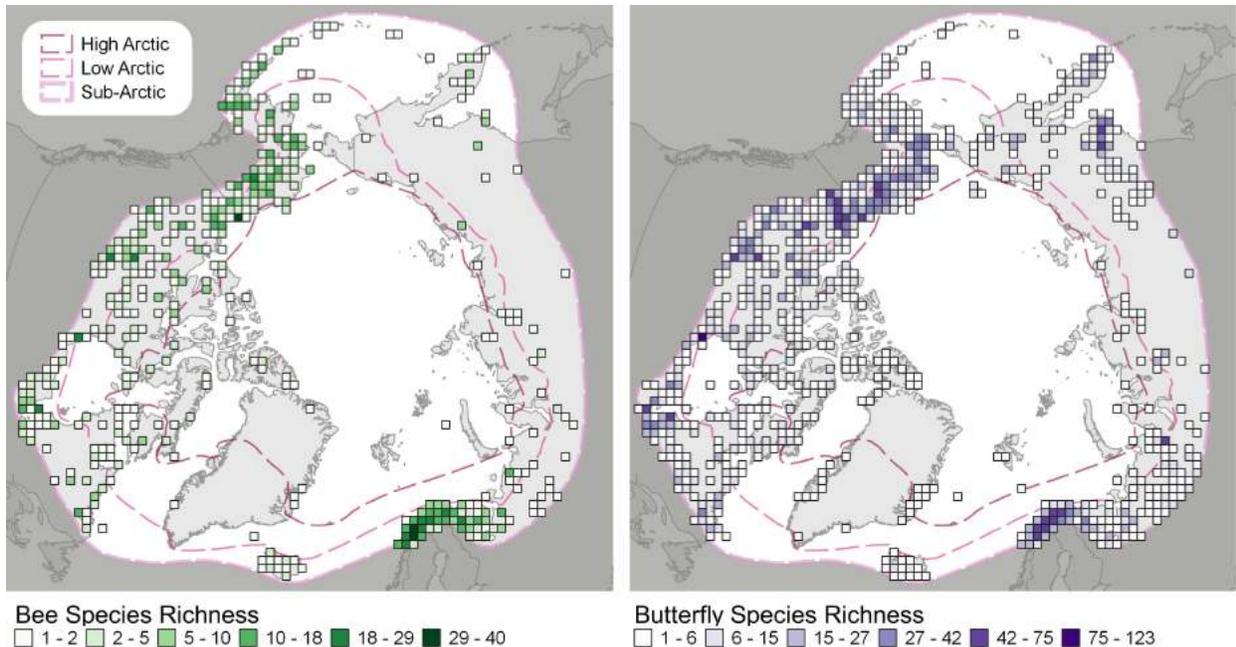
Fig. 2. Arctic spatial distributions of bee and butterfly species richness based on Global Biodiversity Information Facility (GBIF) records.

There are 21 bumble bee (*Bombus*) species associated with the three Arctic zones in the U.S. and Canada, six of which occur in the high Arctic (Table 1). Bumble bees in this region are well-represented by the tundra specialist subgenus *Alpinobombus* and the more generalist subgenus *Pyrobombus*. Twenty-four species of solitary (non-social) bees have been collected in the low Arctic in North America, and none have been recorded in the high Arctic (Table 1). These species tend to be abundant generalist pollinators with widespread distributions in the adjacent sub-Arctic. Within the low Arctic, these solitary bee species are largely associated with floodplains and south-facing bluffs, and warm and dry microsites with sandy substrates that provide suitable habitat for these primarily ground-nesting species. The importance of intensive inventory is highlighted in Fig. 2, where a single dark pixel near the Canada-US border represents 732 records of 35 bee species within the diverse ecosystems of Ivvavik National Park and Qikiqtaruk Territorial Park, Yukon, Canada.

Table 1. Arctic bee list and numbers of known bee species from each genus by Arctic zone, by total number of species restricted to only the High and/or Low Arctic zones and by country based on records primarily from 1990-2022. The full species richness is unknown.

Genus	English Common Name	High Arctic Zone	Low Arctic Zone	Sub-Arctic Zone	High/Low Arctic Only	US	Ca	Gr	Ic	No	Sw	Fi	Ru
Andrena	Mining Bees	-	5	10	-	4	7	-	-	6	4	3	7
Bombus	Bumble Bees	14	38	62	4	21	25	2	7	30	25	23	46
Coelioxys	Cuckoo Leaf-cutter Bees	-	2	2	-	-	2	-	-	-	-	-	-
Colletes	Plasterer Bees	-	1	2	-	1	2	-	-	1	-	-	2
Halictus	Sweat Bees	-	1	2	-	1	1	-	-	-	-	-	1
Lasioglossum	Sweat Bees	-	3	8	-	4	4	-	-	3	2	2	5
Megachile	Leaf-cutter Bees	-	4	5	-	2	4	-	-	-	1	-	2
Nomada	Wandering Cuckoo Bees	-	2	4	1	1	2	-	-	1	2	1	2
Osmia	Mason Bees	-	5	12	-	5	2	-	-	4	5	5	9
Panurginus	Fairy Bees	-	1	1	-	1	-	-	-	-	-	-	-
Stelis	Cuckoo Carder Bees	-	1	1	1	1	1	-	-	-	-	-	-
Other Species -	Sub-Arctic Only	-	-	5	-	1	2	-	1	2	2	2	3
Bee Totals		**14**	**63**	**114**	**6**	**42**	**52**	**2**	**8**	**47**	**41**	**36**	**77**

- = no species records known to authors. US = United States, Ca = Canada, Gr = Greenland, Ic = Iceland, No = Norway, including Svalbard and Jan Mayen, Sw = Sweden, Fi = Finland, Ru = Russia. Complete species table is available at: https://geo.abds.is/

A total of 61 butterfly species are recorded in low Arctic North America; 15 of these are also known from the high Arctic. *Colias johanseni*, endemic to Nunavut, is the only species known to be restricted to the Arctic. Flies and other insect pollinating groups such as beetles, moths, and wasps are poorly known in Arctic North America.

Nordic Region: Country-level inventories in the Nordic region are robust for most countries (Gillespie et al. 2020b), but data on species distributions outside of mainland Europe, as well as trends in abundance and diversity generally are lacking. Improvements are likely, with monitoring due to start at the Rif Station in Iceland (Gillespie et al. 2020a) and already underway at Ny Ålesund in Svalbard. Additionally, plans for national pollinator monitoring schemes are in advanced stages in Norway, Sweden, and Finland, although not necessarily in representative sub-Arctic sites yet (e.g., Åström et al. 2020).

The most comprehensive knowledge of temporal trends in this region come from the Zackenberg Research Station in East Greenland, which has recorded annual pitfall trap catches of insects since 1996. Family-level analyses of 25 years of data demonstrated variable trends among pollinator groups, dependent on habitat type (Fig. 3; Høye et al. 2021). For example, nymphalid butterflies (two recorded species) have been declining steadily in abundance since 1996, but only in mesic heath habitat. In contrast, muscid flies (37 species) have declined in the wet fen sampling sites, but populations have fluctuated in arid heath. At the species level, trends are also variable, with declines in abundance of seven out of 14 muscid species between 1996 and 2014, and over 80% decreases in diversity and abundance in some habitat types (Gillespie et al. 2020b).
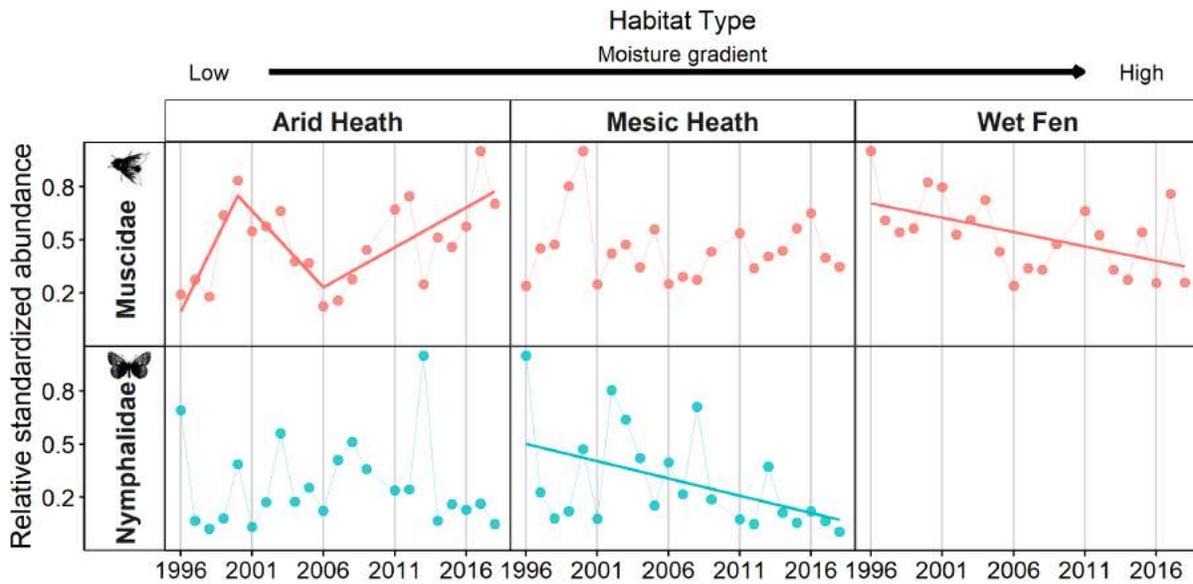
Fig. 3. Long-term trends in relative standardized insect abundance (individuals per trapping day) by family for the primary pollinator groups at Zackenberg, East Greenland. Solid lines indicate significant (p<0.05) best fitting linear or segmented regression lines (Høye et al. 2021).

In the high and low Arctic Nordic region, the most important pollinators are likely flies. In Greenland, there are only two bumble bees and eight established butterfly species, but muscid flies, particularly in the genus *Spilogona*, are more abundant and frequent flower visitors (Gillespie et al. 2020b). In Iceland, syrphid flies are more widespread with most bumble bee and butterfly species restricted to the sub-Arctic south and a general lack of solitary bees. Bees and butterflies are absent from Jan Mayen and Svalbard, where flies often make up the majority of flower visits.

In northern Norway, Sweden, and Finland, the bee and butterfly fauna are more diverse (Tables 1 and 2), closely linked to southern populations and habitats, and likely more important for wildflower pollination. Tundra and alpine specialists are found in the region, together with more widespread temperate species. However, few studies have focused attention on the status and trends of the sub-Arctic ranges of these species.

Table 2. Arctic butterfly list and numbers of known butterfly species from each genus by Arctic zone, by total number of species restricted to only the high and/or low Arctic zones, and by country based on records primarily from 1990-2022. The full species richness is unknown.

Genus	English Common Name	High Arctic Zone	Low Arctic Zone	Sub-Arctic Zone	High/Low Arctic only	US	Ca	Gr	Ic	No	Sw	Fi	Ru
Aglais	Tortoiseshells	-	1	3	-	1	1	1	2	2	1	2	2
Agriades	Blues	1	2	2	-	2	2	1	-	-	-	-	-
Anthocharis	Orange-tips	-	1	1	-	-	-	-	-	1	1	1	1
Aporia	Black-veined Whites	-	1	1	-	-	-	-	-	1	-	1	1
Boloria	Fritillaries	7	16	17	1	9	10	2	-	11	11	11	16
Brenthis	Fritillaries	-	1	1		-	-	-	-	-	1	-	1
Callophrys	Elfins / Hairstreaks	-	1	4	-	2	2	-	-	1	1	1	1
Carterocephalus	Skippers	-	2	2	-	1	1	-	-	1	-	1	2
Celastrina	Spring Azures	-	1	2	-	1	1	-	-	1	-	1	1
Coenonympha	Ringlets	-	1	3	-	1	1	-	-	1	1	2	3
Colias	Sulphurs	3	9	13	1	8	10	1	1	3	3	3	6
Cupido	Tailed Blues	-	2	2	-	1	1	-	-	1	1	-	1
Cyaniris	Blues	-	1	1	-	-	-	-	-	1	1	-	1
Erebia	Alpines	1	13	25	-	11	9	-	-	7	3	5	20
Erynnis	Duskywings	-	1	3	-	1	3	-	-	-	-	-	-
Euchloe	Marbles	-	1	5	-	2	3	-	-	-	-	-	4
Euphydryas	Checkerspots	-	2	4	-	1	1	-	-	1	1	1	3
Glaucopsyche	Silvery Blues	-	1	1	-	1	1	-	-	-	-	-	1
Hesperia	Branded Skippers	-	1	1	-	1	1	-	-	1	1	1	1
Icaricia	Mission Blues	-	1	1	-	1	1	-	-	-	-	-	-
Issoria	Fritillaries	-	1	1	-	-	-	-	-	-	-	-	1
Limenitis	Admirals	-	1	2	-	1	1	-	-	-	-	-	1
Lycaena	Coppers	1	2	7	-	2	3	1	-	3	2	3	5
Nymphalis	Tortoiseshells	-	2	3	-	2	3	-	1	1	1	1	3
Oeneis	Arctics	2	8	13	-	8	9	-	-	2	2	2	9
Papilio	Swallowtails	-	2	2	-	2	2	-	1	1	1	1	1
Parnassius	Parnassians	-	2	6	1	2	2	-	-	-	-	-	6
Phyciodes	Crescents	-	1	2	-	1	2	-	-	-	-	-	-
Pieris	Whites	-	3	6	-	1	3	-	3	4	1	3	4
Plebejus	Blues	-	5	6	-	1	1	-	-	5	4	3	6
Polygonia	Commas	-	2	5	-	2	4	-	1	1	-	-	1
Polyommatus	Blues	-	2	3	-	-	-	-	-	1	2	1	3
Pontia	Checkered Whites	-	2	4	-	1	2	-	-	1	-	2	2
Pyrgus	Grizzled Skippers	-	2	2	-	1	1	-	-	2	2	2	2
Vanessa	Ladies and Admirals	2	1	2	-	-	2	2	2	2	2	2	2
Other Species -	Sub-Arctic Only	-	-	31	-	2	9	-	2	9	1	6	21
Butterfly Totals		**17**	**95**	**186**	**3**	**70**	**92**	**8**	**13**	**65**	**44**	**56**	**132**

- = no species records known to authors. US = United States, Ca = Canada, Gr = Greenland, Ic = Iceland, No = Norway, including Svalbard and Jan Mayen, Sw = Sweden, Fi = Finland, Ru = Russia. Complete species table is available at: https://geo.abds.is/

Russia: Russia has a long history of engaging in insect conservation, but there is generally a lack of systematic pollinator monitoring (Fig. 2). Nevertheless, contributions to biodiversity databases reveal particularly high species richness (132 butterfly, 46 bumble bee, and 31 other bee species) across the three Arctic zones, including many taxa not represented in the other Arctic countries (Tables 1 and 2).

Bumble bees appear to be well-represented in low Arctic regions, in particular species in the subgenus *Alpinobombus* and other more widespread species, whereas only nine species are found in the high Arctic. Recent research on *Bombus glacialis*, found only on Wrangel, Novaya Zemlya, and Kolguyev Islands, demonstrates that these isolated populations are under considerable threat from climate change (Potapov et al. 2021).

Across the circum-Arctic, only four bee and one butterfly species are restricted to only the high and low Arctic zones, whereas many species are shared with the sub-Arctic and beyond. The largest proportion of high and low Arctic species are low Arctic species that also are found in the sub-Arctic. These species may, however, be restricted to isolated tundra habitats in the sub-Arctic.

Current coordination efforts and next steps

The February 2022 Conservation of Arctic Flora and Fauna (CAFF) Arctic Pollinator Monitoring Workshop convened experts to communicate existing and upcoming Arctic pollinator research, identify knowledge gaps, and build new partnerships towards coordinating monitoring efforts. This workshop was inspired in part by recent syntheses of status and trends of Arctic insects (Gillespie et al. 2020b) and the CAFF State of the Arctic Terrestrial Biodiversity Report (Aronsson et al. 2021). Research needs identified at the workshop include shared inventory and monitoring protocols, centralized data storage, increased taxonomic and ecological attention to flies, and long-term studies on ecologically important Arctic bee species to better understand the effects of climate change and other stressors on bee abundance, phenology, and distribution.

National and continental-scale monitoring projects are in development in North America and Europe that intersect the Arctic. Cooperation with monitoring in adjacent boreal forests provides a wealth of data, expertise, and collaborative opportunities, as these areas are intrinsically linked ecologically to the more northerly latitudes. Indigenous-led monitoring and observation platforms, including programs through the Gwich'in Tribal Council, Nunavik Sentinels, and the SIKU.org app, provide local training and employment opportunities for Indigenous Peoples while generating critical pollinator data and insights.

DNA barcoding, digital imagery, and machine learning are increasingly valuable tools for monitoring and research, as demonstrated by the multinational BITCue project, furthering understanding of the relative importance of Arctic pollinator species (Mann et al. 2022). There is great potential and need for partnerships with Indigenous governments and communities; for leveraging ongoing monitoring in existing non-pollinator research networks (e.g., Program for Regional and International Shorebird Monitoring/PRISM); and for citizen science platforms (e.g., iNaturalist). Building and maintaining long-term partnerships at multiple scales supports pollinator monitoring that is coordinated, has robust spatial coverage, is cost-effective, and helps identify shared priorities for the future of Arctic pollinator monitoring.

Methods and data

Online data were accessed from publicly available resources. Nordic and Russia data from GBIF.org occurrence data were downloaded August 2022. North American data from Philip and Ferris (2016), Rykken (2017), University of Alaska Museum (2021), GBIF.org were downloaded February 2021, Alaska Center for Conservation Science (2022), https://www.leifrichardson.org/bumble-bees-of-north-america.html were downloaded August 2022, Dumesh and Sheffield (2014), Canadian Endangered Species Conservation Council (2016), and Layberry et al. (1998).

Acknowledgments

References

Alaska Center for Conservation Science, 2022: Seward Peninsula bees identified from USGS bycatch. Unpublished data, University of Alaska Anchorage.

Aronsson, M., and Coauthors, 2021: State of the Arctic Terrestrial Biodiversity Report. Conservation of Arctic Flora and Fauna International Secretariat, Akureyri, Iceland. ISBN 978-9935-431-94-3.

Åström, S., J. Åström, K. Bøhn, J. O. Gjershaug, A. Staverløkk, S. Dahle, and F. Ødegaard, 2020: Nasjonal overvåking av dagsommerfugler og humler i Norge. Oppsummering av aktiviteten i 2019. (National monitoring of butterflies and bumble bees in Norway. Summary of activities in 2019). NINA Report 1811. Norwegian Institute for Nature Research. Trondheim, May 2020. ISBN: 978-82-426-4569-2.

Canadian Endangered Species Conservation Council, 2016: Wild Species 2015: The General Status of Species in Canada. National General Status Working Group, https://www.wildspecies.ca/reports.

Dumesh, S., and C. S. Sheffield, 2014: Illustrated Keys to the Bees of the Northwest Territories, Canada. Government of the Northwest Territories, Culture & Communications.

Gillespie, M. A. K., and Coauthors, 2020a: Circumpolar terrestrial arthropod monitoring: A review of ongoing activities, opportunities and challenges, with a focus on spiders. *Ambio*, **49**, 704-717, https://doi.org/10.1007/s13280-019-01185-y.

Gillespie M. A. K., and Coauthors, 2020b: Status and trends of terrestrial arthropod abundance and diversity in the North Atlantic region of the Arctic. *Ambio*, **49**, 718-731, https://doi.org/10.1007/s13280-019-01162-5.

Hodkinson, I. D., 2018: Insect Biodiversity: Science and Society, Volume II. Insect Biodiversity, R. G. Foottit and P. H. Adler, Eds., John Wiley & Sons Ltd., 15-57, https://doi.org/10.1002/9781118945582.ch2.

Høye, T. T., 2020: Arthropods and climate change - arctic challenges and opportunities. *Curr. Opin. Insect Sci.*, **41**, 40-45, https://doi.org/10.1016/j.cois.2020.06.002.

Høye, T. T., S. Loboda, A. M. Koltz, M. A. K. Gillespie, J. J. Bowden, and N. M. Schmidt, 2021: Nonlinear trends in abundance and diversity and complex responses to climate change in Arctic arthropods. *P. Natl. Acad. Sci.*, **118**(2), e2002557117, https://doi.org/10.1073/pnas.2002557117.

Koch, V., L. Zoller, J. M. Bennett, and T. M. Knight, 2020: Pollinator dependence but no pollen limitation for eight plants occurring north of the Arctic Circle. *Ecol. Evol.*, **10**(24), 13664-13672, https://doi.org/10.1002/ece3.6884.

Layberry, R. A., P. W. Hall, and J. D. Lafontaine, 1998: The Butterflies of Canada. University of Toronto Press, Toronto.

Mann, H. M. R., A. Iosifidis, J. U. Jepsen, J. M. Welker, M. J. J. E. Loonen, and T. T. Høye, 2022: Automatic flower detection and phenology monitoring using time-lapse cameras and deep learning. *Remote Sens. Ecol. Conserv.*, https://doi.org/10.1002/rse2.275.

Philip, K. W., and C. D. Ferris, 2016: Butterflies of Alaska: A Field Guide. 2nd ed. Alaska Entomological Society.

Potapov, G. S., and Coauthors, 2021: The last refugia for a polar relict pollinator: isolates of *Bombus glacialis* on Novaya Zemlya and Wrangel Island indicate its broader former range in the Pleistocene. *Polar Biol.*, **44**, 1691-1709, https://doi.org/10.1007/s00300-021-02912-6.

Rykken, J., 2017: Insect pollinators of Gates of the Arctic NPP: A preliminary survey of bees (Hymenoptera: Anthophila) and flower flies (Diptera: Syrphidae). Natural Resource Report NPS/GAAR/NRR-2017/1541. National Park Service, Fort Collins, CO.

Tiusanen, M., P. D. N. Hebert, N. M. Schmidt, and T. Roslin, 2016: One fly to rule them all-muscid flies are the key pollinators in the Arctic. *P. Roy. Soc. B.-Biol. Sci.*, **283**, 20161271, https://doi.org/10.1098/rspb.2016.1271.

University of Alaska Museum, 2021: Arctos database. https://arctos.database.museum/collection/UAMObs:Ento, accessed February 2021.

December 2, 2022

Lessons From Oceans Melting Greenland, a NASA Airborne Mission

J. K. Willis[1] and M. Wood[1,2]

[1]Jet Propulsion Laboratory, California Institute of Technology, Pasadena, CA, USA
[2]Moss Landing Marine Laboratories, San José State University, San José, CA, USA

Highlights

- From 2015 through 2021, NASA's Oceans Melting Greenland (OMG) experiment measured pan-Greenland changes in near-coast ice elevation, ocean temperature and salinity, and the near-shore ocean bathymetry that connects them.
- OMG showed that ice loss through glaciers at the ice sheet's margin is strongly affected by ocean temperatures on the continental shelf.
- Argo-like profiling floats offer a robust, easily deployed, and economical tool to continue monitoring Greenland's shelf waters.

Introduction

Greenland's ice sheet is disappearing. Each year, the snow added in the winter falls short of replenishing the summer melt and ice loss through Greenland's marine-terminating glaciers (see essay *Greenland Ice Sheet*). Because so many of Greenland's glaciers reach the ocean and sit in hundreds of meters of water (Morlighem et al. 2017), they can be directly influenced by ocean conditions. But how much of Greenland's ice loss is driven by the oceans? It was this question that inspired NASA's 6-year long airborne mission called Oceans Melting Greenland—OMG, for short.

While it was already known that some glaciers could be strongly influenced by ocean conditions (Holland et al. 2008; Straneo and Heimbach 2013), OMG set out to determine how widespread this influence could be and to quantify it. During its mission, OMG collected comprehensive observations of ocean depth on the shelf and near many glacier termini, ice elevation change measurements of all marine-terminating glaciers where they met the ocean, and widespread observations of ocean temperature and salinity on the continental shelf around the entire ice sheet (Fig. 1). Armed with this extensive set of new observations, OMG showed Greenland's glaciers are extremely sensitive to changes in ocean temperature. In the process, OMG also discovered new techniques for measuring ocean conditions in key locations on Greenland's continental shelf.
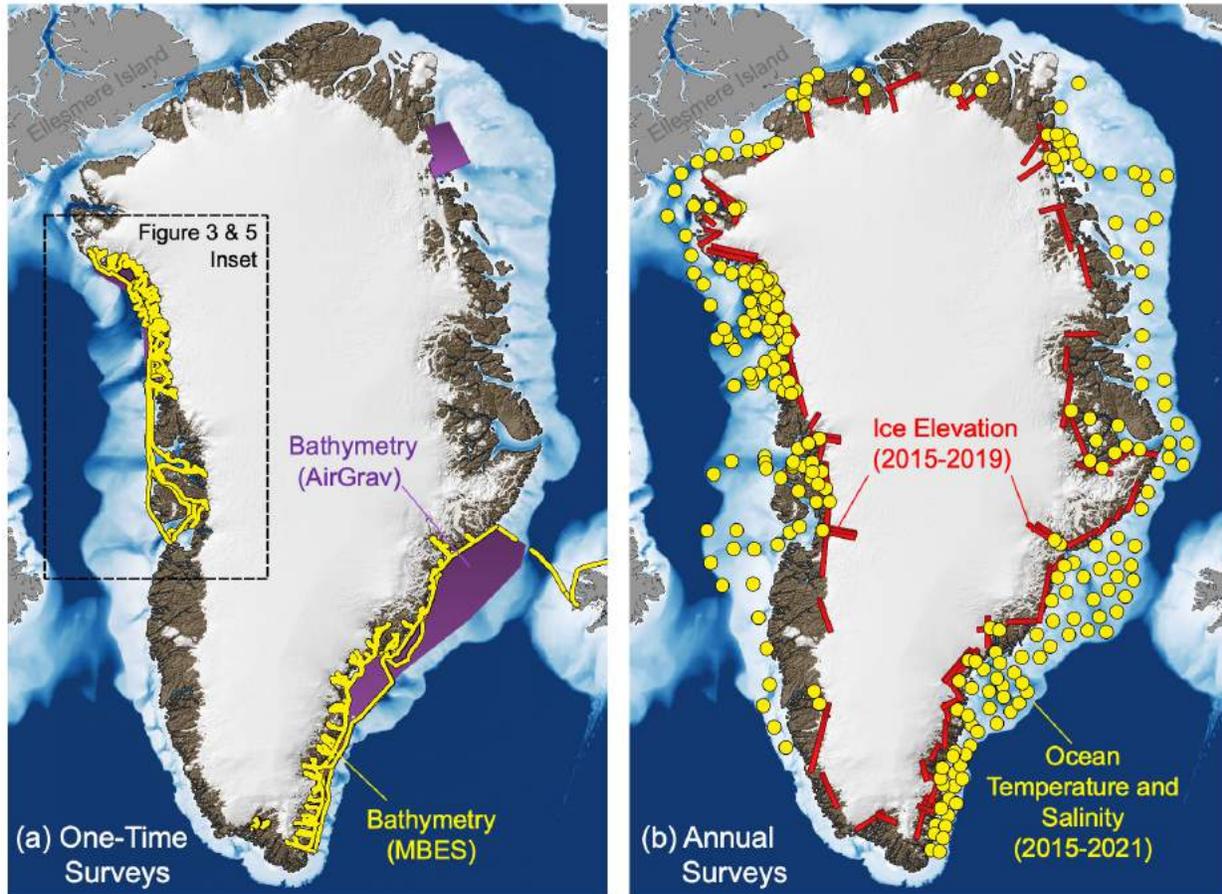
Fig. 1. Locations of measurements taken during NASA's Ocean Melting Greenland campaign 2015-21. Panel (a) shows bathymetry measurement locations collected during one-time surveys from AirGrav (purple) and multi-beam echo sounding (yellow). Panel (b) shows locations of ice elevation from airborne radar interferometry (red), and ocean temperature and salinity (yellow) measurements collected in annual surveys during the mission.

Pervasive Atlantic water and its variability

All around Greenland, warm, salty water from the Atlantic Ocean lies beneath a layer of colder, fresher water that comes from the Arctic (Fig. 2). Because this warm water sits deeper than 100 to 200 m below the ocean surface, it is impossible to use remote sensing techniques to directly observe these temperatures, and even inferred estimates face complex challenges and depend strongly on local oceanographic conditions (Snow et al. 2021). This means that direct, in situ observations of waters on the shelf are critically important for explaining ongoing ice loss and projecting future sea level rise.
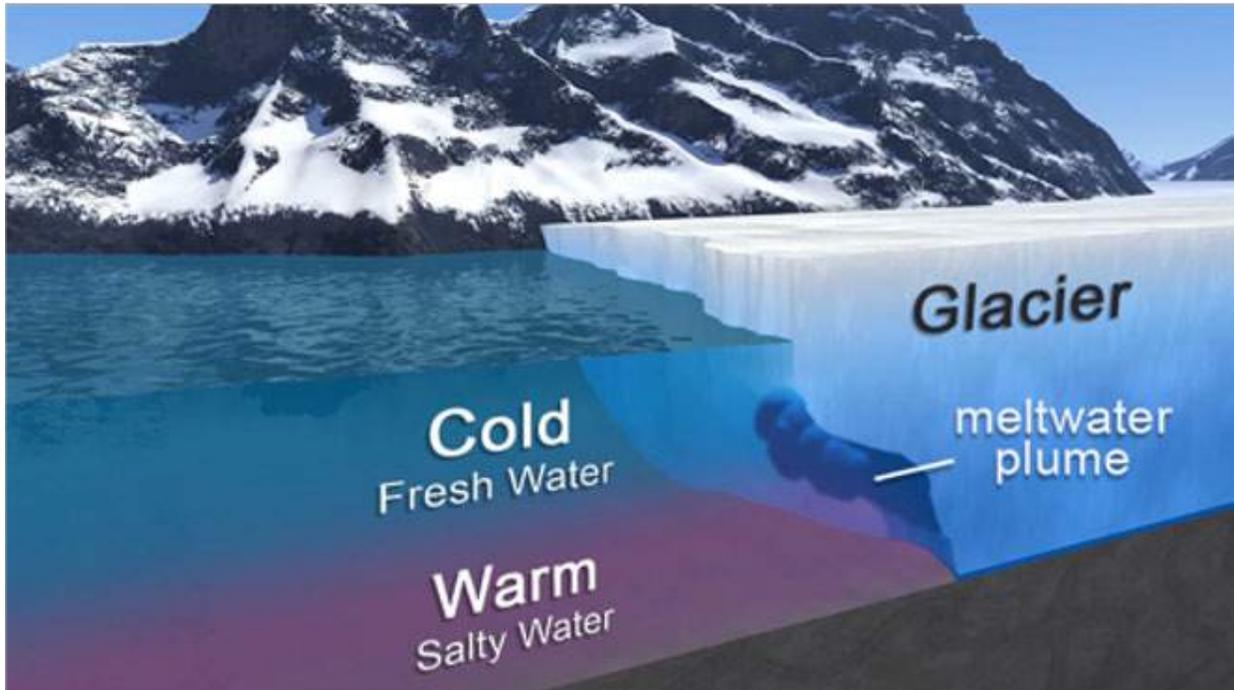
Fig. 2. Artist's impression of a meltwater plume at a typical Greenland marine-terminating glacier. Meltwater plumes, driven by subglacial discharge, entrain warm salty water at depth, causing high melt rates underneath the glacier front. See this video for more details.

OMG surveys showed that large-scale patterns of ocean temperature variability can persist on the shelf for years. Figure 1 shows locations of all the temperature and salinity profiles collected during a typical yearly ocean survey. The survey was conducted by aircraft and typically took 3-6 weeks to deploy approximately 250 expendable air-launched conductivity, temperature and depth sensors (AXCTDs). Figure 3 shows a subset of these locations along with insets depicting average temperature profiles from three different survey years, over three different regions along the west coast, along with a one-standard error uncertainty bound. The subsurface temperature maximum of approximately 2°C clearly shows the deep, warm layer, and between 2016 and 2018, this layer cooled by almost 1°C in all three regions—a temperature decline that can be traced back through the boundary current, which circulates around the southern half of Greenland (Khazendar et al. 2019). Subsequently, this layer warmed again in recent years in the western region, but not in the northwest.
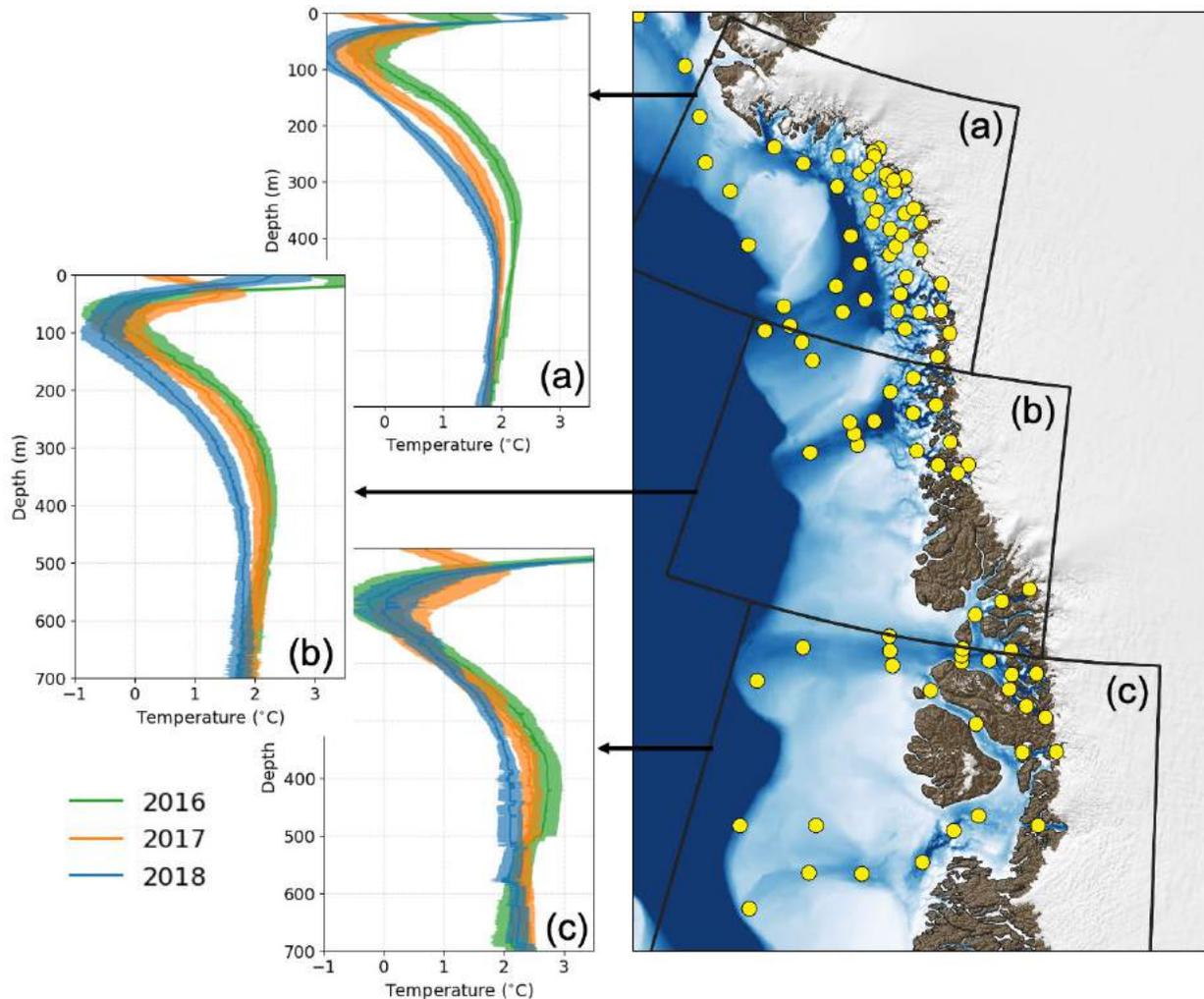
Fig. 3. West Greenland variations in ocean temperature in (a) Melville Bay, (b) Ummannaq Bay, and (c) Disko Bay measured by OMG Airborne Expendable CTDs (AXCTDs) during 2016-18. The map on the right shows the locations where temperature-salinity profiles were collected.

Linking temperature change with ice loss

With more than 70 peer-reviewed publications making use of the observations, the OMG data have revolutionized our knowledge of the coastal bathymetry (Morlighem et al. 2017) and the vulnerability of glaciers to ocean-driven ice loss. In many sectors of the ice sheet, major glaciers with significant potential to raise sea level are susceptible to destabilization by warmer subsurface water. On the central west coast, Greenland's fastest glacier (Sermeq Kujalleq or Jakobshavn Isbræ) can be dramatically altered by changes in ocean temperature, retreating and accelerating in warming conditions (Holland et al. 2008) and reversing those trends in cooler conditions (Khazendar et al. 2019). Likewise, its northern counterparts Zachariae Isstrøm and Humboldt Gletscher have been retreating and accelerating as a result of increased ocean melt over the past several decades (An et al. 2020; Rignot et al. 2021).

Taken together, OMG's observations show how ocean conditions surrounding Greenland could change the entire ice sheet's discharge by as much as a factor of two over the next century and beyond (Wood et al. 2021), which numerical climate projections must account for (Choi et al. 2021). But these

measurements also revealed a looming gap: if ocean conditions are driving widespread ice loss in Greenland, how do we continue to observe them after OMG's end?

OMG floats

During its final years, OMG tested autonomous, Argo-like floats as a tool for monitoring Greenland coastal waters (Fig. 4). Since 2017, seventeen Alamo floats and six APEX floats were deployed on the continental shelf and programmed to collect profiles usually once every 5 days, throughout both summer and winter. Data were collected in roughly the same geographic location by "parking" the floats on the bottom, which limited their drift between profiles.

Fig. 4. Flight Engineer Gerald Cirtwell (Kenn Borek Air) prepares to launch an APEX float from a DC-3 aircraft in 2020 during OMG.

In the first few years, most were lost after a short time due to equipment malfunction or operator error. However, since 2020, four of the APEX floats and two of the Alamo floats not only remained on the shelf but also survived sea ice cover through at least one winter (and in some cases two). In winter, when the floats are unable to surface due to pervasive sea ice, they store data onboard and transmit them later in the summer when access to the surface is again feasible. Although GPS positions are missing for the winter profiles, because the floats park on the shelf, profile positions during the winter can be assigned to those data with high confidence. This small array of floats has begun to build a more robust time series of ocean temperature and salinity in several key regions along Greenland's west coast (Fig. 5).
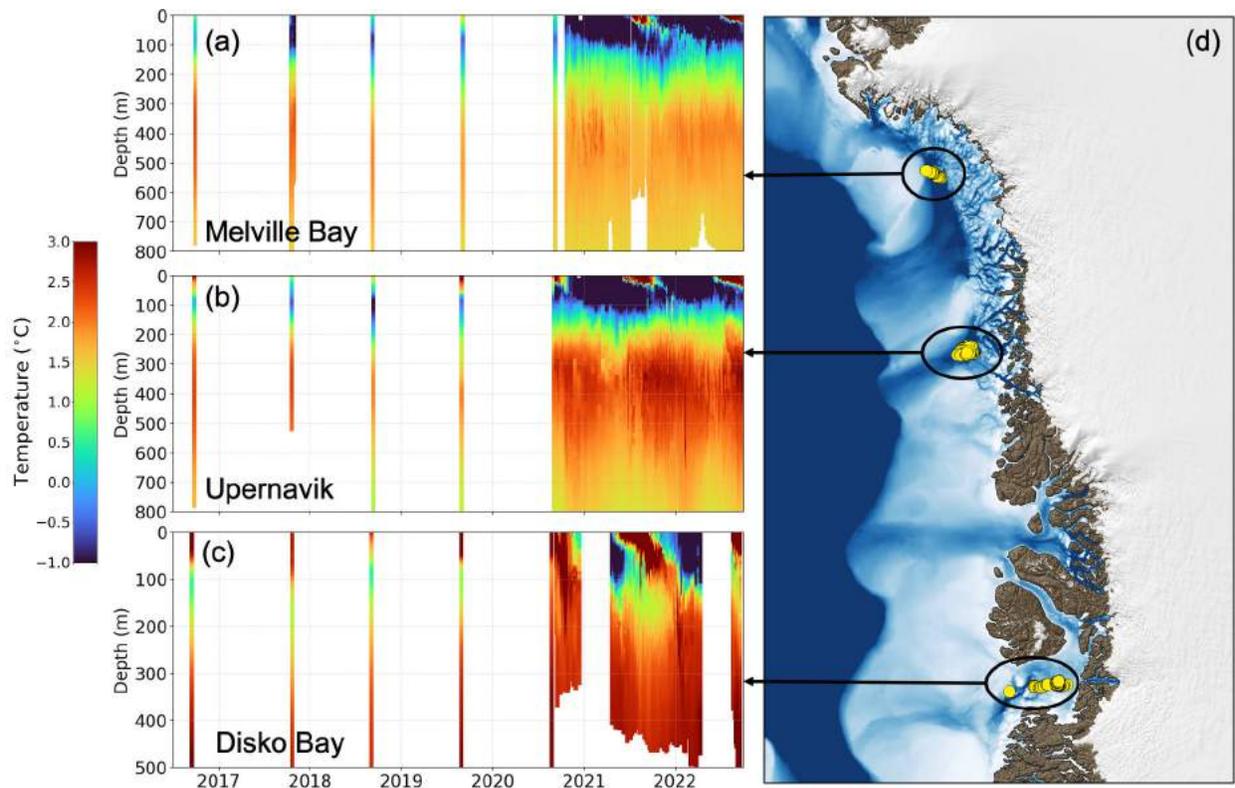
Fig. 5. Time series of temperature profiles along the west coast of Greenland in Melville Bay (a), Upernavik (b), and Disko Bay (c) from a combination of AXCTD and float observations. The discrete narrow bands in the early years correspond to the AXCTD surveys, conducted over a few weeks in late summer. The continuous time series were collected by floats. Yellow dots (right) show the locations where profiles are plotted.

A window to the future

Building on a decade of prior work, OMG demonstrated that the narrow strip of ocean surrounding Greenland provides a window into the future of its ice sheet. Accurate predictions of ice loss and sea level rise will hinge on observation of these waters—especially over interannual to decadal time scales. With the conclusion of OMG, the widespread surveys of the continental shelf have come to an end, and despite their importance, there is no plan to monitor these waters over the long term.

Autonomous floats provide a possible path forward, especially on the west coast where OMG focused its float deployments. Compared to moorings, floats are relatively inexpensive and easier to deploy. Now that OMG has demonstrated their ability to remain on the shelf and survive through the winter, they provide a promising solution for long-term monitoring. Furthermore, the international Argo program has already built infrastructure to maintain an array of more than 4000 of these instruments in the global oceans, and to distribute their data in near real time at no cost. An expansion of the Argo array to include a modest number of floats that park on Greenland's continental shelf would fill a critical gap in the global climate observing system and would align with recent assessments (Weller et al. 2019; Straneo et al. 2019) that call for sustained ocean observations to serve a variety of scientific and societal purposes.

Methods and data

All data collected during the OMG mission can be found at the Physical Oceanography Distributed Active Archive Center. In Fig. 3, all AXCTD observations from each year's surveys were averaged together using a simple mean. The band around each mean profile shows the standard error on the mean for each of these estimates. Because each survey was completed in a period of less than 6 weeks, these provide an estimate of the spatial variations of temperature within each region.

Acknowledgments

References

An, L., E. Rignot, M. Wood, J. K. Willis, J. Mouginot, and S. A. Khan, 2020: Ocean melting of the Zachariae Isstrøm and Nioghalvfjerdsfjorden glaciers, northeast Greenland. *P. Natl. Acad. Sci.*, **118**(2), e2015483118, https://doi.org/10.1073/pnas.2015483118.

Choi, Y., and Coauthors, 2021: Ice dynamics will remain a primary driver of Greenland ice sheet mass loss over the next century. *Commun. Earth Env.*, **2**, 26, https://doi.org/10.1038/s43247-021-00092-z.

Holland, D. M., R. H. Thomas, B. De Young, M. H. Ribergaard, and B. Lyberth, 2008: Acceleration of Jakobshavn Isbræ triggered by warm subsurface ocean waters. *Nat. Geosci.*, **1**, 659-664, https://doi.org/10.1038/ngeo316.

Khazendar, A., and Coauthors, 2019: Interruption of two decades of Jakobshavn Isbræ acceleration and thinning as regional ocean cools. *Nat. Geosci.*, **12**, 277-283, https://doi.org/10.1038/s41561-019-0329-3.

Morlighem, M., and Coauthors, 2017: BedMachine v3: Complete bed topography and ocean bathymetry mapping of Greenland from multibeam echo sounding combined with mass conservation. *Geophys. Res. Lett.*, **44**, 11,051- 11,061, https://doi.org/10.1002/2017GL074954.

Rignot, E., and Coauthors, 2021: Retreat of Humboldt Gletscher, north Greenland, driven by undercutting from a warmer ocean. *Geophys. Res. Lett.*, **48**, e2020GL091342, https://doi.org/10.1029/2020GL091342.

Snow, T., and Coauthors, 2021: More than skin deep: Sea surface temperature as a means of inferring Atlantic Water variability on the southeast Greenland continental shelf near Helheim Glacier. *J. Geophys. Res.-Oceans*, **126**(4), https://doi.org/10.1029/2020JC016509.

Straneo, F., and P. Heimbach, 2013: North Atlantic warming and the retreat of Greenland's outlet glaciers. *Nature*, **504**, 36-43, https://doi.org/10.1038/nature12854.

Straneo F., and Coauthors, 2019: The case for a sustained Greenland Ice Sheet-Ocean Observing System (GrIOOS). *Front. Mar. Sci.*, **6**, 138, https://doi.org/10.3389/fmars.2019.00138.

Weller R. A., D. J. Baker, M. M. Glackin, S. J. Roberts, R. W. Schmitt, E.S. Twigg, and D. J. Vimont, 2019: The challenge of sustaining ocean observations. *Front. Mar. Sci.*, **6**, 105, https://doi.org/10.3389/fmars.2019.00105.

Wood, M., and Coauthors, 2021: Ocean forcing drives glacier retreat in Greenland. *Sci. Adv.*, **7**, eaba7282, https://doi.org/10.1126/sciadv.aba7282.

November 23, 2022

Partnering in Search of Answers: Seabird Die-offs in the Bering and Chukchi Seas

R. Kaler[1], G. Sheffield[2], S. Backensto[3], J. Lindsey[4], T. Jones[4], J. Parrish[4], B. Ahmasuk[5], B. Bodenstein[6], R. Dusek[6], C. Van Hemert[7], M. Smith[7], and P. Schwalenberg[8]

[1]U.S. Fish & Wildlife Service, Alaska Region, Anchorage, AK, USA
[2]Alaska Sea Grant, Marine Advisory Program, University of Alaska Fairbanks, Nome, AK, USA
[3]National Park Service, Fairbanks, AK, USA
[4]Coastal Observation and Seabird Survey Team, University of Washington, Seattle, WA, USA
[5]Marine Advocate, Kawerak Inc., Nome, AK, USA
[6]National Wildlife Health Center, U.S. Geological Survey, Madison, WI, USA
[7]Alaska Science Center, U.S. Geological Survey, Anchorage, AK, USA
[8]Alaska Migratory Bird Co-Management Council, Anchorage, AK, USA

Highlights

- During 2022, the northern Bering and southern Chukchi Sea region reported the sixth consecutive year of higher-than-expected beach-cast seabirds (2017-22).
- Reports of beach-cast carcasses ranged from Point Hope to Izembek Lagoon and numbered ~450, fewer than in the preceding several years but a continued concern for coastal communities.
- Tracking the duration, geographic extent, and magnitude of seabird bird die-offs across Alaska's expansive and remote coastline is only possible through well-coordinated communication and a dedicated network of Tribal, State, Federal, and university academic partners.

Introduction

Prior to 2015, seabird die-offs in Alaskan waters were rare; they typically occurred in mid-winter, linked to epizootic disease events or above-average ocean temperatures associated with strong El Niño-Southern Oscillation events (Bodenstein et al. 2015; Jones et al. 2019; Romano et al. 2020). Since 2015, the U.S. Fish and Wildlife Service (USFWS) has monitored mortality events that have become annual occurrences in Alaska (Fig. 1). Since 2017, communities on the coasts of the northern Bering and southern Chukchi Seas have annually observed dead and dying seabirds along their coasts (Fig. 2). Affected species included birds that consume plankton such as auklets (*Aethia* spp.), plankton and fish consumers such as shearwaters (*Ardenna* spp.) and northern fulmars (*Fulmarus glacialis*), primarily fish-consuming murres (*Uria* spp.), puffins (*Fratercula* spp.), and kittiwakes (*Rissa* spp.), as well as low numbers of benthic feeding sea ducks (*Somateria* spp.) (U.S. Geological Survey 2022). The range of seabird and prey species involved, the timing of these die-offs throughout summer, and the localization of events over widespread areas indicate environmental causes at multiple trophic levels. Such wildlife mortality events are a public health concern for coastal communities that rely on ocean resources for

their nutritional, cultural, and economic well-being. They have also been seen as a harbinger of concern for the state of the Arctic Ocean itself.
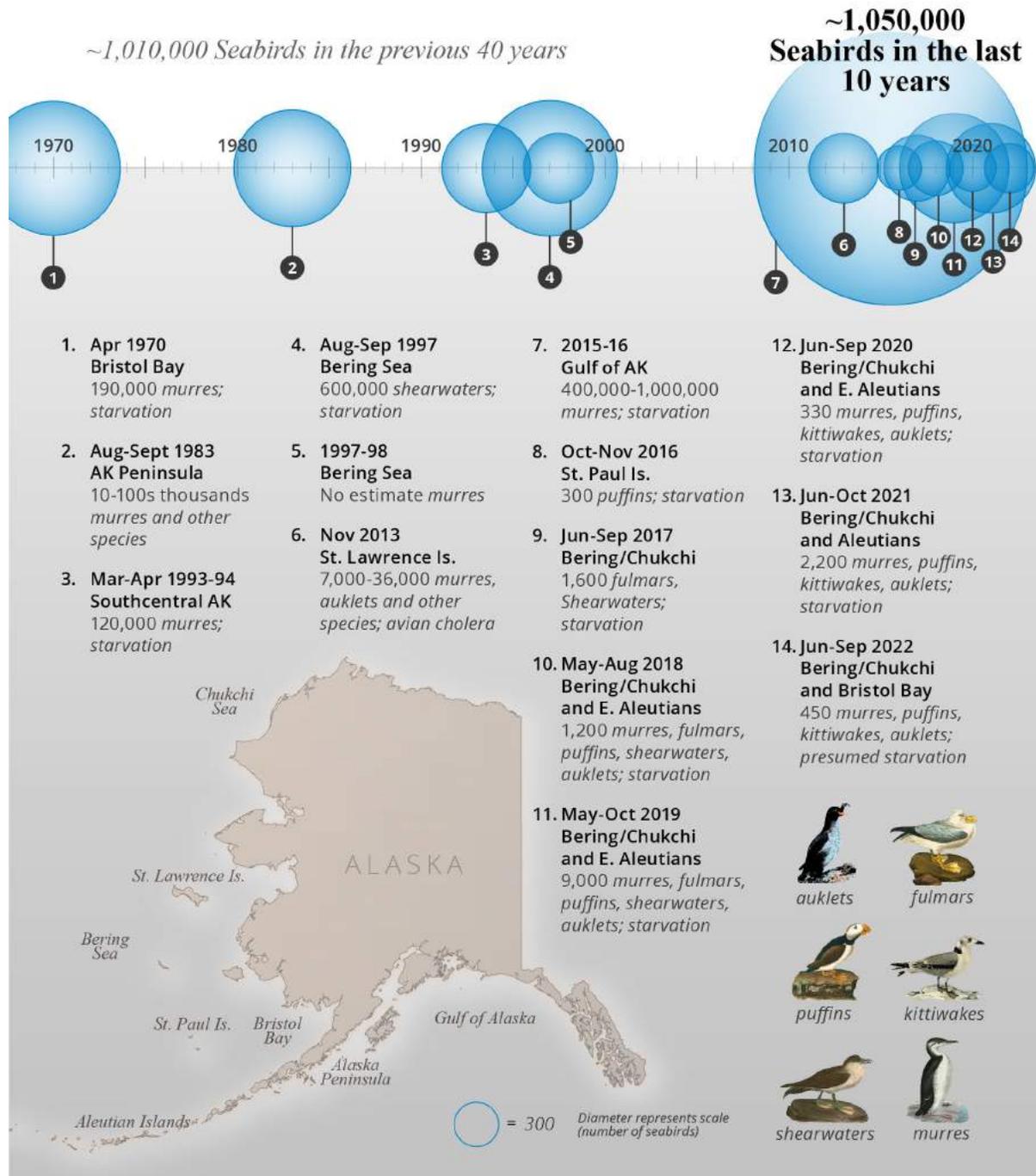

Fig. 1. Alaska seabird die-offs, 1970 to present. Since 2015, mass die-offs have annually occurred in Alaska. Species primarily affected include murres, puffins, auklets, shearwaters, fulmars, and kittiwakes. (Credit: Sarah Battle, NOAA/PMEL; modified original by Robert Kaler)
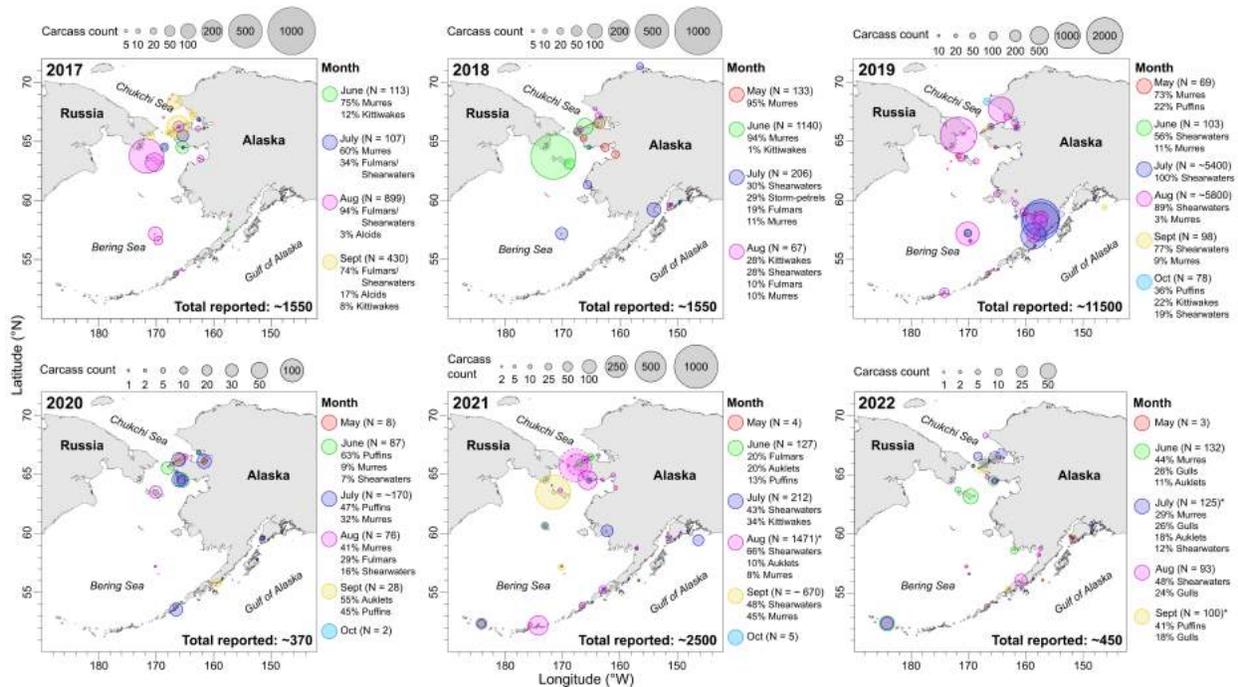
Fig. 2. Alaska seabird mortality records, 2017-22. Size of concentric circles indicates the cumulative count of seabird carcasses reported each month of the corresponding year, aggregated into 100×100 km grid cells overlaid onto the map. Note that locations with no reported carcass counts may result from remoteness and/or lack of visitation or reporting capacity, rather than a lack of seabird carcass deposition. Species/species groups are summarized by month, indicated by color of circle, and percent (%) of total reported (N) each month. Reports courtesy of Tribal, State, and Federal partners.

Seabirds are sentinels of the status of marine ecosystems and these die-offs are concurrent with a massive ecological shift resulting from the loss of sea ice extent and duration in the Bering and Chukchi Seas (Stabeno et al. 2019). Seabirds are top predators, with many consuming forage fish. For example, Pacific sand lance (*Ammodytes hexapterus*), which are a small forage fish found in the nearshore area, are a high-quality prey item, rich in nutrients and calories (Robards et al. 1999). Similarly, Pacific capelin (*Mallotus villosus*) are associated with cold water and are high in nutrients and calories (Montevecchi and Piatt 1984). With increasing ocean temperatures, the numbers of sand lance and capelin have declined, while the numbers of juvenile (Age-0) walleye pollock (*Gadus chalcogrammus*) and Pacific cod (*Gadus macrocephalus*), which are lower quality prey compared to sand lance and capelin, have increased (Duffy-Anderson et al. 2019). Age-0 walleye pollock and its caloric value have been compared to "junk food" (Romano et al. 2006). A drastically increased abundance of Age-0 pollock in warm years (Renner et al. 2016) may compensate for low-energy content of individual fish (Kokubun et al. 2018). Lastly, planktivorous seabirds consume Euphausiids (krill), which are high-value but only locally and seasonally available, and copepods—a group of small crustaceans that vary in size and energy value. As an example of metabolic rate, common murres (*Uria aalge*) are thought to consume 10-30% of their 1050-gram body mass every day, which equates to ~90-300 fish per day (Ainly et al. 2002). While the specific cause of why seabird die-offs have increased in frequency remains largely unknown, the decrease in sea ice extent and lipid-rich ice algae along with warmer ocean conditions are likely involved.

Findings to date, 2017-21

Apparent emaciation was the most significant factor contributing to death based on a combination of field reports, laboratory assessments, and ancillary test results of examined carcasses (Table 1; Bodenstein et al. 2022). Researchers continue to evaluate possible contributing factors. Sample size was limited in 2022, but Highly Pathogenic Avian Influenza (HPAI H5 or H7; see HPAI discussed in *Arctic Geese* essay) has not been confirmed in seabird carcasses except for gulls (*Larus* spp.) and jaegers (*Stercorarius* spp.), which scavenge on carcasses of other birds and mammals. Additionally, H10N6 (a Low Pathogenic Avian Influenza) was detected in two murres samples from St. Lawrence Island in 2018 (Will et al. 2020a).

Table 1. Summary of Bering and Chukchi Seas seabird necropsies, 2017-21. More than 14,000 dead seabirds were reported and a total of 117 carcasses were examined. 92 cases had emaciation identified as the Cause Of Death (COD), seven cases where COD was undetermined, and 17 cases where COD was determined as "Other", which included predation, trauma, encephalitis, peritonitis, and bacterial infection. Low Pathogenic Avian Influenza (n=4) and saxitoxin (n=15) were also detected; however, the virus and biotoxin were not determined to be the COD except for one case in 2020 where saxitoxin toxicosis was suspected.

	2017	2018	2019	2020	2021	Total
Total Reported	>1,600	>1,200	>9,000	>330	>2,200	>14,330
Total Examined	19	25	39	20	14	117
Reported Cause of Death						
Emaciation	17	19	31	13	12	92
Undetermined	0	3	2	1	1	7
Other	2	3	6	6	1	18
Avian Influenza Detected	0	2	0	1	1	4
Saxitoxin Detected	11	BDL*	3	1[&]	BDL*	15

*BDL - Below detection limits for the laboratory test used.
[&]Saxitoxin toxicosis was also suspected to be the cause of death.

Exposure to harmful algal bloom biotoxins (e.g., saxitoxin, associated with paralytic shellfish poisoning) has been detected in seabird tissues in the region, including a puffin from Unalaska Island in 2020. In 2017, saxitoxin was detected in the majority of northern fulmar carcasses collected during a mortality event; however, direct neurotoxic action by saxitoxin could not be confirmed and starvation appeared to be the proximate cause of death (Van Hemert et al. 2021). Little is known about the occurrence of these biotoxins or their impacts on wild seabirds and USGS Alaska Science Center researchers continue investigations (Matthew Smith, USGS, Alaska Science Center, 2022, personal communication).

Beach-cast seabirds continue to be reported over a wide geographic range and throughout summer and fall on an annual basis, albeit at much reduced numbers in some recent years (2020 and 2022). Observations at northern seabird breeding colonies indicate lack of breeding attempts or very late and unsuccessful breeding over several years (Romano et al. 2020; Will et al. 2020b). These observations together with the northward expansion of gadid fishes (Pacific cod, pollock; Duffy-Anderson et al. 2019) suggest that the seabird die-offs stem from a lack of food or unfavorable foraging conditions, indicating

ecosystem changes that may be associated with abnormally high ocean water temperatures (Will et al. 2020a). Additional work is needed to understand links between prey availability and the health and productivity of local seabird populations.

Conclusions

Seabirds and their eggs are an important subsistence food for remote communities in rural Alaska. Rural residents and particularly Alaska Native peoples are concerned about impacts to subsistence food resources. Members of subsistence communities in the northern Bering and southern Chukchi Sea region are frustrated by the lack of timely answers regarding the cause of seabird die-off events and whether birds and eggs are safe to consume. Some communities have requested assistance to document these die-offs and collect samples for testing. The past three years have been especially challenging owing to the global COVID-19 pandemic, which limited abilities to conduct full necropsies on carcasses to determine causes of death, as well as due to increased concerns regarding HPAI in 2022. The USFWS continues to collaborate with numerous partners, including the Alaska Migratory Bird Co-Management Council, Alaska Department of Fish and Game, National Oceanic and Atmospheric Administration, National Park Service, and coastal subsistence communities to monitor and assess seabird die-offs. The USFWS also collaborates with the University of Washington Coastal Observation and Seabird Survey Team, University of Alaska Fairbanks/Alaska Sea Grant Program, University of Alaska Fairbanks Institute for Arctic Biology, USGS (National Wildlife Health Center and Alaska Science Center), and other State and Federal agencies to document and report die-off events.

The next decades will be critical for determining how coastal species and communities in northern Alaska adapt to a fast-changing environment. With Alaska's vast coastline and remote communities, State and Federal agencies lack adequate resources required to investigate changes and document these now annually occurring seabird mortality events. Efforts have led to several lessons learned. Firstly, reports and observations are property; permission must be granted prior to using or sharing observational data and acknowledgment of partner contributions is essential. Secondly, maintaining clear channels of communication, especially regarding shared priorities and mutual expectations, is critical throughout the response process. Thirdly, outreach and information exchange are dynamic, and partners must strive to be consistent, reliable, and inclusive. Lastly, moments of misunderstanding or disagreement provide opportunities for patience and listening. Success begins with small steps.

Acknowledgments

References

Ainly, D., and Coauthors, 2002: Common murre (*Uria aalge*), The Birds of North America, No. 666., A. Poole and F. Gill, Eds., The Birds of North America, Inc. Philadelphia, PA.

Bodenstein, B., and Coauthors, 2015: Avian cholera causes marine bird mortality in the Bering Sea of Alaska. *J. Wildlife Dis.*, **51**, 934-937, https://doi.org/10.7589/2014-12-273.

Bodenstein, B. L., R. J. Dusek, M. M. Smith, C. R. Van Hemert, and R. S. A. Kaler, 2022: USGS National Wildlife Health Center necropsy results to determine cause of illness/death for seabirds collected in Alaska from January 1, 2017 through December 31, 2021: U.S. Geological Survey data release, https://doi.org/10.5066/P9XHBX75.

Duffy-Anderson, J. T., and Coauthors, 2019: Responses of the northern Bering Sea and southeastern Bering Sea pelagic ecosystems following record-breaking low winter sea ice. *Geophys. Res. Lett.*, **46**, 9833-9842, https://doi.org/10.1029/2019GL083396.

Jones, T., and Coauthors, 2019: Unusual mortality of Tufted puffins (*Fratercula cirrhata*) in the eastern Bering Sea. *PLoS ONE*, **14**, e0216532, https://doi.org/10.1371/journal.pone.0216532.

Kokubun, N., and Coauthors, 2018: Inter-annual climate variability affects foraging behavior and nutritional state of thick-billed murres breeding in the southeastern Bering Sea. *Mar. Ecol. Prog. Ser.*, **593**, 195-208, https://doi.org/10.3354/meps12365.

Montevecchi, W. A., and J. F. Piatt, 1984: Composition and energy content of mature inshore spawning capelin (*Mallotus villosus*): Implications for seabird predators. *Comp. Biochem. Phys. A*, **78**(1), 10-20, https://doi.org/10.1016/0300-9629(84)90084-7.

Renner, M., and Coauthors, 2016: Timing of ice retreat alters seabird abundances and distributions in the southeast Bering Sea. *Biol. Letters*, **12**, 20160276, https://doi.org/10.1098/rsbl.2016.0276.

Robards, M., M. Willson, R. Armstrong, and J. Piatt, 1999: Sand lance as cornerstone prey for predator populations. USDA Forest Service - Research Papers PNW-RP, 17-44.

Romano, M., J. F. Piatt, D. D. Roby, 2006: Testing the junk-food hypothesis on marine birds: Effects of prey type on growth and development. *Waterbirds*, **29**(4), 407-524, https://doi.org/10.1675/1524-4695(2006)29[407:TTJHOM]2.0.CO;2.

Romano, M., and Coauthors, 2020: Die-offs, reproductive failure, and changing at-sea abundance of murres in the Bering and Chukchi Seas in 2018. *Deep-Sea Res. Pt. II*, **181-182**, 104877, https://doi.org/10.1016/j.dsr2.2020.104877.

Stabeno, P. J., R. L. Thoman, and K. Wood, 2019: Recent warming in the Bering Sea and its impacts on the ecosystem. *Arctic Report Card 2019*, J. Richter-Menge, M. L. Druckenmiller, and M. Jeffries, Eds., https://www.arctic.noaa.gov/Report-Card.

US Geological Survey, 2022: Wildlife Health Information Sharing Partnership—event reporting system (WHISPers) on-line database, accessed October 2022, https://whispers.usgs.gov/.

Van Hemert, C., and Coauthors, 2021: Investigation of algal toxins in a multispecies seabird die-off in the Bering and Chukchi seas. *J. Wildlife Dis.*, **57**(2), 399-407, https://doi.org/10.7589/JWD-D-20-00057.

Will, A., and Coauthors, 2020a: Investigation of the 2018 thick-billed murre (*Uria lomvia*) die-off on St. Lawrence Island rules out food shortage as the cause. *Deep-Sea Res., Pt. II*, **181**, 104879, https://doi.org/10.1016/j.dsr2.2020.104879.

Will, A., and Coauthors, 2020b: The breeding seabird community reveals that recent sea ice loss in the Pacific Arctic does not benefit piscivores and is detrimental to planktivores. *Deep-Sea Res., Pt. II*, **181-182**, 104902, https://doi.org/10.1016/j.dsr2.2020.104902.

December 9, 2022

Consequences of Rapid Environmental Arctic Change for People

SEARCH[1], O. Ahkinga[1], E. Alexander[1], M. D. Apassingok[1], B. Baker[1], M. Baker[1], M. Berman[1], M. Blair[1], E. Bloom[1], N. J. Burns[1], A. E. Copenhaver[1], E. Q. Cravalho[1], J. Donatuto[1], K. Dunton[1], S. V. Fletcher[1], E. Froehlich[1], J. C. George[1], C. Harris[1], M. Heavner[1], M. Hoffbeck[1], M. Holland[1], M. T. Jorgenson[1], B. P. Kelly[1]*, E. Kerttula[1], G. W. Kling[1], C. W. Koch[1], L. Landrum[1], S. Lange[1], M. K. Lukin[1], E. Marino[1], V. K. Metcalf[1], C. Nunn[1], R. Pincus[1], P. Pungowiyi[1], M. Robards[1], J. Q. Schaeffer[1], A. Shahbazi[1], A. Shultz[1], D. T. Turner[1], J. E. Walsh[1], F. Wiese[1], and G. Wong[1]

Wilson Justin[2,3]

[1]Study of Environmental Arctic Change
[2]Althsetnay Headwaters People Clan, Ahtna Dine' Storyteller, Elder Ambassador Cheesh'na Tribe, Chistochina, AK, USA
[3]Chair, Mt. Sanford Tribal Consortium Board of Directors, Chistochina, AK, USA

*Corresponding author

Highlights

- People experience the consequences of a rapidly changing Arctic as the combined effects of physical conditions; responses of biological resources; impacts on infrastructure; decisions influencing adaptive capacities; and both environmental and international influences on economics and well-being.
- Living and innovating in Arctic environments over millennia, Indigenous Peoples have evolved holistic knowledge providing resilience and sustainability. Indigenous expertise is augmented by scientific abilities to reconstruct past environments and to model and predict future changes. Applying the combined understanding of Indigenous and scientific experts will be important if decision makers (from communities to governments) are to help mitigate and adapt to a rapidly changing Arctic.
- Considerable discussion among diverse collaborators suggests that addressing unprecedented Arctic environmental changes requires hearing one another, aligning values, and collaborating across knowledge systems, disciplines, and sectors of society.

Ahtna Dine' Storyteller Wilson Justin's Oral Account: https://youtu.be/gBBffAtqMsc

Introduction

The vital signs and key indicators tracked in the Arctic Report Card since 2006 detail rapid environmental changes in the Arctic. In this essay and the accompanying oral history, Indigenous, scientific, and decision-making experts collaboratively describe just some consequences of these rapid changes for people. Here, we focus on people in the Arctic while acknowledging that the changing Arctic has important impacts on people beyond the region. We also highlight the necessity of diverse, complex collaborations as one of the tools needed to advance policy solutions to the profound consequences of these changes for people.

If current rates of greenhouse gas emissions continue, Arctic people will increasingly experience in this century "extremes in sea ice, temperature, and precipitation phase far outside anything experienced in the past century and probably much longer" (Landrum and Holland 2020). People experience the consequences of these extremes not as individual events but as the composite of multiple events. Understanding the impacts of environmental shifts and extremes requires assessments of the drivers of change; their direct, indirect, and compounding consequences on human well-being, economics, and international cooperation; as well as the modifying effects of community and governmental actions from local to international scales (e.g., Fisher et al. 2020; Harper et al. 2020; Landrum and Holland 2020; Schaeffer 2021). Because these consequences and modifying effects compound over varying time periods, we do not limit our consideration to 2022 or any other particular year.

In his oral account, Ahtna Dine' Storyteller Wilson Justin explains that the Arctic environment has already changed (see 17:08), and we must work to overcome the colonial divide and determine together "how we're going to speak to each other in terms of not only rebuilding, but what it is we are going to rebuild" (see 17:17-17:50). Similarly, Vera Kingeekuk Metcalf has led her Study of Environmental Arctic Change (SEARCH) colleagues in understanding the importance of language and knowing "when we are saying the same thing" (see also Metcalf 2021; see 14:34-15:00).

Recognizing that the human consequences of Arctic environmental changes result from their compounding effects helps structure cross-cultural syntheses. Increasing temperature, diminishing ice, thawing permafrost, increasing frequency and severity of storms, wildfires, and other forces disrupt mechanisms that ensure safety, food security, and other aspects of human well-being (see essays *Surface Air Temperature*, *Sea Surface Temperature*, *Sea Ice*, *Tundra Greenness*, and *Precipitation*). Indigenous Knowledge holders possess specialized understanding of the Arctic and view these impacts

as part of an interconnected universe. Justin suggests that we need more holistic observations and syntheses, and Metcalf describes an Indigenous approach in which elders meet daily to share and synthesize recent environmental observations from which they predict future conditions (Apassingok et al. 2022).

Integrating diverse perspectives and knowledge systems is necessary but insufficient to mitigate and adapt to change in ways that preserve the health and well-being of people. It also is vital that we use our collective understanding to offer practical solutions to problems experienced at all levels of community, business, and government, which necessitates collaborating with experts in decision making as well as Indigenous and scientific knowledge.

As a team of Indigenous, scientific, and decision-making experts, we have begun synthesizing the human consequences of environmental change, and here we illustrate with a few brief examples how combinations of environmental changes impact human safety, food security, and health in the Arctic. Our examples are focused on Alaska, but our broader work considers the entire Arctic.

Safety. Arctic Indigenous Peoples interact intimately with their environments, and their safety depends to a large degree on knowing how to operate on land and sea (see Fig. 1). For example, the distribution, quality, thickness, and timing of ice on the ocean, lakes, and rivers drive nearly every aspect of life on Arctic coasts, from boating to whaling and seal hunting to the safety of fishing and foraging (see 12:00-12:35).

Fig. 1. St. Lawrence Island Yupik butcher a bowhead whale on shorefast ice adjacent to Gambell, Alaska, circa 1960. Butchering and dividing the harvest ideally took place after pulling the whale onto the ice or, if need be, from the ice edge and boats as seen here. Increasingly, suitable shorefast ice is absent or too thin for either method, and butchering must take place entirely in the water. Credit: Francis H. Fay.

The danger and costs of whale harvesting have been driven higher by diminishing sea ice and distant military conflict. The number of days spent hunting bowhead whales in open water during fall at Utqiaġvik, Nuiqsut, and Kaktovik has doubled over the past 40 years as the duration and extent of sea ice cover declined. At the same time, wave height has increased with sea ice retreat, increasing risks to hunters. The diminished sea ice and associated increases in waves have driven some villages to purchase larger boats for whale hunting but at great up-front expense. Larger boats are also more expensive to operate, doubling or tripling fuel consumption. The war in Ukraine has driven fuel costs even higher, exacerbating the local impact of ice retreat on the costs of whaling.

For walrus hunters, the increased speed and magnitude of sea ice retreat forces much longer excursions in small skiffs (see Fig. 2). Perry Pungowiyi of Savoonga, for example, reports hunters traveling as much as 100 miles from St. Lawrence Island to reach walruses during the spring harvest. In the Chukchi Sea, some seal hunting communities are hampered by decreasing duration and thinning of the sea ice cover (Huntington et al. 2016). Darlene Tocktoo Turner describes traditional on-ice hunting routes around Shishmaref as no longer safe.

Fig. 2. Yupik hunters offshore of St. Lawrence Island. February 2021. Credit: Justina Noongwook.

Changes in seasonal patterns for harvesting (see Food Security section below) have dramatic consequences for safety. Fatal falls through sea, lake, and river ice in Alaska, which disproportionately involve Indigenous People, are increasing (Fleischer et al. 2014; see essay *Lake Ice*). Maija Lukin from Kotzebue, Alaska has described—in powerful terms—the human costs of these tragedies (Fisher et al. 2020).

Food Security. Understanding the impacts of environmental change on Inuit food security is greatly enhanced by an Inuit holistic view considering the influences and interactions of environmental stability, resource availability and accessibility, decision-making power, culture, and health and wellness (ICC-Alaska 2015; Johnson et al. 2021; see 02:20-02:43). Such understanding is being forced to evolve rapidly, however, because of shifts in the migratory patterns of Arctic animals including caribou, walrus, whales, birds, and fish (ICC-Alaska 2015). For example, bowhead whales now migrate earlier in spring and later

in fall, forcing whale hunting crews at Utqiaġvik to hunt both earlier in spring to make use of more stable shorefast ice and much later into autumn to harvest the preferred younger whales that arrive later in the migration. Similarly, geese hunting is happening earlier in Utqiaġvik to avoid soft snow cover in late May, while fall fishing, which relies on snow machine access, occurs later due to delayed freeze up (see essay *Arctic Geese*).

While access to food species is rapidly changing, laws and other policies regulating harvests will struggle to keep up (see essays *Arctic Ocean Primary Productivity: The Response of Marine Algae*; *Partnering in Search of Answers: Seabird Die-offs in the Bering and Chukchi Seas*). For example, expanding legal harvesting to other species of whales will likely soon be critical to the health and quality of life of Indigenous communities, but securing permissions from international and national authorities could take decades (Fisher et al. 2020).

Human Health. As the changing Arctic environment affects the health of Arctic people, the consequences can be exacerbated by limited and compromised infrastructure (Schaeffer 2021). For example, the consequences of wildfires impact people through disturbance of the landscape and negative impacts on respiratory health. Some regions of the Arctic, such as Siberia and Alaska, have seen increasingly large areas burned in the past 40 years (York et al. 2020). Burns accelerate atmospheric warming through decreased surface albedo and increased carbon losses during combustion and subsequent permafrost thaws. Smoke compromises breathing, interrupts aviation, and interferes with traditional subsistence activities. Arctic communities typically lack air conditioning, and Savannah Fletcher described how increasing summer air temperatures in Fairbanks have required ventilating buildings with open windows, exacerbating exposure to wildfire smoke.

Access to clean water is a major health challenge across much of the Arctic (Harper et al. 2020). At the same time, climate-induced changes on land surfaces are causing dramatic shifts in the availability of water (see essay *Tundra Greenness*). Permafrost thaw is often implicated, and in 2022, a tundra lake near Kotzebue, Alaska, supplying freshwater to some residents abruptly drained. Nonetheless, quantitative projections of climate change impacts on drinking water in the Arctic are lacking (Harper et al. 2020).

In September 2022, typhoon Merbok demonstrated the inextricable linkage of environmental change and impacts on human safety, food security, and health. The storm—fueled by unusually warm water in the subtropical North Pacific Ocean—flooded several Bering Sea communities; damaged or destroyed homes, hunting camps, boats, and other subsistence infrastructure; and disrupted vital fall subsistence harvests (see Fig. 3).

Fig. 3. Surging Bering Sea waters, driven inland as a consequence of typhoon Merbok in September 2022, damaged one third of the homes in Golovin, Alaska. Credit: Josephine Daniels.

Future directions

The examples presented here just scratch the surface of the compound impacts to people of rapid Arctic change. As we expand understanding of how people experience dramatic environmental changes, Wilson Justin, Maija Lukin, and other Indigenous experts point us to a deeper, more soulful appreciation of the human hardships and costs. They make clear the importance of actions rooted in shared values (see 17:34) and recognition of the intersectional nature of the problem, in which people are simultaneously burdened by crises of safety, food security, and health (see essay *Satellite Record of Pan-Arctic Maritime Ship Traffic*).

SEARCH is integrating and synthesizing the perspectives of Indigenous Knowledge holders, scientists, and policy experts with the intent of co-developing practical solutions, which could range from changes in behavior to new partnerships to policy proposals. We have learned that hearing one another, aligning values, and working in concert require new collaborations across knowledge systems, disciplines, and sectors of society. This essay resulted from a series of facilitated discussions over the course of a year among the 42 authors. Specifics of each author's contributions are detailed on the SEARCH website. These complex collaborations are key to advancing timely, evidence-based, and practical solutions for communities, businesses, and governments (Kelly and Fisher 2021).

References

Apassingok, M. D., V. K. Metcalf, and B. P. Kelly, 2022: Moving to the back of the boat: how a new approach to Arctic research can help us better understand and respond to environmental change. ArcticToday. September 9, 2022. https://www.arctictoday.com/moving-to-the-back-of-the-boat/.

Fisher, A. M., B. P. Kelly, and G. W. Kling (eds.), 2020: *Arctic Futures 2050 Conference Report*. Washington, D.C., Study of Environmental Arctic Change. https://doi.org/10.6084/m9.figshare.12148770. 48 pp.

Fleischer, N. L., P. Melstrom, E. Yard, M. Brubaker, and T. Thomas, 2014: The epidemiology of falling-through-the-ice in Alaska, 1990-2010. *J. Public Health (Oxford),* **36**(2), 235-242, https://doi.org/10.1093/pubmed/fdt081.

Harper, S. L., C. Wright, S. Masina, and S. Coggins, 2020: Climate change, water, and human health in the Arctic. *Water Secur.*, **10**, 100062, https://doi.org/10.1016/j.wasec.2020.100062.

Huntington, H. P., M. Nelson, and L. T. Quakenbush, 2016: Traditional knowledge regarding ringed seals, bearded seals, and walrus near Shishmaref, Alaska. Final report to the Eskimo Walrus Commission, the Ice Seal Committee, and the Bureau of Ocean Energy Management for contract #M13PC00015. 9 pp.

ICC-Alaska, 2015: Alaskan Inuit Food Security Conceptual Framework: How to Assess the Arctic from an Inuit Perspective: Summary and Recommendations Report, Inuit Circumpolar Council-Alaska, https://iccalaska.org/wp-icc/wp-content/uploads/2016/03/Food-Security-Summary-and-Recommendations-Report.pdf.

Johnson, N., and Coauthors, 2021: The Impact of COVID-19 on Food Access for Alaska Natives in 2020. *Arctic Report Card 2021*, T. A. Moon, M. L. Druckenmiller, and R. L. Thoman, Eds., https://doi.org/10.25923/5cb7-6h06.

Kelly, B. P., and A. M. Fisher, 2021: Complex collaboration tools for a sustainable Arctic. *Wither the Arctic Ocean? Research, Knowledge Needs, and Development en Route to the New Arctic*, P. Wassman, Ed., Fundación BBVA, 43-51.

Landrum, L., and M. M. Holland, 2020: Extremes become routine in an emerging new Arctic. *Nat. Climate Change*, **10**, 1108-1115, https://doi.org/10.1038/s41558-020-0892-z.

Metcalf, V. K., 2021: Nangaghneghput – our way of life. *Front. Ecol. Environ.*, **19**(8), 427, https://doi.org/10.1002/fee.2409.

Schaeffer, J. Q., 2021: Climate change and its impacts on Indigenous People. *Science, Technology and the Path Forward for a New Arctic*, J. Kim & O. Young, Eds., Korea Maritime Institute & East-West Center, 118-125.

York, A., U. S. Bhatt, E. Gargulinski, Z. Grabinski, P. Jain, A. Soja, R. L. Thoman, and R. Ziel, 2020: Wildfire in High Northern Latitudes. *Arctic Report Card 2020*, R. L. Thoman, J. Richter-Menge, and M. L. Druckenmiller, Eds., https://doi.org/10.25923/2gef-3964.

Authors and Affiliations

O. Ahkinga, Study of Environmental Arctic Change

B. Ahmasuk, Marine Advocate, Kawerak Inc., Nome, AK, USA

E. Alexander, Study of Environmental Arctic Change

M. D. Apassingok, Study of Environmental Arctic Change

S. Backensto, National Park Service, Fairbanks, AK, USA

B. Baker, Study of Environmental Arctic Change

M. Baker, Study of Environmental Arctic Change

T. J. Ballinger, International Arctic Research Center, University of Alaska Fairbanks, Fairbanks, AK, USA

P. A. Berkman, Science Diplomacy Center, Falmouth, MA, USA; Program on Negotiation at Harvard Law School, Cambridge, MA, USA; United Nations Institute for Training and Research (UNITAR), Geneva, Switzerland

M. Berman, Study of Environmental Arctic Change

L. T. Berner, School of Informatics, Computing and Cyber Systems, Northern Arizona University, Flagstaff, AZ, USA

U. S. Bhatt, Geophysical Institute, University of Alaska Fairbanks, Fairbanks, AK, USA

S. Bigalke, Plants, Soils and Climate Department, Utah State University, Logan, UT, USA

J. W. Bjerke, Norwegian Institute for Nature Research, FRAM - High North Research Centre for Climate and the Environment, Tromsø, Norway

M. Blair, Study of Environmental Arctic Change

E. Bloom, Study of Environmental Arctic Change

B. Bodenstein, National Wildlife Health Center, U.S. Geological Survey, Madison, WI, USA

B. Brettschneider, National Weather Service Alaska Region, NOAA, Anchorage, AK, USA

L. C. Brown, Department of Geography, Geomatics and Environment, University of Toronto Mississauga, Mississauga, ON, Canada

C. T. Burns, Bureau of Land Management, U.S. Department of the Interior, Anchorage, AK, USA

M. L. Burns, U.S. Fish & Wildlife Service, Anchorage, AK, USA

N. J. Burns, Study of Environmental Arctic Change

S. Cannings, Canadian Wildlife Service, Environment and Climate Change Canada, Whitehorse, YT, Canada

M. L. Carlson, Alaska Center for Conservation Science, University of Alaska Anchorage, Anchorage, AK, USA

D. Causey, Arctic Domain Awareness Center, University of Alaska, Anchorage, AK, USA

J. C. Comiso, Cryospheric Sciences Laboratory, Goddard Space Flight Center, NASA, Greenbelt, MD, USA

L. W. Cooper, Chesapeake Biological Laboratory, University of Maryland Center for Environmental Science, Solomons, MD, USA

A. E. Copenhaver, Study of Environmental Arctic Change

S. Coulson, University Centre in Svalbard, Longyearbyen, Svalbard, Norway

E. Q. Cravalho, Study of Environmental Arctic Change

B. L. Daniels, Yukon Delta National Wildlife Refuge, U.S. Fish & Wildlife Service, Bethel, AK, USA

B. Decharme, Centre National de Recherches Météorologiques, Météo-France, Toulouse, France

C. Derksen, Climate Research Division, Environment and Climate Change Canada, Toronto, ON, Canada

D. Divine, Norwegian Polar Institute, Fram Centre, Tromsø, Norway

L. M. Divine, Aleut Community of St. Paul Island Tribal Government, St. Paul Island, AK, USA

J. Donatuto, Study of Environmental Arctic Change

J. Dooley, Division of Migratory Bird Management, U.S. Fish & Wildlife Service, Vancouver, WA, USA

M. L. Druckenmiller, National Snow and Ice Data Center, University of Colorado Boulder, Boulder, CO, USA; Cooperative Institute for Research in Environmental Sciences, University of Colorado Boulder, Boulder, CO, USA

C. R. Duguay, Department of Geography and Environmental Management, University of Waterloo, Waterloo, ON, Canada

K. Dunton, Study of Environmental Arctic Change

R. Dusek, National Wildlife Health Center, U.S. Geological Survey, Madison, WI, USA

A. Elias Chereque, Department of Physics, University of Toronto, Toronto, ON, Canada

H. E. Epstein, Department of Environmental Sciences, University of Virginia, Charlottesville, VA, USA

S. Farrell, Department of Geographical Sciences, University of Maryland, College Park, MD, USA

R. S. Fausto, Geological Survey of Denmark and Greenland, Copenhagen, Denmark

L. M. Fernandez, Department of Economics, Center for Environmental Studies, Virginia Commonwealth University, Richmond, VA, USA

X. Fettweis, SPHERES Research Unit, University of Liège, Liège, Belgium

G. J. Fiske, Woodwell Climate Research Center, Falmouth, MA, USA

S. V. Fletcher, Study of Environmental Arctic Change

B. C. Forbes, Arctic Centre, University of Lapland, Rovaniemi, Finland

K. E. Frey, Graduate School of Geography, Clark University, Worcester, MA, USA

E. Froehlich, Study of Environmental Arctic Change

G. V. Frost, Alaska Biological Research, Inc., Fairbanks, AK, USA

C. Garcia-Eidell, Global Ocean Monitoring and Observing Program, NOAA, Silver Spring, MD, USA

J. C. George, Study of Environmental Arctic Change

S. Gerland, Norwegian Polar Institute, Fram Centre, Tromsø, Norway

M. A. K. Gillespie, Department of Environmental Sciences, Western Norway University of Applied Sciences, Sogndal, Vestland, Norway

S. J. Goetz, School of Informatics, Computing and Cyber Systems, Northern Arizona University, Flagstaff, AZ, USA

J. M. Grebmeier, Chesapeake Biological Laboratory, University of Maryland Center for Environmental Science, Solomons, MD, USA

A. Greene, Kotzebue, AK, USA

E. Hanna, Department of Geography and Lincoln Climate Research Group, Lincoln, UK

I. Hanssen-Bauer, Norwegian Meteorological Institute, Oslo, Norway

C. Harris, Study of Environmental Arctic Change

M. Heavner, Study of Environmental Arctic Change

S. Hendricks, Alfred Wegener Institute, Helmholtz Centre for Polar and Marine Research, Bremerhaven, Germany

M. Hoffbeck, Study of Environmental Arctic Change

M. Holland, Study of Environmental Arctic Change

T. T. Høye, Department of Ecoscience and Arctic Research Center, Aarhus University, Aarhus, Denmark

C. D. Jensen, Danish Meteorological Institute, Copenhagen, Denmark

T. Jones, Coastal Observation and Seabird Survey Team, University of Washington, Seattle, WA, USA

L. L. Jørgensen, Institute of Marine Research, Tromsø, Norway

M. T. Jorgenson, Study of Environmental Arctic Change

W. Justin, Althsetnay Headwaters People Clan, Ahtna Dine' Storyteller, Elder Ambassador Cheesh'na Tribe, Chistochina, AK, USA; Chair, Mt. Sanford Tribal Consortium Board of Directors, Chistochina, AK, USA

R. Kaler, U.S. Fish & Wildlife Service, Alaska Region, Anchorage, AK, USA

L. Kaleschke, Alfred Wegener Institute, Helmholtz Centre for Polar and Marine Research, Bremerhaven, Germany

K. E. Kapsar, Center for Systems Integration and Sustainability, Department of Fisheries and Wildlife, Michigan State University, East Lansing, MI, USA

B. P. Kelly, Study of Environmental Arctic Change

E. Kerttula, Study of Environmental Arctic Change

S. -J. Kim, Korea Polar Research Institute, Incheon, Republic of Korea

G. W. Kling, Study of Environmental Arctic Change

C. W. Koch, Study of Environmental Arctic Change

Z. Labe, Atmospheric and Oceanic Sciences Program, Princeton University, Princeton, NJ, USA; Geophysical Fluid Dynamics Laboratory, NOAA, Princeton, NJ, USA

R. Lader, International Arctic Research Center, University of Alaska Fairbanks, Fairbanks, AK, USA

L. Landrum, Study of Environmental Arctic Change

S. Lange, Study of Environmental Arctic Change

M. J. Lara, Department of Plant Biology, University of Illinois, Urbana, IL, USA; Department of Geography, University of Illinois, Urbana, IL, USA

J. Leafloor, Aquatic Unit, Environment and Climate Change Canada, Winnipeg, MB, Canada

J. Lindsey, Coastal Observation and Seabird Survey Team, University of Washington, Seattle, WA, USA

B. D. Loomis, Goddard Space Flight Center, NASA, Greenbelt, MD, USA

D. Lorenzini, AAC SpaceQuest, Fairfax, VA, USA

M. K. Lukin, Study of Environmental Arctic Change

K. Luojus, Arctic Research Centre, Finnish Meteorological Institute, Helsinki, Finland

M. J. Macander, Alaska Biological Research, Inc., Fairbanks, AK, USA

D. MacNearney, Wildlife Research Division, Environment and Climate Change Canada, Ottawa, ON, Canada

K. D. Mankoff, National Snow and Ice Data Center, University of Colorado Boulder, Boulder, CO, USA; Cooperative Institute for Research in Environmental Sciences, University of Colorado Boulder, Boulder, CO, USA

E. Marino, Study of Environmental Arctic Change

S. A. McAfee, Department of Geography, University of Nevada Reno, Reno, NV, USA

W. N. Meier, National Snow and Ice Data Center, Boulder, CO, USA; Cooperative Institute for Research in Environmental Sciences, University of Colorado Boulder, Boulder, CO, USA

V. K. Metcalf, Study of Environmental Arctic Change

T. A. Moon, National Snow and Ice Data Center, University of Colorado Boulder, Boulder, CO, USA; Cooperative Institute for Research in Environmental Sciences, University of Colorado Boulder, Boulder, CO, USA

T. L. Mote, Department of Geography, University of Georgia, Athens, GA, USA

L. Mudryk, Climate Research Division, Environment and Climate Change Canada, Toronto, ON, Canada

C. Nunn, Study of Environmental Arctic Change

E. Oberndorfer, Agriculture and Agri-Food Canada, Goose Bay, NL, Canada

J. E. Overland, Pacific Marine Environmental Laboratory, NOAA, Seattle, WA, USA

J. Parrish, Coastal Observation and Seabird Survey Team, University of Washington, Seattle, WA, USA

V. Patil, Alaska Science Center, U.S. Geological Survey, Anchorage, AK, USA

J. M. Pearce, Alaska Science Center, U.S. Geological Survey, Anchorage, AK, USA

D. Perovich, Thayer School of Engineering, Dartmouth College, Hanover, NH, USA

A. Petty, Goddard Space Flight Center, NASA, Greenbelt, MD, USA

G. K. Phoenix, School of Biosciences, University of Sheffield, Sheffield, UK

R. Pincus, Study of Environmental Arctic Change

K. Pletnikoff, Aleutian Pribilof Islands Association, Anchorage, AK, USA; Aleut International Association, Anchorage, AK, USA

K. Poinar, Department of Geology, University at Buffalo, Buffalo, NY, USA

P. Pungowiyi, Study of Environmental Arctic Change

R. Ricker, NORCE Norwegian Research Centre, Tromsø, Norway

M. Robards, Study of Environmental Arctic Change

J. J. Rykken, Alaska Center for Conservation Science, University of Alaska Anchorage, Anchorage, AK, USA

J. Q. Schaeffer, Study of Environmental Arctic Change

P. Schwalenberg, Alaska Migratory Bird Co-Management Council, Anchorage, AK, USA

S. P. Serbin, Environmental and Climate Sciences Department, Brookhaven National Laboratory, Upton, NY, USA

M. C. Serreze, National Snow and Ice Data Center, University of Colorado Boulder, Boulder, CO, USA

T. L. Sformo, Department of Wildlife Management, North Slope Borough, Utqiaġvik (Barrow), AK, USA; Institute of Arctic Biology, University of Alaska Fairbanks, Fairbanks, AK, USA

A. Shahbazi, Study of Environmental Arctic Change

G. Sheffield, Alaska Sea Grant, Marine Advisory Program, University of Alaska Fairbanks, Nome, AK, USA

A. Shultz, Study of Environmental Arctic Change

D. S. Sikes, University of Alaska Museum, University of Alaska Fairbanks, Fairbanks, AK, USA

M. Smith, Alaska Science Center, U.S. Geological Survey, Anchorage, AK, USA

L. V. Stock, Cryospheric Sciences Laboratory, Goddard Space Flight Center, NASA, Greenbelt, MD, USA

M. Tedesco, Lamont-Doherty Earth Observatory, Columbia University, Palisades, NY, USA; Goddard Institute of Space Studies, NASA, New York, NY, USA

R. L. Thoman, Alaska Center for Climate Assessment and Policy, University of Alaska Fairbanks, Fairbanks, AK, USA; International Arctic Research Center, University of Alaska Fairbanks, Fairbanks, AK, USA

X. Tian-Kunze, Alfred Wegener Institute, Helmholtz Centre for Polar and Marine Research, Bremerhaven, Germany

M. -L. Timmermans, Yale University, New Haven, CT, USA

H. Tømmervik, Norwegian Institute for Nature Research, FRAM - High North Research Centre for Climate and the Environment, Tromsø, Norway

D. T. Turner, Study of Environmental Arctic Change

C. Van Hemert, Alaska Science Center, U.S. Geological Survey, Anchorage, AK, USA

D. A. Walker, Institute of Arctic Biology, University of Alaska Fairbanks, Fairbanks, AK, USA

J. E. Walsh, International Arctic Research Center, University of Alaska Fairbanks, Fairbanks, AK, USA; Study of Environmental Arctic Change

M. Wang, Pacific Marine Environmental Laboratory, NOAA, Seattle, WA, USA; Cooperative Institute for Climate, Ocean, and Ecosystem Studies, University of Washington, Seattle, WA, USA

M. Webster, Geophysical Institute, University of Alaska Fairbanks, Fairbanks, AK, USA

A. Wehrlé, Department of Geography, University of Zurich, Zurich, Switzerland

F. Wiese, Study of Environmental Arctic Change

J. K. Willis, Jet Propulsion Laboratory, California Institute of Technology, Pasadena, CA, USA

G. Wong, Study of Environmental Arctic Change

M. Wood, Jet Propulsion Laboratory, California Institute of Technology, Pasadena, CA, USA; Moss Landing Marine Laboratories, San José State University, San José, CA, USA

D. Yang, Environmental and Climate Sciences Department, Brookhaven National Laboratory, Upton, NY, USA; Department of Ecology and Evolution, Stony Brook University, Stony Brook, NY, USA

O. R. Young, Bren School of Environmental Science & Management, University of California Santa Barbara, Santa Barbara, CA, USA